Final Report

Technical Subtopic 2.1: Modeling Variable Refrigerant Flow Heat Pump and Heat Recovery Equipment in EnergyPlus

September 2013

DOE/NETL Award DE-EE0003848

FSEC-CR-1968-13

Floida Solar Energy Center
Richard Raustad
Dr. Bereket Nigusse
Chandan Sharma
Jamie Cummings

Electric Power Research Institute
Dr. Ron Domitrovic
Harshal Upadhye

Florida Solar Energy Center
Buildings Research Division
University of Central Florida
1679 Clearlake Road

Cocoa, FL 32922

Phone: 321-638-1454
Fax: 321-638-1439
http://www.fsec.ucf.edu

Table of Contents

List of Figures

List of Tables

NOMENCLATURE

a – f	Equation coefficients determined through regression analysis
AFUE	Annual fuel utilization efficiency, (%)
AHRI	Air-Conditioning, Heating and Refrigeration Institute
ANSI	American National Standard Institute
COP	Heating or cooling coefficient of performance, (-).
CR	Combination ratio, (-)
CAPFF	Quadratic or cubic capacity modifying curve as a function of flow fraction, (-)
CAPFT	Bi-quadratic or cubic capacity modifying curve as a function of temperature, (-)
Cv	Coefficient of variation of the root-mean-square error
DB	Dry bulb
DBT	Dry bulb temperature, °C (°F)
DX	Direct expansion
EEV	Electronic expansion valve
EIRFT	Bi-quadratic EIR modifying curves as a function of temperature, (-)
FF	Ratio of actual to rated air mass flow rate through an indoor coil, (-)
h	Enthalpy, J/kg (Btu/lb)
HP	Heat pump
HRCapMod	Heat recovery mode capacity modifier fraction, (-)
HRPowerMod	Heat recovery mode electric power modifier factor, (-)
ID	Indoor
IDU	Indoor unit
k	Fraction of steady-state VRF electric power at beginning of heat recovery mode
IAT	Indoor –unit return-air temperature °C (°F)
MBh	Thousand Btu's per hour
$\dot{m}$	Mass flow rate, kg/s (lb/hr)
n	Sample size, or number of indoor coils
OAT	Outdoor air temperature °C (°F)
OD	Outdoor
P	Electric power, W
$\overline{P}$	Normalized electric power, (-)
PFPLR	Electric power modifier factor as a function of part-load ratio, (-)
PL	Piping loss due to refrigerant tubing
PLR	Heating or cooling part-load-ratio, (-)
$\dot{Q}$	Rate of heat transfer, W (Btu/hr)
Q	Heating or cooling load delivered or capacity, W (Btu/hr)
$\overline{Q}$	Normalized cooling or heating capacity, (-)
r	Sample correlation coefficient
RAT	Return air temperature, °C (°F)
RA-DBT	Return air – dry bulb temperature, °C (°F)
RA-WBT	Return air – wet bulb temperature, °C (°F)
RH	Relative humidity (%)
RTF	System runtime fraction, (-)
T	Temperature, °C (°F)
$\overline{T}$	Average temperature, °C (°F)
τ	Time constant to reach steady-state operation, (hours)

U	Heat transfer coefficient, W/m^{2}K (Btu/ft^{2}hr°F)
UA	Heat transfer coefficient time area, W/K (Btu/hr°F)
V	Supply air volume flow rate, m^3/s (ft^3/hr)
VRF	Variable refrigerant flow
VRF-HR	Variable refrigerant flow – heat recovery
w	Humidity ratio, g/g (lb/lb)
WB	Wet bulb
WBT	Wet bulb temperature, °C (°F)
X	Measured and predicted output variables

SUBSCRIPTS

actual	actual load or electric power
auxiliary	auxiliary electric power
Crankcase	crank case heater
cool	cooling operation mode
cap	capacity
db	dry-bulb
defrost	defrost operating mode
e	electric power
evapcooler	evaporative cooler
fan	terminal units or indoor units fan
Full	full-load capacity of an indoor coil or outdoor unit
heat	heating operation mode
hp	heat pump operating mode
hr	heat recovery operating mode
ID	indoor coil or indoor coil entering air condition
i, j	Indices
L	Heating or cooling load
m	measured variable
OD	outdoor coil or outdoor air condition
opr	actual operating condition
Rated	AHRI rated test conditions
ref	reference or rated condition
Sys	VRF system or outdoor unit
S	simulation variable
trns	transition period
TUs	terminal unit or indoor units
wb	wet-bulb

Executive Summary

The University of Central Florida/Florida Solar Energy Center, in cooperation with the Electric Power Research Institute and several variable-refrigerant-flow heat pump (VRF HP) manufacturers, provided a detailed computer model for a VRF HP system in the United States Department of Energy's (U.S. DOE) EnergyPlus™ building energy simulation tool. Detailed laboratory testing and field demonstrations were performed to measure equipment performance and compare this performance to both the manufacturer's data and that predicted by the use of this new model through computer simulation.

The project goal was to investigate the complex interactions of VRF HP systems from an HVAC system perspective, and explore the operational characteristics of this HVAC system type within a laboratory and real world building environment. Detailed laboratory testing of this advanced HVAC system provided invaluable performance information which does not currently exist in the form required for proper analysis and modeling. This information will also be useful for developing and/or supporting test standards for VRF HP systems. Field testing VRF HP systems also provided performance and operational information pertaining to installation, system configuration, and operational controls.

Information collected from both laboratory and field tests were then used to create and validate the VRF HP system computer model which, in turn, provides architects, engineers, and building owners the confidence necessary to accurately and reliably perform building energy simulations. This new VRF HP model is available in the current public release version of DOE's EnergyPlus software and can be used to investigate building energy use in both new and existing building stock.

The general laboratory testing did not use the AHRI Standard 1230 test procedure and instead used an approach designed to measure the field installed full-load operating performance. This projects test methodology used the air enthalpy method where relevant air-side parameters were controlled while collecting output performance data at discreet points of steady-state operation. The primary metrics include system power consumption and zonal heating and cooling capacity. Using this test method, the measured total cooling capacity was somewhat lower than reported by the manufacturer. The measured power was found to be equal to or greater than the manufacturers indicated power. Heating capacity measurements produced similar results. The air-side performance metric was total cooling and heating energy since the computer model uses those same metrics as input to the model. Although the sensible and latent components of total cooling were measured, they are not described in this report.

The test methodology set the thermostat set point temperature very low for cooling and very high for heating to measure full-load performance and was originally thought to provide the maximum available capacity. Manufacturers stated that this test method would not accurately measure performance of VRF systems which is now believed to be a true statement. Near the end of the project, an alternate test method was developed to better represent VRF system performance as if field installed. This method of test is preliminarily called the Load Based Method of Test where the load is fixed and the indoor conditions and unit operation are allowed to fluctuate. This test method was only briefly attempted in a

laboratory setting but does show promise for future lab testing. Since variable-speed air-conditioners and heat pumps include an on-board control algorithm to modulate capacity, these systems are difficult to test. Manufacturers do have the ability to override internal components to accommodate certification procedures, however, it is unknown if the resulting operation is replicated in the field, or if so, how often. Other studies have shown that variable-speed air-conditioners and heat pumps do out perform their single-speed counterparts though these field studies leave as many questions as they do provide answers.

The measured performance of all VRF systems tested did show remarkable agreement with the shape of the manufacturers performance data (i.e., the slope of the measured data versus outdoor temperature had the same or similar slope as reported by the manufacturer). This outcome supports the use of manufacturers performance data, in a normalized format, as performance inputs to the VRF computer model. The questionable model inputs are the rated capacity and COP which, during this project, were found at times to be quite different than reported by manufacturers. Of course, these differences are inherently caused by the different test procedures used to measure performance.

Given the accelerated use of variable-speed equipment, further research is warranted to understand the performance of these systems in real world applications. Additional laboratory testing, review and critique of Standards test methods, and further comparison of field measured performance to computer models will provide information necessary to better understand the operational and economic benefits of these systems.

1. Introduction

Variable Refrigerant Flow HVAC systems, although not new, are gaining more popularity in American HVAC markets. Variable Refrigerant Flow (VRF) technology is becoming attractive due to their reported high efficiency over a wide range of part-load operation, capability of providing cooling and heating simultaneously when run in heat recovery mode, and individual terminal unit or zone control features (Geotzler et al., 2004; Aynur et. al., 2009; Aynur, 2010; Li and Wu 2010). The VRF technology is a modular design split DX-system with multiple indoor coils connected to a single outdoor unit where the refrigerant flow is controlled using a variable speed compressor (or a combination of variable and constant speed compressors). The compressor, or one or more of multiple compressors, is driven by a variable frequency inverter. The indoor terminal unit coils use electronic-expansion valves (EEV) to control the indoor coil capacity. Although VRF systems have been available in the market for more than two decades (Dyer, 2006), VRF modeling capabilities in non-proprietary building and energy simulation tools has been lagging (Geotzler, 2007; Zhou et al., 2007; Zhou et al., 2008). For this reason, the Department of Energy (DOE) sponsored this project to incorporate a variable refrigerant flow (VRF) heat pump and heat recovery computer model in DOE's EnergyPlus building simulation software.

The objectives of this project were: (1) develop a VRF heat pump and heat recovery computer model and implement that model in DOE's EnergyPlus software, (2) conduct laboratory and field VRF performance measurement to help the formulation and validation of the model, (3) verify the computer model using manufacturers performance data and (4) perform parametric analysis to test the new model and quantify the various advantages of the VRF system compared to conventional HAVC systems.

A VRF Heat Pump system model with cooling and heating only mode has been implemented in EnergyPlus and first released in version V7.0 (US Department of Energy, 2011). The VRF heat recovery and water-cooled model was first released in V7.2 (US Department of Energy, 2012b). The EnergyPlus VRF heat pump model is a semi-empirical equation fit model, primarily based on performance curves generated from published manufacturer's data. The description of the heat pump and heat recovery computer model are provided in Chapter 2 and Chapter 5, respectively. Part of this DOE project also involved verifying the VRF computer model to identify programming errors, and validate the model using field measured data. The VRF heat pump computer model was verified against publicly available manufacturer's performance data. The verification is focused in particular on the system performance at full and part-load over a wide range of indoor and outdoor weather conditions in cooling and heating only modes of operation. Chapter 3 discusses the verification methodology and results. Chapter 4 discusses the independent laboratory testing to understand and characterize the performance of VRF heat pump and heat recovery models.

Chapter 6 discusses the VRF system field performance monitoring and measurement. The objective of these tests was to investigate VRF system performance in the field. The operational performance of the VRF system was monitored and recorded over a period of at least six months at two different sites. The heat recovery operating mode selection, operating mode switching procedure, and assumptions in formulating the VRF heat recovery model control are described in Chapter 7. The VRF computer model was also validated using the field measured data. The validation methodology and results are presented in Chapter 8. The validation was performed using daily energy data that spans more than six months and included cooling only, heating only and simultaneously heating and cooling operating modes. In Chapter 9 the VRF computer model was fully investigated through parametric simulation studies to quantify the potential benefits of VRF systems compared to central variable-air-volume and large rooftop packaged HVAC systems. The systems were compared using four different building types and in one representative city from each of the eight US climate zones. A project overview is provided here to summarize the original intent of this research. Task 2-9 correspond to chapters 2-9 in this report.

1.1 Project Task Description

The project task list as specified in the original statement of work is described here.

Task 1.0 – Project Management Plan

Scope: The University of Central Florida (UCF) / Florida Solar Energy Center (FSEC) will provide a detailed plan to manage and execute the proposed work during the 3 year period of performance. This plan will be provided to the DOE COR for preliminary review and acceptance. This plan will be updated on a regular basis throughout the period of performance to provide a project status update at regular intervals and describe the effort and scheduling of tasks required for successful project completion.

An original project management plan was provided to the DOE project manager. Regular updates were provided when requested.

Task 2.0 – Implementing a VRF heat pump model in U.S. DOE's EnergyPlus software tool

Scope: UCF/FSEC proposes to implement an existing computer model for a VRF heat pump system in a future release of U.S. DOE's EnergyPlus software tool. This specific computer model is appropriate for cooling-only or heating-only (heat pump) applications and is the basis for the overall VRF system computer model.

This existing computer model has been previously approved by DOE's EnergyPlus development team and will be incorporated into the U. S. DOE's EnergyPlus simulation tool according to the Module Development Guide standards for acceptable practice. This process includes formulating the Input Data Dictionary (IDD) input syntax, developing the model's mathematical equations through software programming, and providing a generic working example of a VRF heat pump system. The decision point is identified as the documentation and code submittal.

The Variable Refrigerant Flow (VRF) heat pump model was implemented in DOE's EnergyPlus simulation software V7.0.0.036. Reference documents describe the mathematical model and requisite model inputs. EnergyPlus V7.0 also includes an example file illustrating the use of this new model. FSEC contract report descriptor: FSEC-CR-1960-11.

Task 3.0 – Validation of the VRF heat pump model using manufacturers performance data

Scope: The VRF heat pump model will be validated by comparing the computer simulated performance to publically available manufacturer's performance data and measurements made during laboratory testing in Task 4. The model validation process compares the measured performance data with steady-state performance predicted by the computer simulation tool. Specific parameters such as system capacity, power, and system operating conditions (e.g., temperature and humidity ratio) will be examined to ensure that an accurate and robust model is included in the public release version of U. S. DOE's EnergyPlus simulation software tool. It is anticipated that minimal revisions to the previously defined computer model will be required. This task will required a close working relationship with industry partners to ensure an accurate representation of the existing VRF technology.

The Variable Refrigerant Flow (VRF) heat pump model was implemented in DOE's EnergyPlus simulation software V7.0.0.036. To ensure an accurate implementation, the VRF heat pump computer model was extensively tested to identify possible discrepancies between the simulation results and manufacturer's performance data. FSEC contract report descriptor: FSEC-CR-1961-12.

Task 4.0 – Independent Lab Testing of Two VRF AC Systems in Heat Pump and Heat Recovery Mode

Scope: Two VRF systems—one each VRF heat pump and VRF heat recovery heat pump—will be laboratory tested at the Electric Power Research Institute's Knoxville, TN laboratory. Testing will be conducted in EPRI's thermal testing facility which includes controlled climate chambers and a complete data acquisition system. Testing will characterize the VRF system's performance in a variety of operating modes and at multiple entering air conditions to provide data for model development and validation.

Two Variable Refrigerant Flow (VRF) heat pumps were tested at the Electric Power Research Institute's (EPRI) Knoxville, TN laboratory. These systems were not tested in accordance with the Standard method of test as described by ANSI/AHRI Standard 1230. Instead, these systems were tested in an attempt to measure performance as if these systems were field installed. Given the method of test chosen, the results may not necessarily reflect actual operation. The method of test chosen was the air enthalpy method with fixed operating conditions. As the results show, the performance measured did not agree with manufacturer's published performance data. It is believed that this specific method of test is not appropriate for testing advanced variable-speed heating and cooling equipment and that alternate test methods should be investigated to determine the most appropriate, or a more appropriate, test method for these system types. Project participants have suggested that a calorimetric test method may more accurately represent performance and allow the control algorithms to better respond to imposed loads. One method currently being investigated through other funding sources is to impose a fixed load (both sensible and latent) on the system and allow that system to operate as it would in a real application. If the steady-state operation did not provide the desired operating conditions, minor adjustments to the fixed loads could push the operating conditions toward the desired state point. FSEC contract report descriptor: FSEC-CR-1962-12.

Task 5.0 – Development of a VRF system heat recovery computer model

Scope: Development of an empirical model is primarily based on a thorough examination of existing performance data. Work previously completed during Task 4 provides such a basis for developing an accurate computer model for VRF systems. This task entails identifying an appropriate computer model (i.e., the model's independent variables) and using this model to predict the performance of a VRF system operating in heat recovery mode. The model specifications will be provided to the U. S. DOE's EnergyPlus software development team for review and acceptance. The EnergyPlus software development team will provide the ultimate approval of this model for use in the EnergyPlus software tool.

The Variable Refrigerant Flow (VRF) heat pump model was implemented in DOE's EnergyPlus simulation software V7.0.0.036 (Task 2). For this task, a heat recovery model was developed and presented to the DOE EnergyPlus core development team for approval. The proposed model included documentation describing the mathematical equations used to represent operational performance. FSEC contract report descriptor: FSEC-CR-1963-12.

Task 6.0 – Field Testing Two VRF Systems

Scope: The performance of two VRF systems will be monitored to verify the performance of this unique system type; one providing simple heat pump operation to validate the existing VRF system heat pump model and the other capable of heat recovery for validation of the newly developed VRF heat recovery computer model. EPRI hass installing multiple VRF systems throughout the United States as part of demonstration projects with electric utilities and one of those sites will be instrumented to provide field data input to the model developed in this project. The data collected will serve as a real-world validation check on the model as well as a true measure of field performance of these advanced HVAC systems.

The Electric Power Research Institute (EPRI) field tested a VRF heat pump in a portion of their Knoxville, TN facility. This system was also tested in the laboratory prior to field deployment. The measured performance of another VRF system was also included in this project. FSEC contract report descriptor: FSEC-CR-1964-12.

Task 7.0 – Implementing a VRF AC system heat recovery model in U. S. DOE's EnergyPlus software tool

Scope: Similar to Task 2, the new empirical model developed during Task 5 will be added to the U. S. DOE EnergyPlus building simulation software tool. This new computer model will accurately reflect the performance and energy use for the advanced VRF system's heat recovery operating mode. Deliverables include the completed software code, engineering documentation, an example file to exercise the new computer model, and the requisite user inputs to accurately model this advanced VRF system in heat recovery operating mode.

The Variable Refrigerant Flow (VRF) heat pump model was implemented in V7.0.0.036 (Task 2). This VRF heat recovery model was implemented in V7.2.0.006 on October 15, 2012. FSEC contract report descriptor: FSEC-CR-1965-12.

Task 8.0 – Compare Field Demonstration Building Energy Use to Computer Simulations

Scope: An important aspect of computer simulation tools is the documented performance comparison of specific equipment models with real world applications. This project includes just such a detailed comparison. Task 6 describes the field work to monitor and collect performance data for VRF systems. This field collected performance data will be used to compare to the predicted performance of EnergyPlus computer. One building model will be developed to accurately reflect the field test sites and the installed VRF equipment. A detailed computer simulation will be performed to compare the VRF system computer model to the actual VRF system field performance measured at the field test site.

The Variable Refrigerant Flow (VRF) heat pump model was implemented in V7.0.0.036 (Task 2). This task effort describes the validation methodology and discusses the validation results of the VRF heat pump computer model using field measured data. The VRF heat pump field performance test was conducted in the Electric Power Research Institute (EPRI) test facility at Knoxville, TN. The field measured performance data collected in heat recover operating mode was not adequate for

validation purpose hence, the validation report focused only on the heat pump operating mode. FSEC contract report descriptor: FSEC-CR-1966-13.

Task 9.0 - Parametric Analysis using the EnergyPlus VRF System Model:

Scope: This task involves running a series of parametric simulations to thoroughly exercise the full EnergyPlus VRF model developed as part of previous tasks. It is envisioned that a minimum of three common building types, including an office, retail, and hotel building will be selected. The building models will be taken from the existing DOE Benchmark Commercial Buildings database to maintain standardization. These kinds of buildings typically use either Variable Air Volume (VAV) or large rooftop packaged units. The performance of these systems can be compared with EnergyPlus' new VRF system model. These simulations will be performed for one representative city from each of the eight ASHRAE specified climate locations in the US. Results from these parametric runs will highlight the comparative annual energy use, the thermal comfort within the buildings, the potential reduction in CO2 emissions, and the direct cost savings that might be available after considering operating costs associated with using VRF systems.

Computer simulations were used to test the VRF computer model to identify any programming errors and to also compare simulated energy use to other HVAC system types. The HVAC systems were compared using four different building types and in one representative city from each of the eight U.S. climate zones. The VRF system computer simulations investigated: impacts of duct conduction losses, air distribution losses (duct leakage), fan energy use, system efficiency, and simultaneous heating and cooling operation.

Disclaimer: The parametric simulations discussed in this Task report represent the testing performed to evaluate the new variable refrigerant flow computer model in DOE's EnergyPlus building simulation program. Although the simulation results were reviewed for accuracy, and are believed to be representative of VRF performance, the magnitude of the results described in this report may change as the VRF computer model evolves over time or is changed to provide a better representation of VRF performance. FSEC contract report descriptor: FSEC-CR-1967-13.

1.2 External Agency Contacts

During the course of this project, several agencies became aware of this work and requested updates on work performed, webinar presentation of results, or support for on-going work related to VRF systems. These external agency contacts are:

- ASHRAE TC 8.1 VRF

  The ASHRAE technical committee meetings held at regular conference meetings were attended and provided a forum for discussion of the new VRF computer model, pending laboratory testing, and discussions of future development work benefitting VRF equipment. Four papers were presented at these conference meetings describing project efforts. These papers are:

  Raustad, R.A. (2013). A Variable Refrigerant Flow Heat Pump Computer Model in EnergyPlus. *ASHRAE Transactions*, 119 (Part 1):299-308.

  Nigusse, B., R. Raustad, Verification of a VRF Heat Pump Computer Model in EnergyPlus. ASHRAE Transactions, volume 119, Part 2:101-117. DE-13-010.

  Raustad, R., (2013). Computer Modeling VRF Heat Pumps in Commercial Buildings using EnergyPlus. *ASHRAE Annual Conference*, Denver, Colorado, June 22-27, 2013. DE-13-C071.

  Sharma, C., R. Raustad, Compare Energy Use in Variable Refrigerant Flow Heat Pumps Field Demonstration and Computer Model. *ASHRAE Annual Conference*, Denver, Colorado, June 22-27, 2013. DE-13-C072.

- Variable Capacity Heat Pump Subcommittee

  This web based subcommittee focuses on variable capacity heat pumps (VCHP) which includes VRF as well as other variable-speed equipment. This subcommittee is a Regional Technical Forum for industry professionals and interested parties hosted by Bonneville Power Administration. Several web meetings were attended and presentations were provided at two of these meetings to update the group regarding this work. The two VRF presentations occurred on July 27, 2012 and February 27, 2013. The web site for this forum is: http://rtf.nwcouncil.org/subcommittees/vchp/

- Energy Trust Of Oregon – Building Energy Simulation Forum

  This web based forum is a resource for professionals who work in the field of energy simulation. A participant in this forum, who attended a VCHP Subcommittee web meeting, requested that the VRF information presented in a previous VCHP subcommittee web meeting also be presented to

the Building Energy Simulation Forum. The VRF presentation occurred on May 15, 2013. The web site for this forum is: http://energytrust.org/commercial/building-energy-simulation/

- Compressor Technology Expert Panel

Recruited to participate in an expert panel regarding compressor equipment. Although compression equipment technology is only indirectly related to this project, the panel decided to also include participants who have experience with many HVAC system types, including VRF systems. The panel was moderated by Alan Budovitch of Cladek & Associates, Inc. The discussion began on 5/8/2013 and continued for several weeks. Each day, the group moderator posted new questions and participants answered these questions and also had the opportunity to reply to other participant responses.

Panel participation:

Bill Bush, Carrier (retired), Gene Fields (LG), Eckhard Groll (Purdue University), Guo Defang (Haier), Scott Hix (Bristol Compressors), Noriaki Ishii (Osaka Electro-Communication University), Kun Kim (Toshiba-Carrier), Richard Raustad (University of Central Florida), Tom Roberts (CFM Distributors), Curt Slayton (Ex-Chair, ASHRAE Compressor Committee), William Sun (Danfoss), Simon Wang (Copeland), Xin Ziwen (Xi'an Jiaotong University), Yang Jun (Shanghai Hitachi), You Bin (Midea-GMCC)

2. Implementing a VRF Heat Pump Model in EnergyPlus

The EnergyPlus VRF computer model is a performance based HVAC model similar to other unitary equipment HVAC models. The EnergyPlus VRF model evolved from the previously developed DOE-2 VRF model. The model consists of two main components: indoor unit model, and the outdoor unit. One or more indoor units can be connected to each outdoor unit. Each indoor unit consists of three sub-components: an indoor cooling and/or heating coil, an outdoor air mixer, and a supply fan. The outdoor air mixer and supply fan models are generic component models available in EnergyPlus, while the indoor coil and the outdoor coil are specific to the VRF model of EnergyPlus. These two coil models use performance curves commonly generated from manufacturer's data. A more detailed description of the development and formulation of these component models is documented by Raustad (2013).

2.1 VRF Heat Pump Computer Model

The VRF HVAC computer model is an empirical model that describes several operating characteristics. These performance characteristics are commonly generated from VRF manufacturer's performance data. The VRF computer model and the various performance curve generation techniques are described by Raustad (2012, 2013).

2.1.1 Cooling Operation

Simulating the VRF system model requires model inputs of rated capacity, coefficient of performance (COP), various performance curves for indoor and outdoor coils, piping losses, and operational control parameters. Each indoor coil is simulated to determine the operating coil capacity. The operating coil capacity is calculated from the zone load knowing the indoor and outdoor air conditions. Capacity correction for piping losses are based on manufacturers data and is assumed to be constant throughout the simulation (i.e., piping losses are not based on the number of units actually operating). The system total cooling load is determined by summing the indoor cooling coil loads corrected for piping losses using Eq-1. A similar calculation is performed for zones that have a heating load.

$$\dot{Q}_{Coil,\,Total,\,Cool} = \frac{1}{PL_{Correction,\,Cool}} \sum_{i=1}^{n} \dot{Q}_{Coil,\,i,\,cool} \qquad (1)$$

Figure 1 shows a sample of manufacturer's cooling performance data which has a distinct trend at low and high outdoor air temperature ranges. As outdoor temperature increases, cooling capacity decreases, and cooling power increases after a point is reached when the system can no longer control to meet internal set points. The VRF computer model calculates capacity and electric power using the dual range performance curves. The load-weighted average coil entering air wet-bulb temperature seen by the VRF outdoor unit in cooling operating mode is given by Eq-2. In heating mode load-weighted

average coil entering air dry-bulb temperature is used. This average temperature is used as one of the two independent variables in the capacity and energy input ratio performance curves (Eq-5 and Eq-14).

$$\overline{T}_{wb,\,ID} = \frac{\sum_{i=1}^{n} \dot{Q}_{Coil,\,i,\,Ccool} \cdot T_{wb,\,i,\,ID}}{\dot{Q}_{Coil,\,Total,\,Cool}} \tag{2}$$

$$T_{boundary} = a + b\overline{T}_{wb,\,ID} + c\overline{T}^{2}_{wb,\,ID} + d\overline{T}^{3}_{wb,\,ID} \tag{3}$$

The boundary curve shown in Figure 2-1 and given by Eq-3 calculates the outdoor air dry-bulb boundary temperature as a function of the average indoor coil entering air wet-bulb temperature to distinguish the operating range of the dual range performance curves.

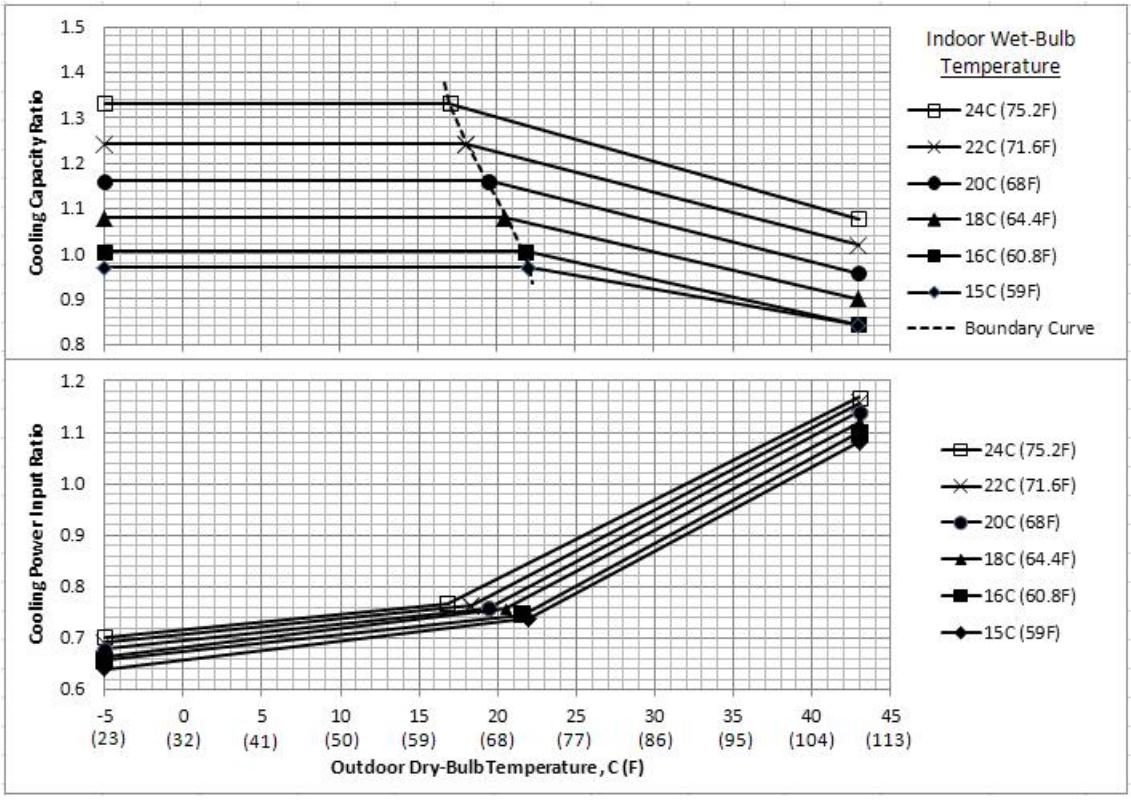

Figure 2-1 Example Variable Refrigerant Flow Cooling Performance Data
Source: Mitsubishi Electric (Mitsubishi, 2009).

The VRF Heat Pump outdoor unit capacity is determined from the rated capacity and the dual range normalized capacity modifier as a function of temperature (CAPFT) curve. These capacity modifier curves represent the cooling performance relative to the reference or rated capacity as defined by Eq-4.

$$CAPFT_{hp,\,cool} = \frac{\dot{Q}_{hp,\,cool}\left(\overline{T}_{wb,\,ID}, T_{db,\,OD}\right)}{\dot{Q}_{hp,\,cool,\,ref}} \tag{4}$$

The capacity modifier bi-quadratic performance curve is shown as Eq-5.

$$CAPFT_{hp,\,cool} = a + b \cdot \overline{T}_{wb,\,ID} + c \cdot \overline{T}^{2}_{wb,\,ID} + d \cdot T_{db,\,OD} + e \cdot T^{2}_{db,\,OD} + f \cdot \overline{T}_{wb,\,ID} \cdot T_{db,\,OD} \quad (5)$$

The total available cooling capacity provided by the VRF Heat Pump outdoor unit is also a function of combination ratio (CR) defined by Eq-6. Manufacturers typically provide combination ratio (CR) performance data that allows generation of coefficients a - d in Eq-7. The total available system cooling capacity is given by Eq-8.

$$CR_{cool} = \frac{\sum_{i=1}^{n} \dot{Q}_{Coil,\,i,\,cool,\,ref}}{\dot{Q}_{hp,\,cool,\,ref}} \quad (6)$$

$$CR_{cool,\,correction} = a + b \cdot CR_{cool} + c \cdot CR^{2}_{cool} + d \cdot CR^{3}_{cool} \;,\; CR_{cool} \geq 1 \quad (7)$$

$$\dot{Q}_{hp,\,total,cool} = \dot{Q}_{hp,cool,\,ref} \cdot CAPFT_{hp,\,cool} \cdot CR_{cool,\,correction} \quad (8)$$

Eq-9 shows that the system part-load ratio (PLR) is calculated as the ratio of the sum of the individual indoor cooling coil total (sensible plus latent) delivered capacity to the available VRF system cooling capacity (Eq-8). If the operating PLR is less than the specified minimum PLR, the VRF compressor will cycle on and off (Eq-10). The VRF system cycling losses are accounted for using an empirical part-load correlation (Eq-11). The runtime fraction (RTF) defines the fractional amount of time the compressor must operate to overcome cycling losses (Eq-12).

$$PLR = \frac{\sum_{i=1}^{n} \dot{Q}_{Coil,\,i,\,Cool}}{\dot{Q}_{HP,\,Total,Cool}} \quad (9)$$

$$C_{Ratio} = PLR / PLR_{\min} \;,\; C_{Ratio} \leq 1 \quad (10)$$

$$C_{RatFrac} = a + b \cdot C_{Ratio} + c \cdot C^{2}_{Ratio} + d \cdot C^{3}_{Ratio} \quad (11)$$

$$RTF_{hp} = C_{Ratio} / C_{RatFrac} \;,\; 0.7 \leq C_{RatFrac} \;\; and \;\; C_{RatFrac} \geq C_{Ratio} \quad (12)$$

The VRF HP outdoor unit energy input is modeled using rated energy inputs and a normalized energy input ratio modifier as a function of the temperature (EIRFT) curve given by Eq-13. The form of the EIRFT curve is shown in Eq-14. A part-load term accounts for changes in the VRF compressor speed above the minimum compressor part-load ratio (Eq-15). When one or more of the indoor coils operate at part-load, the outdoor unit as well operates at a lower part-load ratio (Eq-16). The VRF HP's cooling electric energy input is based on four distinct multipliers and is described by Eq-17.

$$EIRFT_{hp,\,cool,\,j} = \frac{P_{hp,\,cool,\,j} \Big/ \dot{Q}_{hp,\,cool,\,j}}{P_{hp,\,cool,\,ref} \Big/ \dot{Q}_{hp,\,cool,\,ref}} \tag{13}$$

$$EIRFT_{hp,\,cool} = a + b \cdot \bar{T}_{wb,\,ID} + c\bar{T}^{2}_{wb,\,ID} + d \cdot T_{db,OD} + e \cdot T^{2}_{db,OD} + f \cdot \bar{T}_{wb,\,ID} \cdot T_{db,OD} \tag{14}$$

$$EIRFPLR_{hp,\,cool,\,PLR} = \frac{P_{hp,\,cool,\,PLR}}{P_{hp,\,cool,\,ref}},\ PLR \geq PLR_{min} \tag{15}$$

$$EIRFPLR_{hp,\,cool} = a + b \cdot PLR + c \cdot PLR^{2} + d \cdot PLR^{3}\ ,\ PLR \geq PLR_{\min} \tag{16}$$

$$P_{hp,\,cool} = \left(\frac{\dot{Q}_{cool,\,total,\,ref}}{COP_{cool,\,ref}} \right) \cdot CAPFT_{hp,\,cool} \cdot EIRFT_{hp,\,cool} \cdot EIRFPLR_{hp,\,cool} \cdot RTF_{hp} \tag{17}$$

2.1.2 Heating Operation

Heating operation model uses a similar formulation to the cooling mode although there is a subtle difference in the heating performance characteristics. Unlike cooling, the heating operation may involve frost formation on the outdoor coil. The impact of defrost is included in Eq-18, which represents the available heating capacity. When there is no frost the multipliers for defrosting correction are set to 1.0.

$$\dot{Q}_{hp,\,total,heat} = \dot{Q}_{heat,\,total,\,ref} \cdot CAPFT_{hp,\,heat} \cdot CR_{heat,\,correction} \cdot HeatCapFrac_{defrost} \tag{18}$$

Heating electric-power input is given by:

$$P_{hp,\,heat} = \left(\frac{\dot{Q}_{heat,\,total,\,ref}}{COP_{heat,\,ref}} \right) \cdot CAPFT_{hp,\,heat} \cdot EIRFT_{hp,\,heat} \cdot EIRFPLR_{hp,\,heat} \cdot RTF_{hp} \cdot HeatPowFrac_{defrost} \tag{19}$$

2.2 VRF Indoor Coil Model

The capacity of a DX cooling coil is primarily a function of entering air wet-bulb temperature. The outdoor conditions can also affect coil performance but are more predominant in single-speed compression systems. Since a variable-speed compressor can change speed to compensate for variations in outdoor weather, the VRF coil model is assumed to be primarily affected by indoor wet-bulb temperature (Eq-20). If additional information is available that allows the coil performance to be a function of both the indoor wet-bulb and outdoor unit coil entering air temperature, a bi-quadratic form of the equation may be used (Eq-21).

$$CAPFT_{coil,\,cool} = a + b \cdot T_{wb,\,ID} + c \cdot T^{2}_{wb,\,ID} + d \cdot T^{3}_{wb,\,ID} \quad \text{- or} \tag{20}$$

$$CAPFT_{coil,\,cool} = a + b \cdot T_{wb,\,ID} + c \cdot T_{wb,\,ID}^2 + d \cdot T_{db,\,OD} + e \cdot T_{db,\,OD}^2 + f \cdot T_{wb,\,ID} \cdot T_{db,\,OD} \quad (21)$$

The capacity as a function of flow fraction (CAPFF) defined in Eq-23 modifies the cooling coil capacity for changes in supply air flow rates from a reference air flow rate. Given a range of flow fractions (Eq-22), the capacity as a function of flow fraction (CAPFF) equation coefficients may be calculated (Eq-24). The total available cooling capacity is then calculated as shown in Eq-25.

$$ff_i = flow\ fraction = \left(\frac{\dot{m}_i}{\dot{m}_{ref,\,i}} \right) \quad (22)$$

$$CAPFF_{coil,\,cool} = \frac{\dot{Q}_{coil,\,cool}\left(T_{wb,\,ID,\,ref}, T_{db,\,OD,\,ref},\ ff_i\right)}{\dot{Q}_{hp,\,cool,\,ref}} \quad (23)$$

$$CAPFF_{coil,\,cool,\,i} = a + b \cdot ff_i + c \cdot ff_i^2 + d \cdot ff_i^3 \quad (24)$$

$$\dot{Q}_{coil,\,i,\,cool} = \dot{Q}_{coil,\,i,\,ref} \cdot CAPFT_{coil,\,i,\,cool} \cdot CAPFF_{coil,\,i,\,cool} \quad (25)$$

VRF heating coil model calculations are nearly identical to those described for the VRF cooling coil. The only difference is that the heating coil has only a sensible component, and the sensible heat ratio (SHR) is always 1. The model uses the existing single-speed DX heating coil model in EnergyPlus as described in the EnergyPlus engineering reference (U.S. Department of Energy, 2011).

2.3 Summary and Discussion

The EnergyPlus VRF HP computer model is an empirical equation-fit model based on manufacturer's performance data. This performance curve based VRF heat pump computer model has been verified against manufacturers data. The verification confirmed that the model is as good as the accuracy of the performance curves.

3. Verification of the VRF Heat Pump Computer Model in EnergyPlus

3.1 Introduction

Verification and validation of computer models are equally essential to the development of the model. The objective of this task was to verify the equation-fit EnergyPlus VRF heat pump computer model by comparing to published manufacturer's performance data at full and part-load operation over a wide range of indoor and outdoor air conditions. A more detailed description of the verification methodology and results are described in the Task 3 final report (Nigusse and Raustad, 2012). The EnergyPlus VRF heat pump computer model is a semi-empirical model represented by several equation fit performance curves. For each combination of indoor and outdoor coils entering air temperatures and part-load-ratio (*PLR*), these performance curves modify the rated performance values to determine performance at off-rated condition. The VRF-system model illustrated in Figure 3-1 describes the indoor and outdoor coils inputs and outputs relationships.

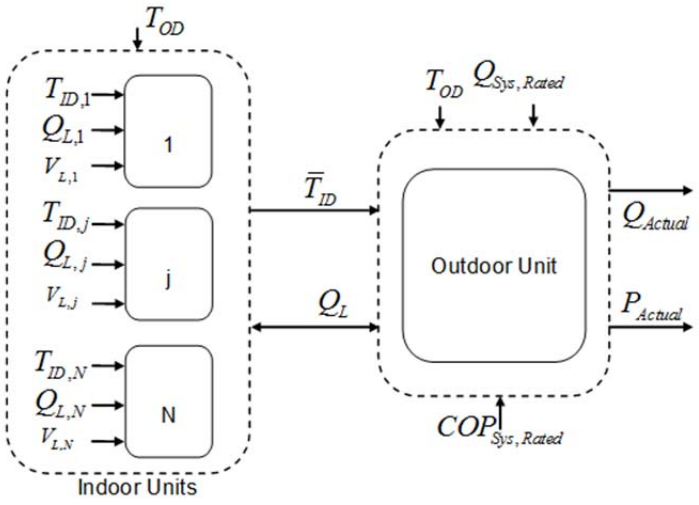

Figure 3-1 VRF DX Coils Input – Output Relationships Representation

The indoor coil model is an extension of the DX coil model that exists in EnergyPlus (Raustad, 2013). The general formulation of the indoor and outdoor coil model is described in Chapter 2. The details of the VRF heat pump computer model verification against manufacturer's data are documented by Nigusse and Raustad (2012; 2013).

3.2 Manufacturer's Data

VRF manufacturers commonly publish performance data that allows establishing the following functional relationships: (1) full-load capacity and electric power as a function of indoor and outdoor coil entering air temperatures, and (2) the system capacity and electric power as a function of *PLR*. The

manufacturers data was regressed against temperature and *PLR* to dual range performance curves; the dual range represents low and high operating ranges (Raustad, 2012). The various performance curves required by the EnergyPlus VRF system model and the coefficients of the curves generated using generalized least square regression technique are published in Task 3 final report (Nigusse and Raustad, 2012). The rated performance parameters of the model used for this verification are provided in Table 3-1.

Table 3-1 System rated performance data of a VRF heat pump model

System Parameter Model Description	Input Value
Rated heating capacity, kW (kBtu/hr)	35.20 (120.0)
Rated heating *COP,* - (Btu/W-hr)	3.55 (12.11)
Rated cooling capacity, W (kBtu/hr)	31.7 (108.0)
Rated cooling *COP,* - (Btu/W-hr)	3.25 (11.09)

3.3 Verification Methodology

The verification compares the system capacity and system electric power at full and part-load conditions. Three data were compared: the EnergyPlus VRF computer model output, a spreadsheet calculation, and manufacturer's data. The EnergyPlus Output is the capacity delivered and electric power input report variables of the EnergyPlus VRF heat pump model at full-load condition[1] normalized using Eq-26 and Eq-27 for various combinations of indoor and outdoor coils entering air temperatures.

$$\overline{Q} = \dot{Q}_{hp,\,full} / \dot{Q}_{ref} \tag{26}$$

$$\overline{P} = P_{hp,\,full} / P_{ref} \tag{27}$$

The spreadsheet calculation uses performance curve values evaluated at the same set of indoor and outdoor coil entering air temperatures as used by the EnergyPlus computer model. The normalized capacity and electric power for the spreadsheet calculation at full load were determined by Eq-28 and Eq-29:

$$\overline{Q} = CAPFT_{hp}\left(\overline{T}_{ID}, T_{OD}\right) \tag{28}$$

$$\overline{P} = CAPFT_{hp}\left(\overline{T}_{ID}, T_{OD}\right) \cdot EIRFT_{hp}\left(\overline{T}_{ID}, T_{OD}\right) \tag{29}$$

The normalized values of the EnergyPlus outputs are expected to exactly match the spreadsheet calculated value if the model is implemented correctly. The VRF heat pump model code was debugged

[1] Full-load condition refers to the condition when the VRF system is operating at full capacity .i.e., when the *PLR* and *RTF* are 1.0 for any given indoor and outdoor coil entering air temperatures.

and corrected line-by-line until the EnergyPlus output matched the spreadsheet values exactly. Thus, the EnergyPlus model output is expected to be as accurate as the performance curves.

3.4 Building and Test Conditions

The VRF heat pump model performance was evaluated in a light weight single-story 61.0 m^2 (6556 ft^2) commercial building with five conditioned zones and a plenum zone. The building has four perimeter zones and one core zone. Each zone has its own thermostat and is served by a single indoor terminal unit. The building description, construction, thermostat settings, internal gain, and infiltration levels used for verification are published in Task 3 final report (Nigusse and Raustad, 2012). The model was simulated using Chicago TMY3 weather during heating operation and Miami, Florida TMY3 weather during cooling operation. Besides the internal gains, various levels of heating and cooling plug loads were used such that the system operates above the minimum operating *PLR* for the different thermostat set points examined under a wide range of heating and cooling outdoor conditions.

3.5 Heating Performance

Figure 3-2 shows the results for heating mode operation normalized heating capacity of the EnergyPlus output, the spreadsheet calculation and the corresponding manufacturer's data for a set of constant indoor coil entering air average dry-bulb temperature. The EnergyPlus output shows exact match to the spreadsheet calculation and a good match to the manufacturer data. Since the VRF heat pump model was tested within the range of temperatures used to create the performance curves, the model accuracy is bound by the margin of errors found when regressing the heating capacity performance curves as shown in Table 3-2.

Table 3-2 Error of normalized heating capacity, EIR and electric power curves

Parameter	Maximum Under prediction error, %	Maximum Over prediction error, %	MPE, %	RMSE
Normalized Capacity	-0.94	0.98	-0.00059	0.003865
Normalized EIR	-3.59	3.88	0.00590	0.015816
Normalized Power	-3.41	3.97	0.00644	0.014566
Number of data points	70			

Figure 3-3 shows the results for the EnergyPlus heating mode output and the manufacturer's normalized heating electric power data for a wide range of outdoor air wet-bulb temperatures and a set of constant indoor coil entering air average dry-bulb temperatures. The full-load predicted normalized heating electric power closely matches the manufacturer's data and is bound by the margin of errors found when regressing the heating electric power performance curves. Manufacturer's provide a power ratio which is then used to create the electric energy input ratio performance curves. This leads to a slight error when converting power input ratio to energy input ratio, and back to power as shown in Figure 3-3.

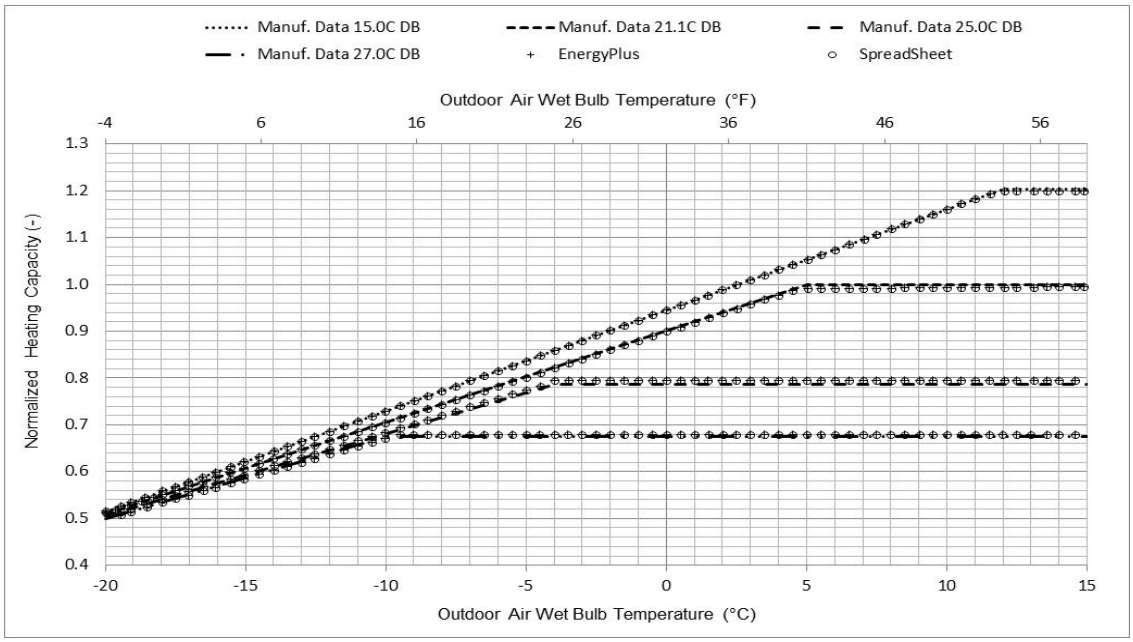

Figure 3-2 Full load normalized heating capacity as a function of temperature

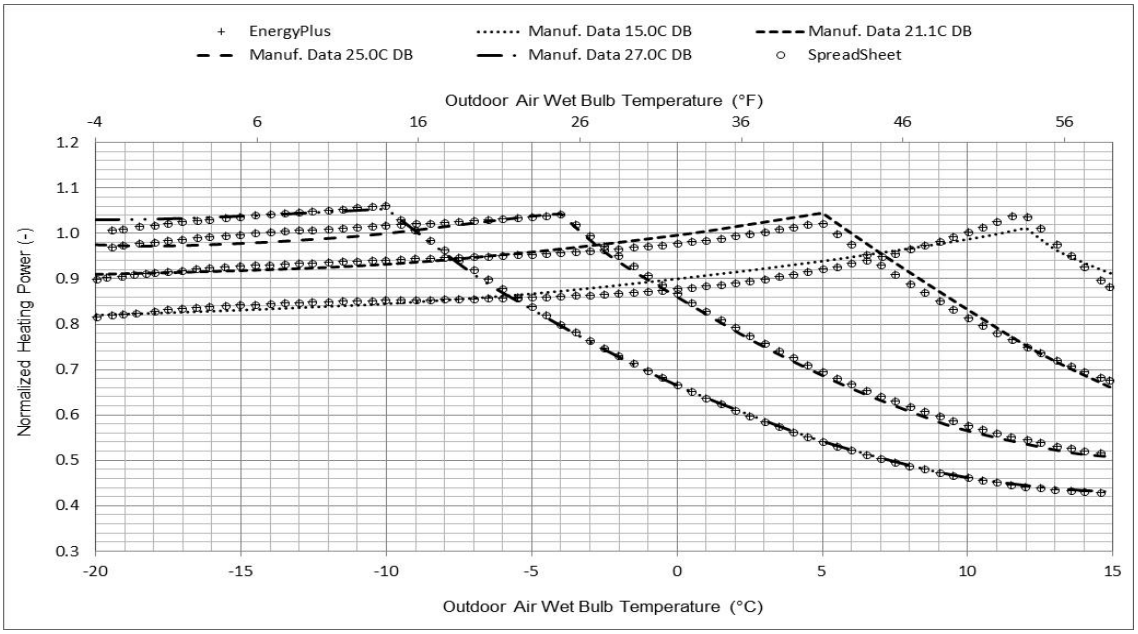

Figure 3-3 Full load normalized heating electric power as a function of temperature

The part-load performance of the VRF heat pump model was investigated to quantify the model prediction compared to the manufacturer's data over wide range of operating part-load ratios. The maximum percent error observed for heating capacity is -0.9% and is within the *CAPFT* bi-quadratic curve error margin provided in Table 3-2. The predicted heating electric power at 21.1°C(70.0°F)/6.1°C(43.0°F)

deviates from the rated value by as high as -2.90% for reasons previously mentioned (i.e., conversion of power input ratio to EIR). The system performance for the off-rated operating conditions follows the trend of the rated system performance but is somewhat offset depending on the coils entering air temperatures.

3.6 Cooling Performance

In cooling operating mode the performance curves use indoor air wet-bulb temperature as one of the independent variables. This wet-bulb temperature is not controlled directly hence it was manually varied the during simulation runs. For this reason, the simulated outputs that were within ±0.02°C/0.04°F and ±0.21°C/0.38°F of the nominal indoor air wet-bulb temperatures were selectively mined for full-load and part-load performance verification. Figure 3-4 and Figure 3-5 show the results for cooling mode normalized cooling capacity and normalized electric power at full load condition. Since the EnergyPlus output and the spreadsheet calculation values match exactly, it is concluded that the EnergyPlus output is bound by the error margins of the normalized cooling capacity performance curves given in Table 3-3.

Table 3-3 Error of normalized cooling capacity, EIR and electric power curves

Parameter	Maximum Under prediction Error, %	Maximum Over prediction Error, %	MPE, %	RMSE
Normalized Capacity	-1.34	1.10	0.0018	0.002863
Normalized EIR	-1.67	1.60	0.0003	0.006017
Normalized Power	-0.85	0.87	0.0005	0.003028
Number of data points				78

The VRF system part-load performance during cooling operation was also compared to the manufacturer's data over a wide range of cooling part-load operation. The predicted cooling capacity for coil entering temperatures of 19.4°C/35.0°C (67.0°F/95.0°F), which is the rated condition, shows a good match to the manufacturer data in spite of the slight variation of indoor coil entering air wet-bulb temperature. As a result of this wet-bulb temperature variation the predicted cooling capacity error ranges from 0.15% to 3.87% and the latter is not within the cooling *CAPFT* bi-quadratic curve prediction error margins. Correcting the predicted cooling capacity for coil entering air wet-bulb temperature variation brought the prediction error in the range 0.64% - 0.72% which is within the *CAPFT* curve error margin given in Table 3-3.

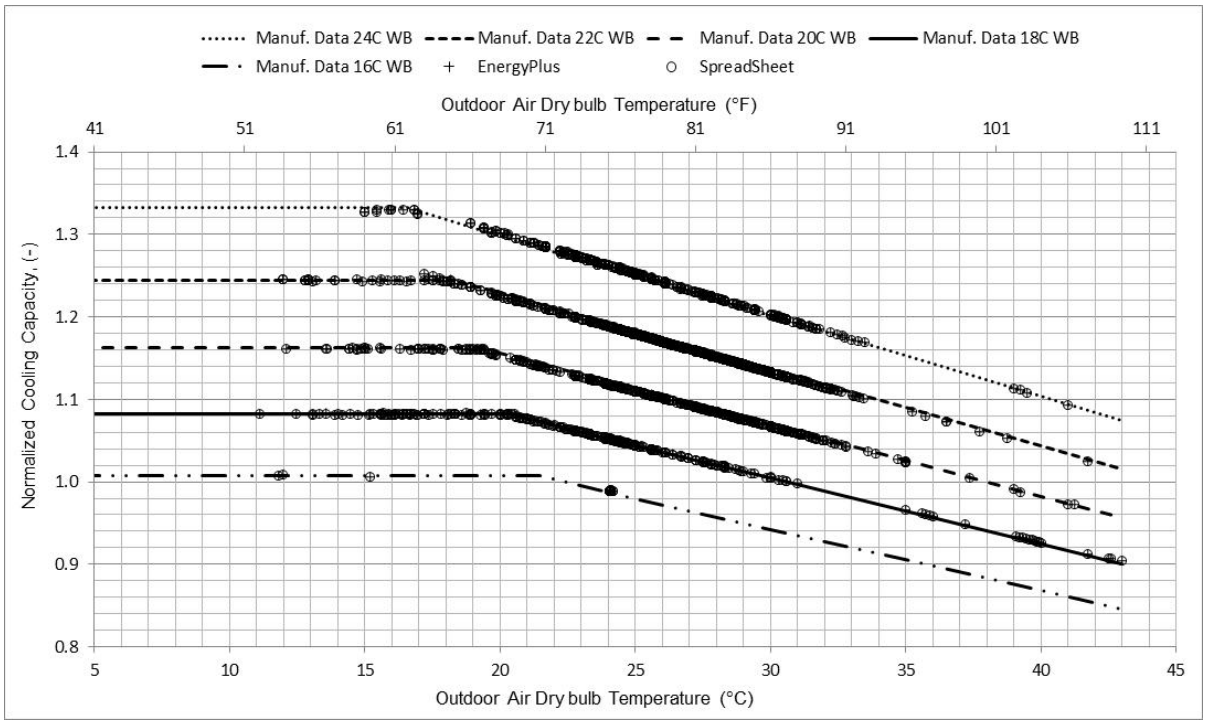

Figure 3-4 Normalized cooling capacity as a function of temperature

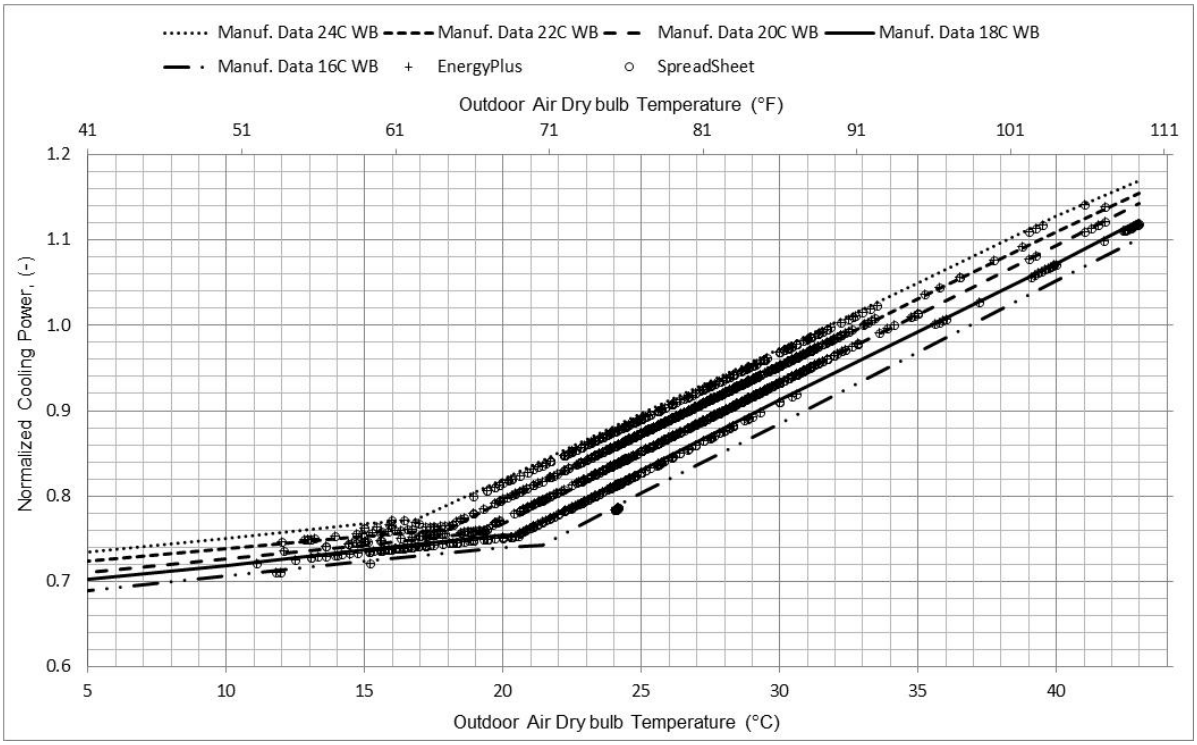

Figure 3-5 Normalized cooling electric power as a function of temperature

Similarly, the predicted cooling electric power nominal coil entering temperatures of 19.4°C/35.0°C (67.0°F/95.0°F), deviates from the rated values in the range from 0.59% to 1.85%. Correcting the predicted cooling electric power for coil entering air wet-bulb temperature variation brought down the prediction error in the range 0.73% - 0.79%, which is within the margin of error of the electric power prediction. The cooling capacities and cooling electric power inputs at off-rated conditions are expected to be bound by cooling capacity and electric power performance curve error margins. These verification results demonstrate that the VRF computer model predicts capacity and electric input within the error of margins of the performance curves hence the model is as accurate as the performance curves, which are typically generated from manufacturers data.

3.7 Conclusion

The EnergyPlus VRF heat pump computer model in cooling-only and heating-only operating modes was verified. In general, the VRF heat pump computer model can predict the capacity and electric power of the manufacturer's performance data within the margins of error found during the regression of capacity and electric power performance curves; hence the EnergyPlus VRF model is as good as the accuracy of the performance data from which the curves are generated. These verification results, therefore, demonstrate that the VRF system can be represented with a black box model, and can predict with an accuracy range similar to packaged and split system HVAC computer models that are commonly found in energy simulation programs. The model assumes that the manufacturer's performance information generally reflects the operation of the VRF system. The verification results based a sample manufacturers data can be summarized as follows:

- The heating capacity is predicted within error margins -0.94% and 0.98%. The heating electric power is predicted within error margins of -3.31% and 3.97%. The heating performance was investigated for an indoor condition range of 15°C to 27°C (59°F to 80.6°F) dry-bulb temperature and an outdoor condition range of -20°C to 15°C (-4.0°F to 59°F) wet-bulb temperature.
- The cooling capacity is predicted within error of margins of -1.34% and 1.10%. The cooling electric power is predicted within error margins of -0.85% and 0.87%. The cooling performance was investigated for an indoor condition range of 16°C to 24°C (60.8°F to 75.2°F) wet-bulb temperature and an outdoor condition range of 11°C to 43°C (51.8°F to 109.4°F) dry-bulb temperature.
- The VRF system part-load performance also shows good match to the manufacturer's data. However, the simulated system capacity ratio was used as a surrogate for the manufacturer's combination ratio since part-load performance data for VRF systems is not published.

4. Independent Lab Testing of Two VRF Systems

4.1 Introduction

This task, which was conducted by the Electric Power Research Institute (EPRI) with assistance from UCF/FSEC, provides a first-of-its-kind third-party analysis and performance characterization of VRF multi-zone heat pump and heat recovery systems. The laboratory-developed performance map will serve as an initial independent reference data set for VRF systems. EPRI's overall effort in performance characterization for VRF heat pump and heat recovery systems was funded by three parties, the Department of Energy (DOE) as a sub-contract through UCF/FSEC, and through Southern California Edison (SCE) and Bonneville Power Administration (BPA) in complementary projects. A more detailed description of the test facility setup, data acquisition system, and data recording are described in the Task 4 final report (Raustad, 2012a).

4.2 Test Stand Design and Testing Methods

A novel setup to test multi-split systems was developed as a part of this project at the EPRI test facility. A duct based test setup was used to condition air entering each of the four indoor units. Each duct supplies specific amounts of conditioned air to the return-air intake of the indoor terminal unit. This setup allows each indoor unit to encounter different temperature and humidity conditions. The range of conditions under which the VRF systems are tested are sufficient to characterize heating and cooling capacity and power use profiles under expected operating conditions. The initial range of tests were determined by the model development requirements as defined by FSEC. Outdoor air temperatures will generally range from 70˚F to 105˚F for cooling operation and 10˚F to 60˚F for heating operation. Within this range of conditions, the typical rating conditions as defined by standards such as AHRI 1230 or AHRI 210/240 were tested as a subset. In heat recovery operation, the outdoor air temperature range is 55˚F to 85˚F. These ranges are expanded or adjusted according to available time and needs as occurred over the course of testing. Two VRF-HR units from different manufacturers were tested in this project. One test unit has a three pipe heat recovery setup (LG Electronics) while the other has a two pipe heat recovery setup (Mitsubishi). Detailed descriptions of these tests can be found in the Task 4 final report (Raustad, 2012a).

The general approach is to control relevant air-side parameters while collecting output performance data at discreet points of steady-state operation. The primary metrics include system power consumption and zonal heating and cooling capacity delivered by the VRF system. The method of test was to set the thermostat set point temperature very low for cooling and very high for heating. This was originally thought to provide the maximum available capacity. In general, the measured operating capacity using this method resulted in lower cooling capacity at a higher power consumption than reported by all manufacturers. Heating results did not seem to be affected by this choice of test methodology.

Manufacturers also stated that this test methodology would not accurately measure performance of VRF systems. Near the end of the project, an alternate test method was developed to better represent VRF system performance as if field installed. This method of test is preliminarily call the Load Based Method of Test where the load is fixed and the indoor conditions and unit operation are allowed to fluctuate. This test method was only briefly attempted in a laboratory setting but does show promise for future lab testing.

General testing for performance mapping fell into 3 general categories: cooling only mode, heating only mode, and heat recovery mode. Both cooling and heating mode tests feature four levels of load to the system, 100% (all four units on), 75% (1 indoor unit off), 50% load (2 indoor units off) and 25% load (3 indoor units off). The thermostat of each indoor unit was set at the lowest or highest possible set point for cooling and heating, respectively. This method of test is not specified in AHRI 1230 and was used here to better represent full-load system operation in the field. The return air supplied to the terminal units were kept at a constant temperature (typically 75°F, 80°F or 85°F for cooling and 65°F, 70°F or 75°F for heating) for any given test. In compliance with ANSI/AHRI Standard 1230, the outdoor unit operated at the manufacturer's specifications, allowing the unit to reach its natural steady-state fan speed as determined by the VRF control system. The percentage of indoor units (% IDU) operating was observed in cooling and heating mode to gain an understanding of the capacity delivered and power consumed in conditions where one or more indoor units were turned off. Situations at less than 100% IDU operation is a frequent occurrence in real world installations which can affect system efficiency and performance characteristics. Since AHRI standard 1230 only requires full-load performance data at 100% IDU operation, this task presents a unique data set for capacity delivered and power consumed in conditions where one or more of the indoor units were turned off.

In heat recovery mode, instead of turning indoor units off, the terminal units were operated either in heating or cooling mode. For example, two units were forced to operate in cooling mode and two units were forced to operate in heating mode. The AHRI simultaneous cooling and heating (SCH) test condition has a set outdoor condition of 47°F DBT and 43°F WBT. The number of units in cooling or heating mode is varied to capture the performance characteristics of the system. Similar to the cooling-only and heating-only data, this data set is one-of-a-kind since the manufacturers only publish data at one point. Alternate tests were also performed. For example, one VRF system was allowed to operate with only 3 IDU's in cooling mode. After steady-state operation was achieved, the 4th IDU was turned on in heating mode. This allowed measurement of the change in cooling side performance as well as overall system power. This specific test was helpful in developing the heat recovery operating mode computer model.

The following tests were conducted by EPRI personnel specifically for this portion of the project.

4.2.1 System A – LG Electronics VRF-HR

A 3-pipe variable refrigerant flow heat recovery system manufactured by LG Electronics was tested as a part of laboratory performance mapping of VRF systems. The tested unit has a Sync II outdoor unit

from LG's Multi V family of VRF systems matched with four ducted low static indoor units and a heat recovery unit. Initial testing showed a lower measured cooling capacity than reported by the manufacturer. A physical inspection of indoor units showed that the coil is wet on the lower portion of the coil and very dry on the upper portion. Proper distribution of refrigerant would result in a fully-wetted coil. Additional instrumentation was installed to understand this low capacity and potential refrigerant mal-distribution problem in the IDU, indicating refrigerant or air mal-distribution in the IDU hindering heat transfer from the air stream to the refrigerant. These results were shared with the manufacturer and the manufacturer visited the laboratory. This issue was not resolved and the terminal units were replaced. A similar issue with low capacity prevailed and it was decided that testing would move forward with a new system from a different manufacturer. It was later deduced that the test method was mostly responsible for these low capacity measurements, however, this system was never reinstalled in the laboratory for additional testing due to time constraints.

4.2.1.1 Effect of Outdoor Dry-Bulb Temperature in Cooling Mode

Figure 4-1 shows the capacity measurements with varying outdoor dry-bulb temperature (OD-DBT) from the manufacturer as well as laboratory measurements from EPRI. Both the manufacturer and EPRI lab data is plotted at a fixed return air wet-bulb temperature (RA-WBT) of 67°F. The manufacturer does not provide performance data for varying RA-DBT. The EPRI lab data includes RA-DBTs of 75°F, 80°F, and 85°F. As previously discussed, the measured capacity of the system was less than the manufacturer's data for all data points and is likely a result of the chosen method of test, although the overall trend in capacity followed that of the manufacturer published data trend.

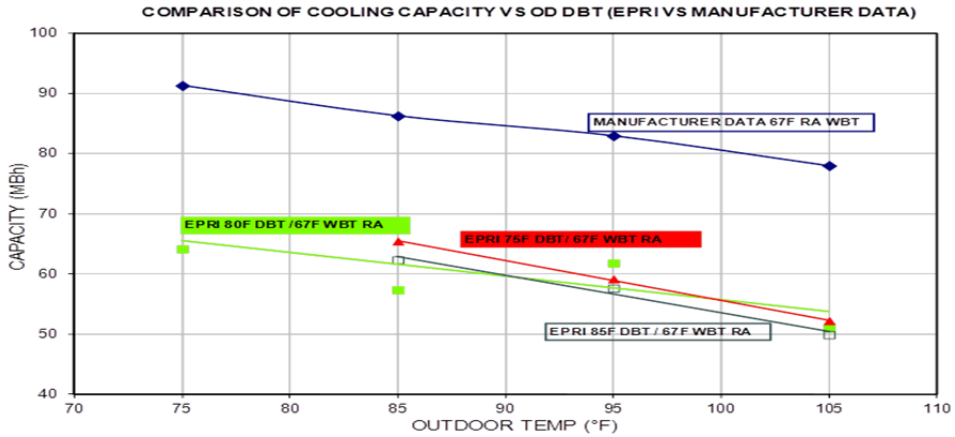

Figure 4-1 LG: Cooling Capacity: Varying OD-DBT, Varying RA–DBT

Figure 4-2 shows the measured power for the same data set shown in Figure 4-1. The laboratory measured power data points were higher by more than 90% compared to the manufacturer's published data, while the overall trend in power is similar to the published data. The method of test is the probable cause for this difference. As the outdoor temperature increases, the power draw increases. The RA-DBT has minimal effect on the power draw, which is evident from the closely grouped data points for each OD-

DBT. This findings further confirm that the capacity is a strong function of RA-WBT and explain the manufacturer's capacity tables, which do not refer to the RA-DBT. At this time, the higher power consumption is believed to be primarily a result of the test method selected for these tests. Future testing with alternative test methods (e.g., using a load based method of test) may prove or disprove these findings.

4.2.1.2 EER Measurements in Cooling Mode

Figure 4-3 shows the effect of OD-DBT on the system energy efficiency ratio (EER). EER is the ratio of delivered capacity to the energy consumption rate. The predicted EER was about 2.5 times lower than the manufacturer's published values because of the lower measured capacity and higher measured power draw. Note the previous discussion of test methodology before making any concluding arguments regarding performance. The overall trend in the EER is very similar to the published performance. From Figure 4-3 we can conclude that the EER is a strong function of OD-DBT and does not vary much with RA-DBT.

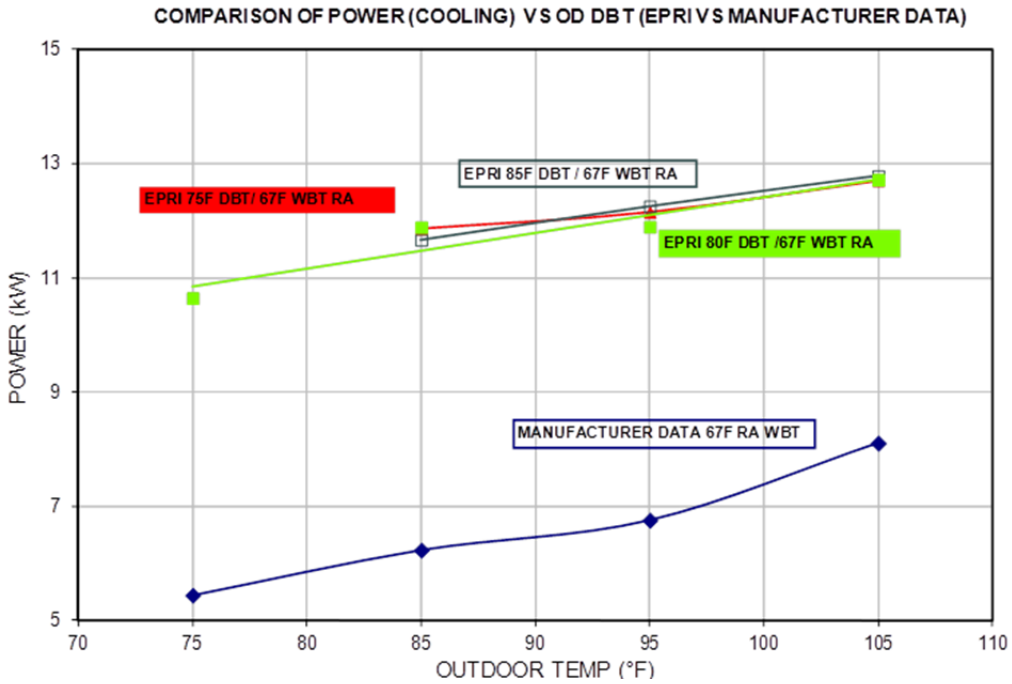

Figure 4-2 LG: Power Cooling Mode: Varying OD-DBT, Varying RA-DBT

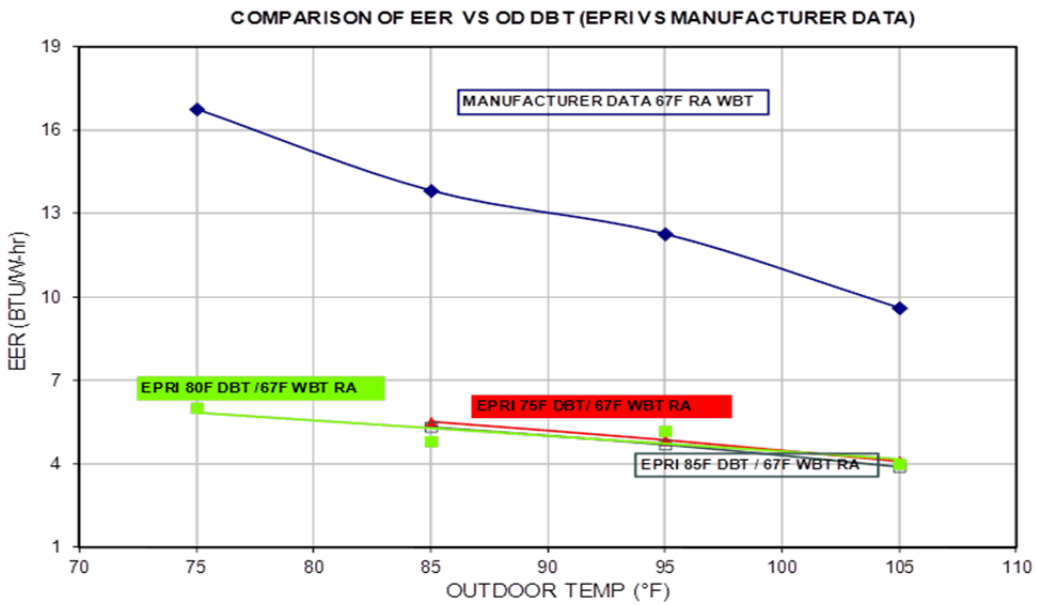

Figure 4-3 LG: EER Cooling Mode: Varying OD-DBT, Varying RA–DBT

4.2.1.3 Percent Indoor Units Running in Cooling Mode

In a multizone system, one or more zones might not require conditioning. The laboratory test results for the system operating with four, three, two, and one indoor units calling for cooling are shown in Figure 4-4. After steady-state operation is reached on all four units, one indoor unit is turned off and the other three indoor units are kept running at the same conditions. Once steady state is reached on the three indoor units, another indoor unit is shut off, and so on. The corresponding steps in percentage IDU running are 100%, 75%, 50%, and 25%.

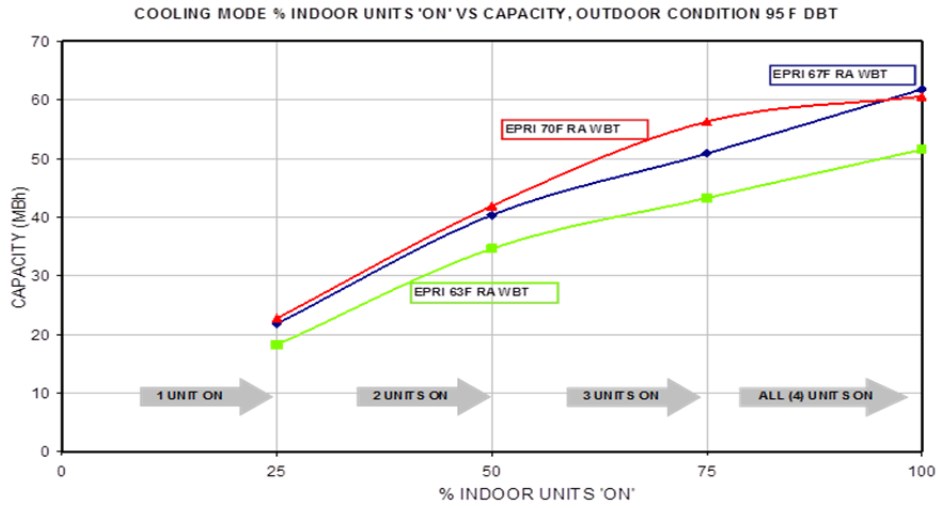

Figure 4-4 LG: Measured Cooling Capacity versus Percent of Operating Indoor Units

4.2.1.4 Effect of Outdoor Dry Bulb Temperature in Heating Mode

Figure 4-5 shows capacity measured by EPRI and manufacturers published values against varying outdoor dry-bulb temperature (DBT). The data at 70°F return air temperature (RAT or indoor air temperature) tracks very closely with the manufacturer published data. The manufacturer's data at 64°F matches very closely to the manufacturer's 70°F data. These data are almost coincidental. In a fixed speed system, we expect the heating capacity to increase with a decrease in RAT but the coincident data for 64°F and 70°F from the manufacturer may be a result of internal control logic. EPRI lab data at 65°F RAT shows some increase in capacity (red data points) compared to 70°F RAT (green data points).

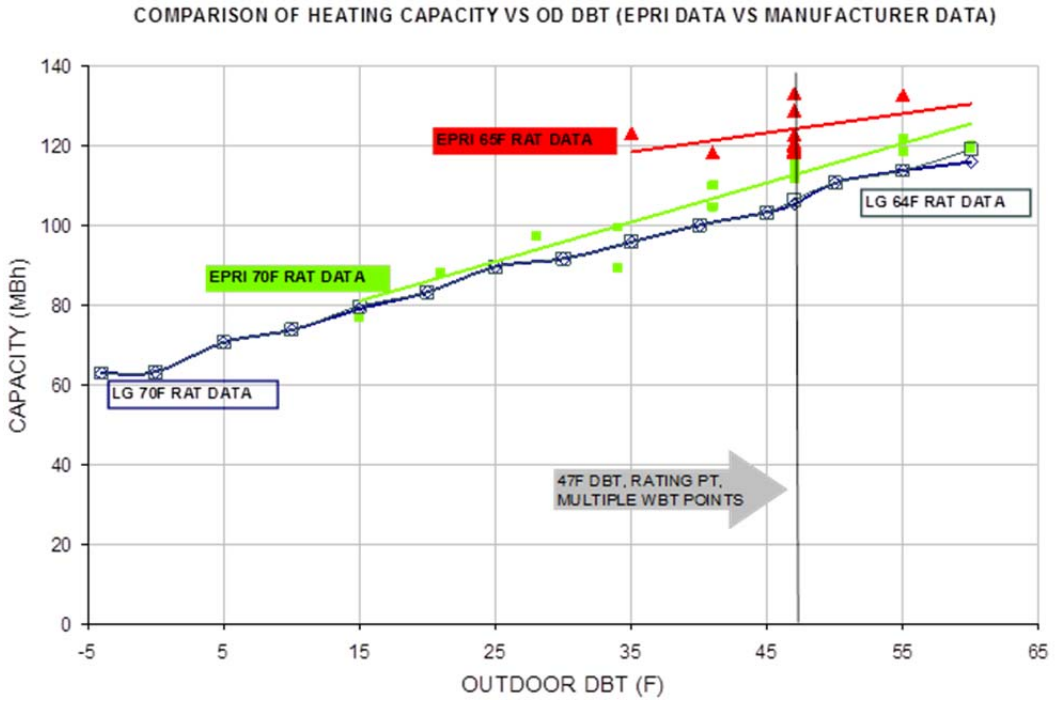

Figure 4-5 LG: Measured and Manufacturers Published Capacity in Heating Mode

Figure 4-6 shows the measured electric consumption rate for the same data set shown in Figure 4-5. The measured power is higher than that of published manufacturers data by about 3kW; however, the overall trend in power is similar to that of the manufacturers published data. Figure 4-7 shows the COP of the system as a function of the outdoor DBT. In this plot we can see that the overall trend of measured COP is very similar to the manufacturer published data. Since the measured capacity are in good agreement with the manufacturer data, the difference in measured COP and manufacturer's COP can be attributed to the chosen test methodology.

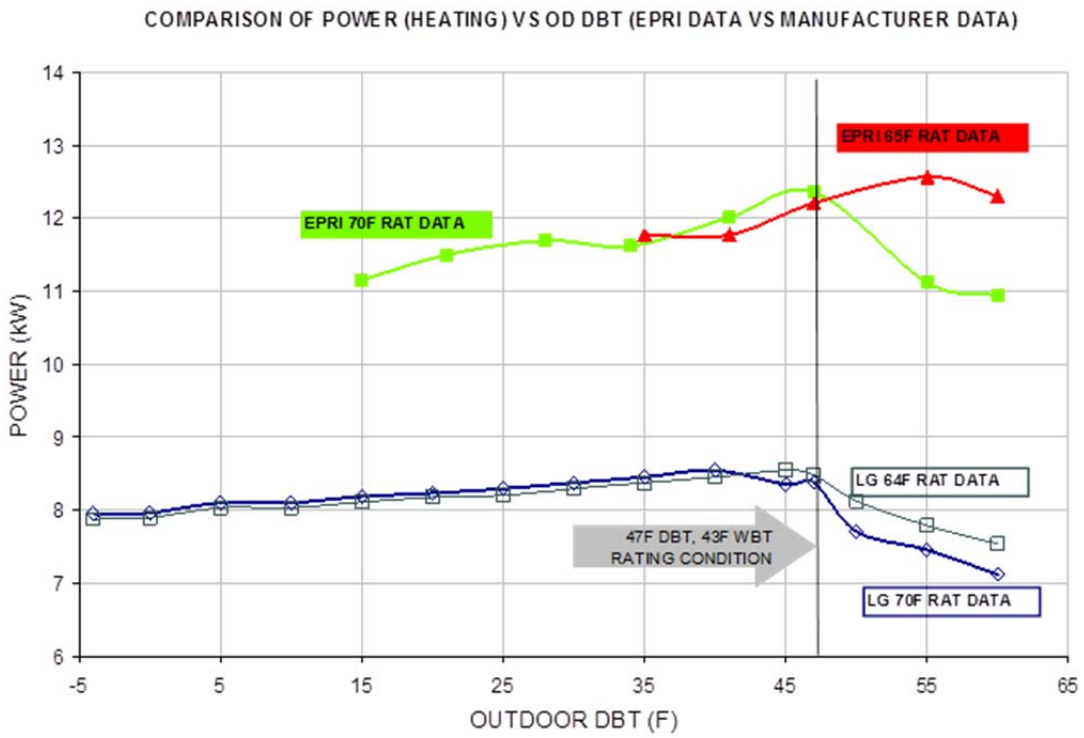

Figure 4-6 LG: Measured and Manufacturers Published Power in Heating Mode

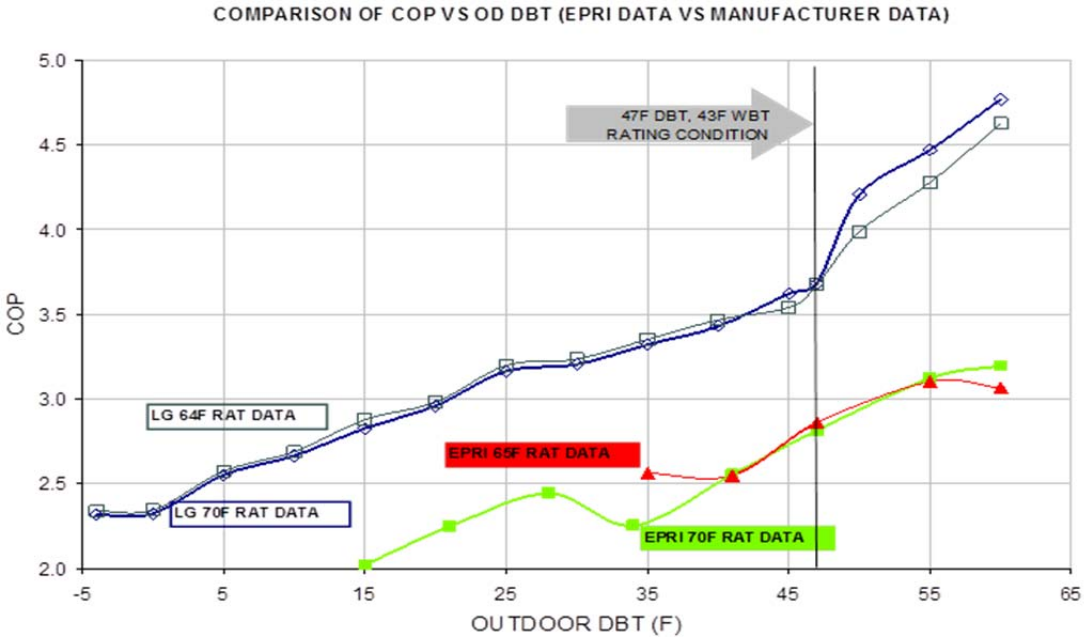

Figure 4-7 LG: Measured and Manufacturers Published COP in Heating Mode

4.2.1.5 Effect of Outdoor Wet-Bulb Temperature in Heating Mode

Outdoor wet-bulb temperature (WBT) is another outdoor parameter that was investigated in laboratory testing. The WBT entering the outdoor unit in heating mode affects the capacity only when there is condensation on the outdoor unit. For these measurements, a fixed outdoor DBT and RA-DBT are selected and the outdoor WBT varied to understand the effect.

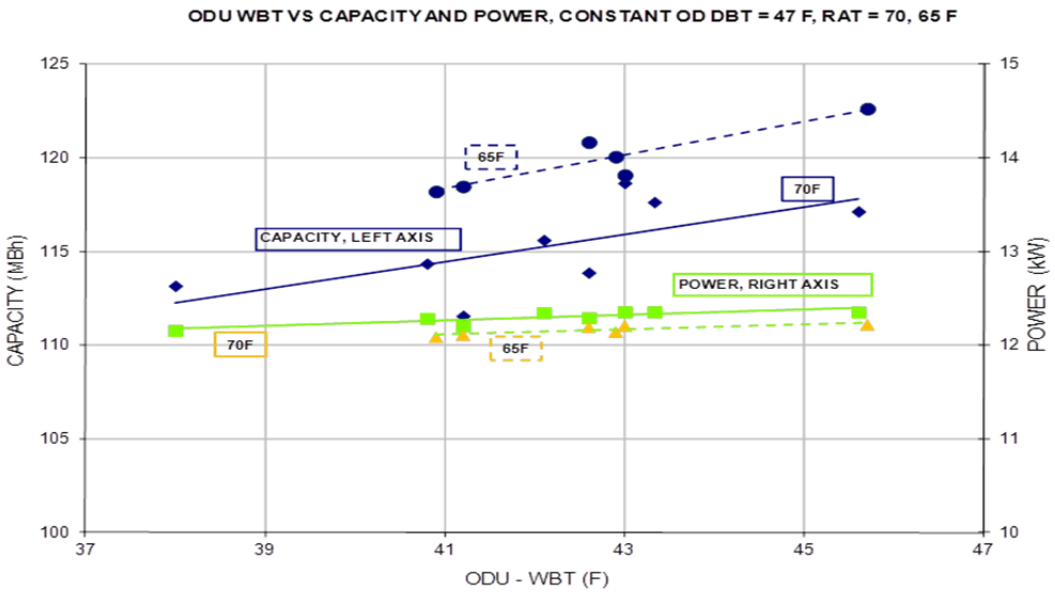

Figure 4-8 LG: Measured Capacity and Power versus Varying OD–WBT, RAT 70° & 65° F

The RAT is constant at 70°F and the outdoor DBT is constant at 47°F. The outdoor WBT is varied from 38°F to 46°F translating to RH of 41% to 91%. As shown in Figure 4-8 the power draw remains almost constant but the capacity increases slightly. At a constant outdoor temperature, the system capacity increases with increasing outdoor WBT indicating that more moisture is condensed on the outdoor unit. Although the phase change of water, from vapor to liquid, results in heat gain and hence capacity, the amount of moisture in cold air is very small. The capacity variation is relatively minor and there is minimal change in the power draw. The constant power draw across the range of WBT of 38°F to 46°F (41%RH to 91%RH) means that the unit is not reacting to the outdoor WBT in heating mode. The same analysis is extended to RAT of 65°F.

4.2.1.6 Broader Comparison of Measured Data with Manufacturers Data

The following two figures show measured heating and cooling performance along with manufacturer's published performance data. In these figures, fan power/heat was not included in the measured capacity or power data. Heating capacity reasonably matches the manufacturers published data while power measurements show much higher than reported by the manufacturer. Cooling capacity shows a lower total cooling rate than reported by the manufacturer whereas measured power is only slightly higher. The manufacturer was on-site during testing but had no explaination as to the cause of these results. It was

originally thought that this system had some hardware defect. After testing the second manufacturers VRF system, it is believed that the method of test is the reason for the differences measured in the laboratory. It was intended that the selected test method show the full-load available capacity and power consumption, however, and to be fair to manufacturers, it is probably rare that VRF systems would encounter this type of over-load condition in the field (i.e., thermostat was buried which means the VRF system's control algorithm may have responded with an unlikely control scenario). The slopes of the measured and manufacturers reported performance data do appear to be similar which means that manufacturers normalized performance information can be used to define performance of the computer model.

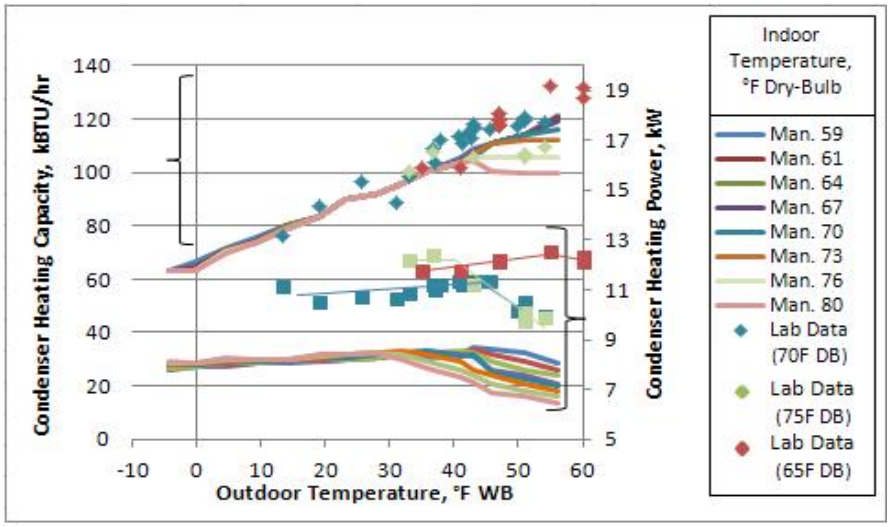

Figure 4-9 LG: Heating Mode Comparison to Manufacturers Data

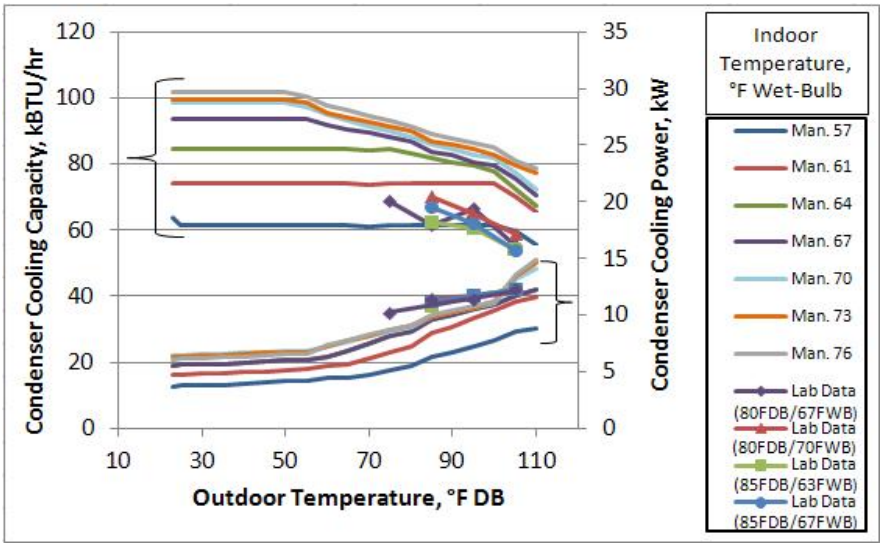

Figure 4-10 LG: Cooling Mode Comparison to Manufacturers Data

4.2.1.7 Percent of Indoor Units Running in Heating Mode

In a multi-zone system, one or more zones might not be calling for heating. Lab test results for the system operating with four, three, two and one indoor units calling for heat are shown in Figure 4-11.

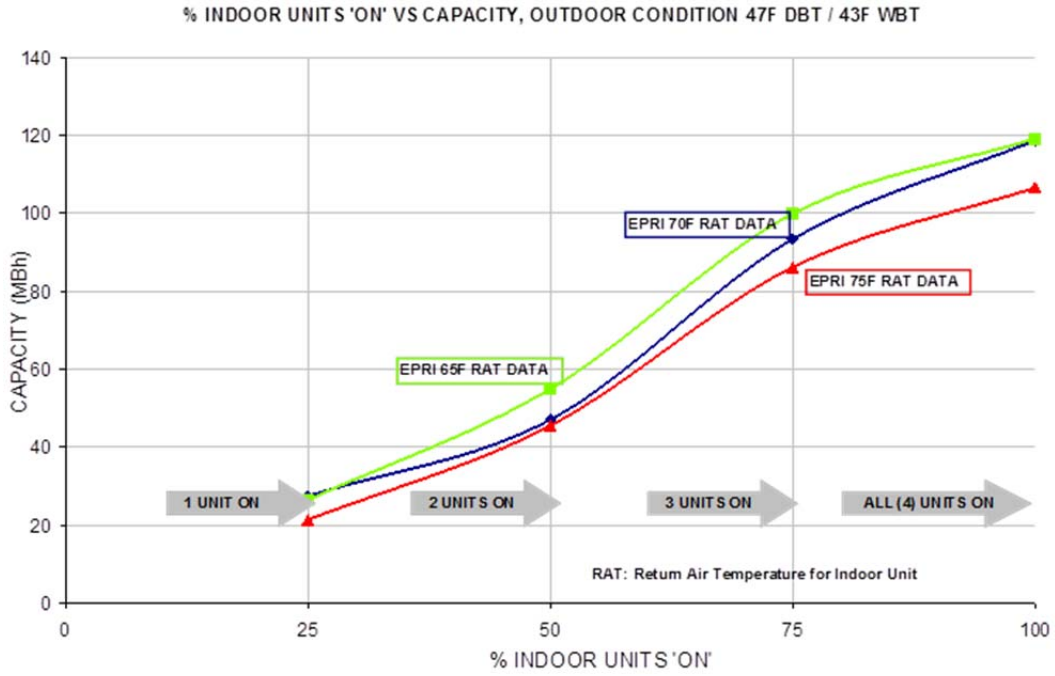

Figure 4-11 LG: Measured Capacity versus Percent Indoor Units Running

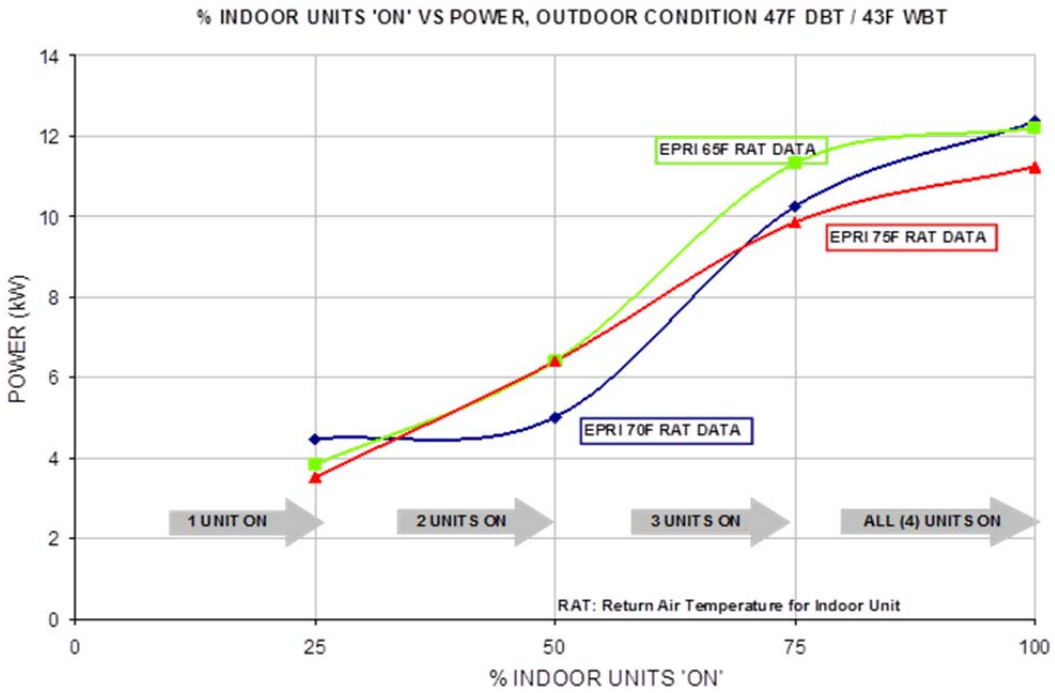

Figure 4-12 LG: Measured Power versus Percent of Operating Indoor Units

The system is operating at outdoor conditions of 47°F DBT and 43°F WBT. Figure 4-11 shows three data sets for RAT of 65°F, 70°F and 75°F. The heating capacity provided by the aggregate system decreases as units are turned 'OFF'. The power draw for the same conditions is shown in Figure 4-12. The power draw reduces as the units are turned 'OFF', but it is important to note that the power draw reduction is not in the same proportion as the reduction in capacity. The COP chart, shown in Figure 4-13 shows that the COP decreases as the units are turned 'OFF'. As previously discussed, this may be an artifact of the test methodology and further testing using alternate test methods may prove or disprove these findings.

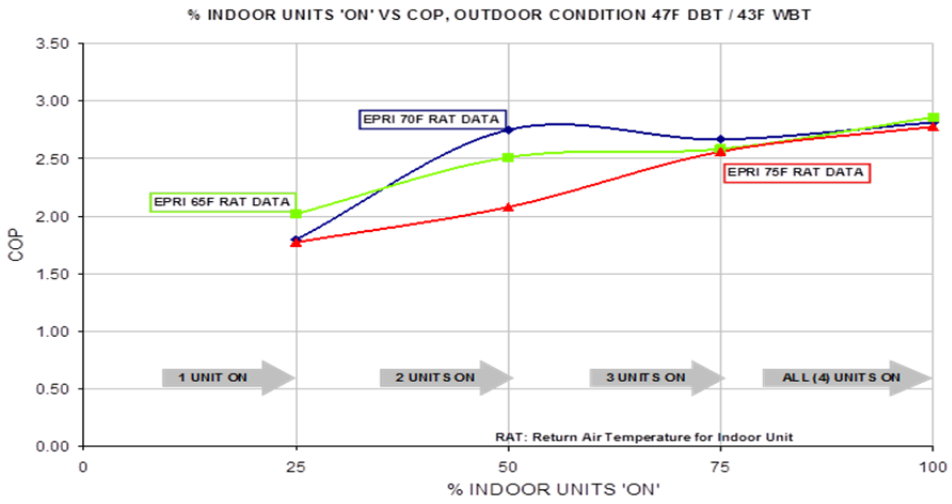

Figure 4-13 LG: Measured COP versus Percent of Operating Indoor Units

4.2.1.8 Simultaneous Cooling and Heating (SCH) Mode

Figure 4-14 shows the effect of changing modes on capacity. The OD-DBT in this case is 75°F and the RAT is at 80°F DB/ 67°F WB in cooling mode and at 70°F in heating mode.

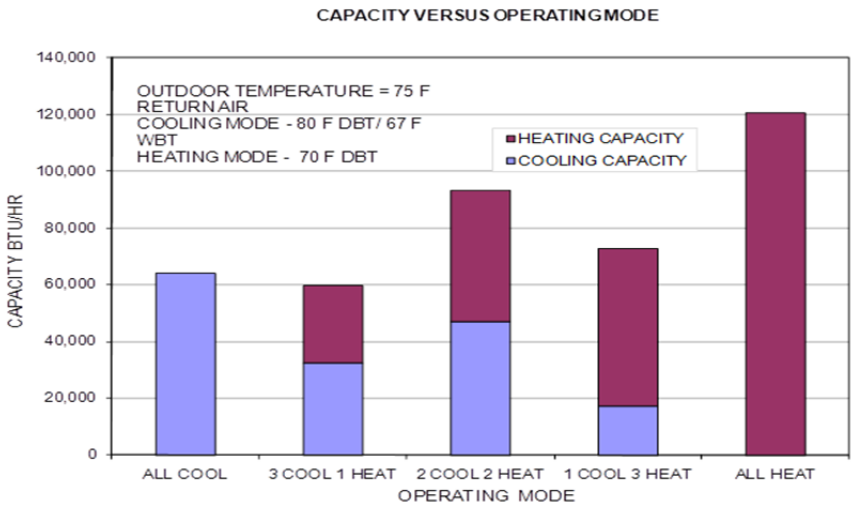

Figure 4-14 LG: Measured Capacity for Changing Operating Modes

The Measured power and EER of the system operating at various conditions is shown in Figure 4-15. The power draw is dependent on the operating mode (cooling or heating) of the outdoor unit and the number of compressors operating. An interesting point of operation is the “2 COOL–2 HEAT” mode, in which the manufacturer-provided information is insufficient to determine the operating mode of the outdoor unit. From Figure 4-15, the power draw in “2 COOL–2 HEAT” mode is more than that in “3 COOL–1 HEAT” mode and in “1 COOL–3 HEAT” mode. It is clear that both the compressors are running, but it is still not clear whether the outdoor unit is acting as a condenser or an evaporator. When analyzing the diagnostic data from EPRI instrumentation, it became clear that in this case the outdoor unit was operating in condensing mode (i.e. in cooling mode operation). This situation was evident from the liquid-line temperature, with verification from the air leaving the outdoor unit.

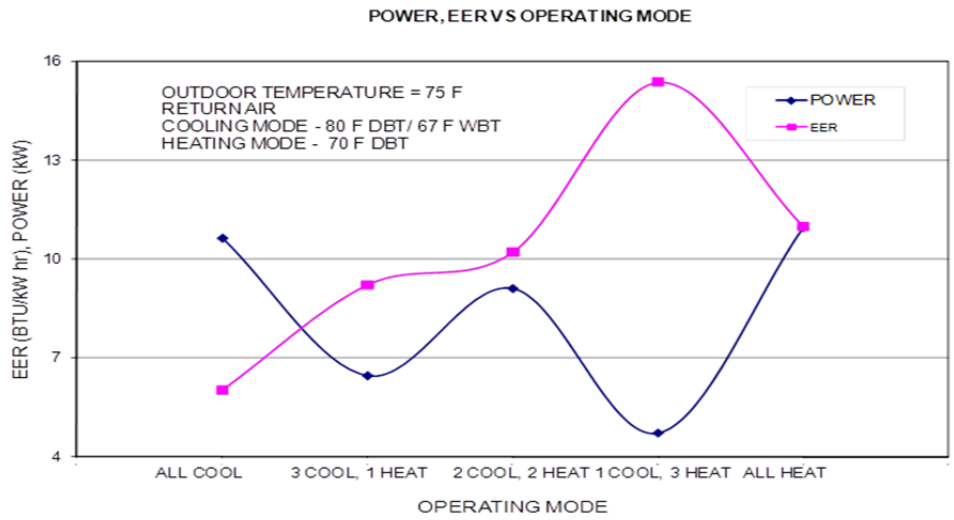

Figure 4-15 LG: Measured Power and EER for Changing Operating Modes

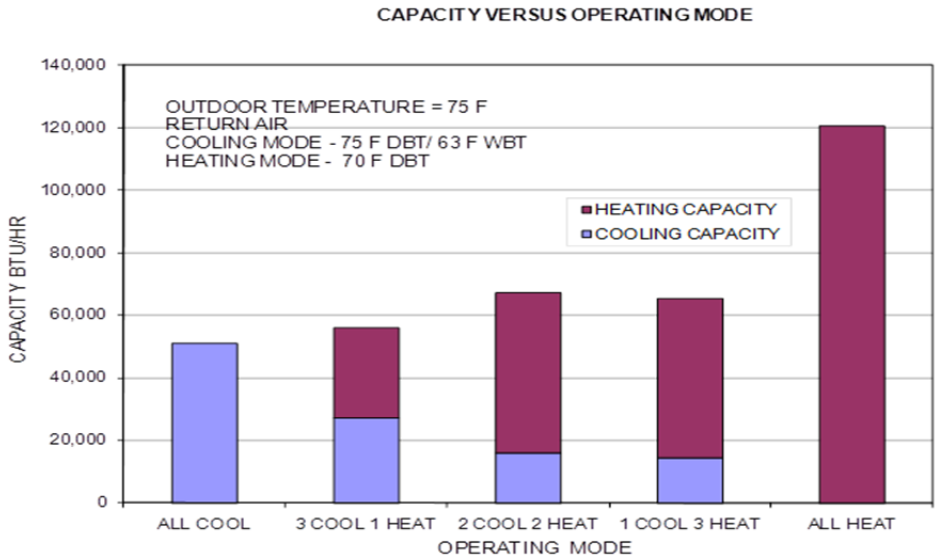

Figure 4-16 LG: Measured Capacity for Changing Operating Modes

4.2.1.9 Lower Cooling Return Air Wet and Dry Bulb Temperatures

Figure 4-17 shows measured capacity similar to the data in Figure 4-14, except that the RA conditions in cooling mode are lower, at 75°F DBT and 63°F WBT. In this case, the "2 COOL–2 HEAT" operation shows different characteristics from those seen in Figure 4-15 and Figure 4-16. The outdoor unit is running in the evaporator mode, and thus it is in the heating-based operation. The operation of the unit in this mode is very similar to the "1 COOL–3 HEAT" mode. Figure 4-15 shows the corresponding measured power draw and EER for the operating conditions shown in Figure 4-17. In the heating-based operation for "2 COOL–2 HEAT mode, only the variable-speed compressor in the outdoor unit is running, resulting in low power draw and hence an increased EER measurement.

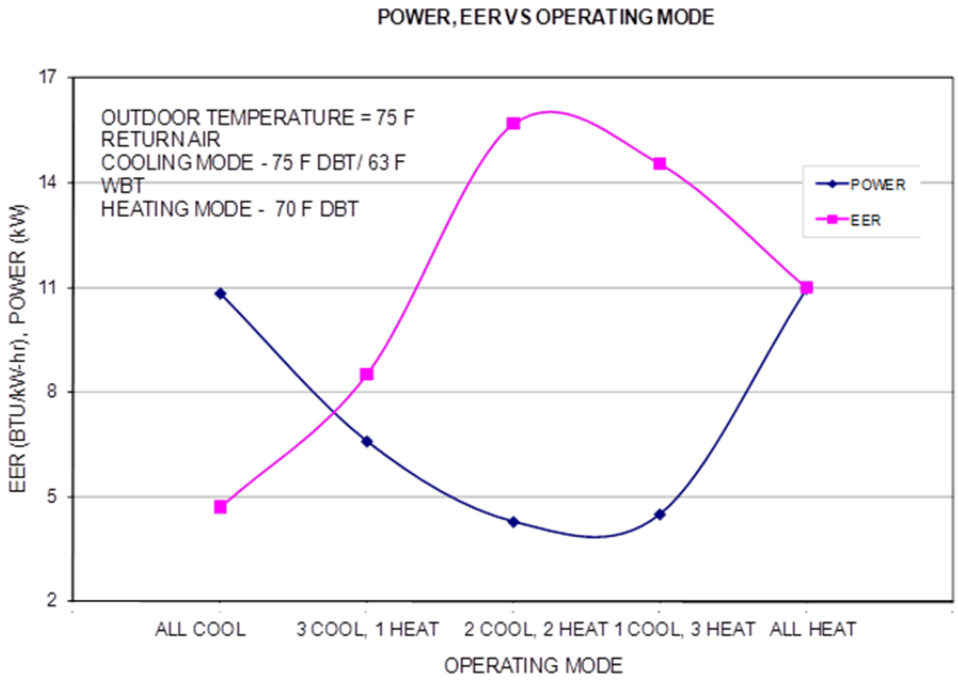

Figure 4-17 LG: Measured Power and EER for Changing Operating Modes

4.2.1.10 SCH Performance at Lower Outdoor Temperatures

Figure 4-18 and Figure 4-19 show measured capacity similar to those in Figure 4-15 and Figure 4-17, but for a lower outdoor temperature of 65°F DBT. The overall trend in capacity at 65°F is very similar to the capacity measured at 75°F. The higher capacity (Figure 4-18) when the return air is at 67°F WBT indicates that the system is in the cooling-based operation in "2 COOL–2 HEAT" mode (similar to that at 75°F OD-DBT). In Figure 4-19, the return air is at 63°F WBT and the system is in the heating-based operation.

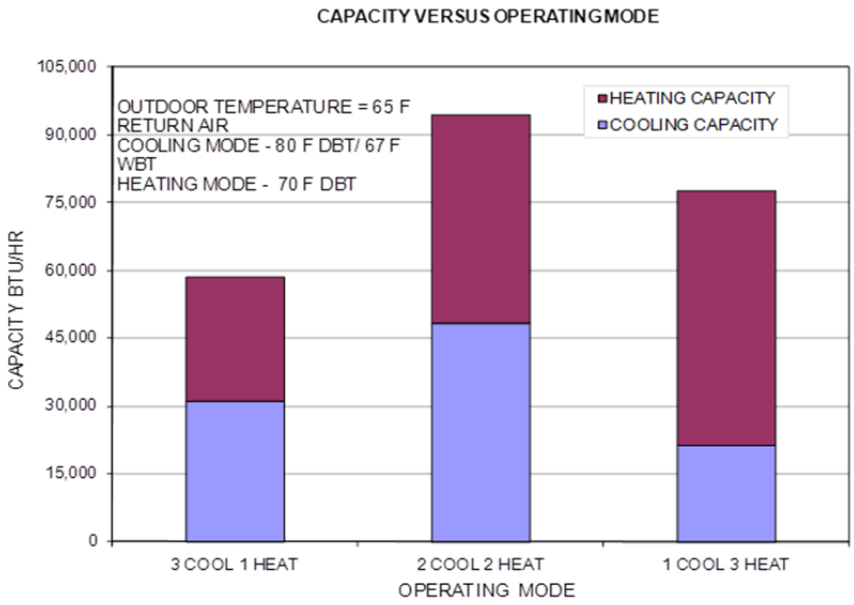

Figure 4-18 LG: Measured Capacity for Changing Operating Modes

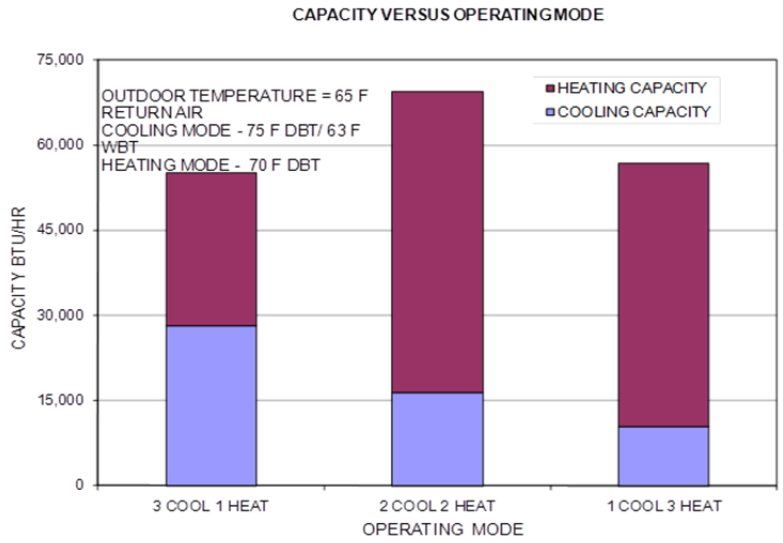

Figure 4-19 LG: Measured Capacity for Changing Operating Modes

Figure 4-20 shows a side-by-side comparison of data from 75°F OD-DBT and 65°F OD-DBT. The plots shows that the outdoor temperature does not have a significant effect on capacity. In SCH mode, the important parameter for units that are operating in cooling mode seems to be the RA-WBT. The RA-WBT effect can be seen in Figure 4-18 and Figure 4-19, in which a higher WBT (67°F) resulted in a higher cooling capacity in units operating in cooling mode. Similar results can also be seen in Figure 4-15 and Figure 4-17.

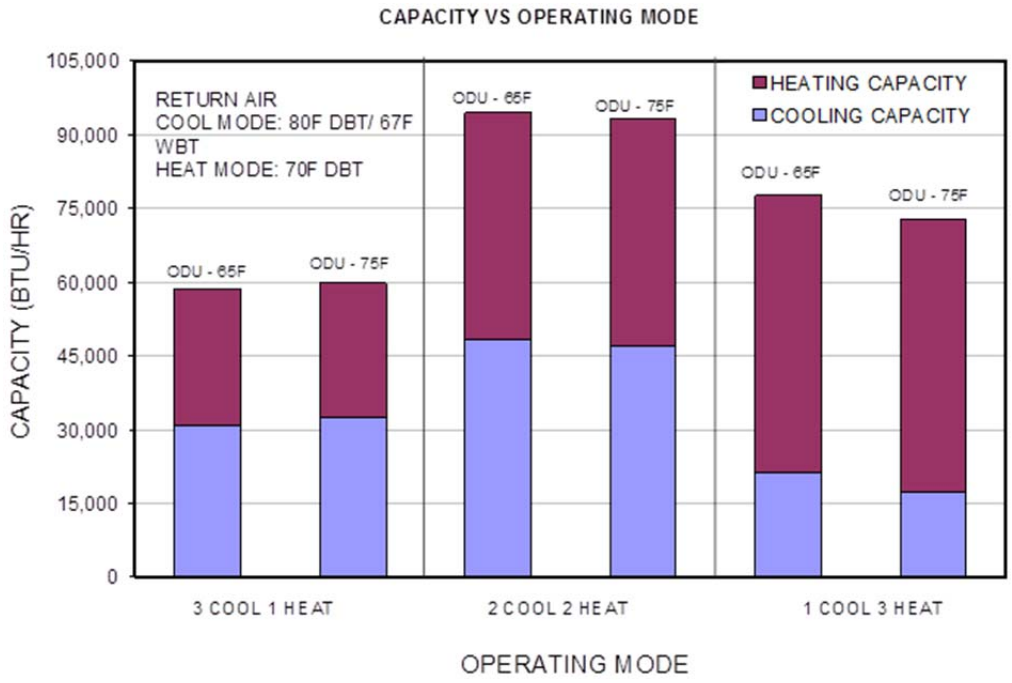

Figure 4-20 LG: Measured Capacity at 75°F and 65°F OD-DBT

4.2.2 System B – Mitsubishi VRF-HR

A 2-pipe variable refrigerant flow heat recovery system manufactured by Mitsubishi Electric was tested as a part of laboratory performance mapping of VRF systems. The tested unit has a City Multi outdoor unit matched with four ducted low static indoor units and a branch controller.

4.2.2.1 Effect of Outdoor Dry-bulb Temperature in Cooling Mode

Figure 4-21 shows total system air-side measured capacity from lab testing, along with manufacturers data at similar conditions. Data is shown for varying outdoor DBT and varying return air WBT. The return air DBT is fixed at 80°F. The manufacturer's data is calculated from capacity charts provided by the manufacturer. The manufacturer's charts and the procedure to calculate capacity and power for the system under test are available in the Task 4 final report (Raustad, 2012a). All data points show a measured capacity 25% less than the manufacturer published data, although the overall trend in capacity followed that of the manufacturer published data trend. Note here that lower measured capacity may be a direct result of the test methodology used in the laboratory.

Figure 4-22 shows the power measurements for the same conditions that are shown in Figure 4-21. The measured power are close to the manufacturers published data. The maximum difference of 10% is observed at lower return air WBT of 60°F. For all other data points the difference between measured and manufacturers published power is within 5%.

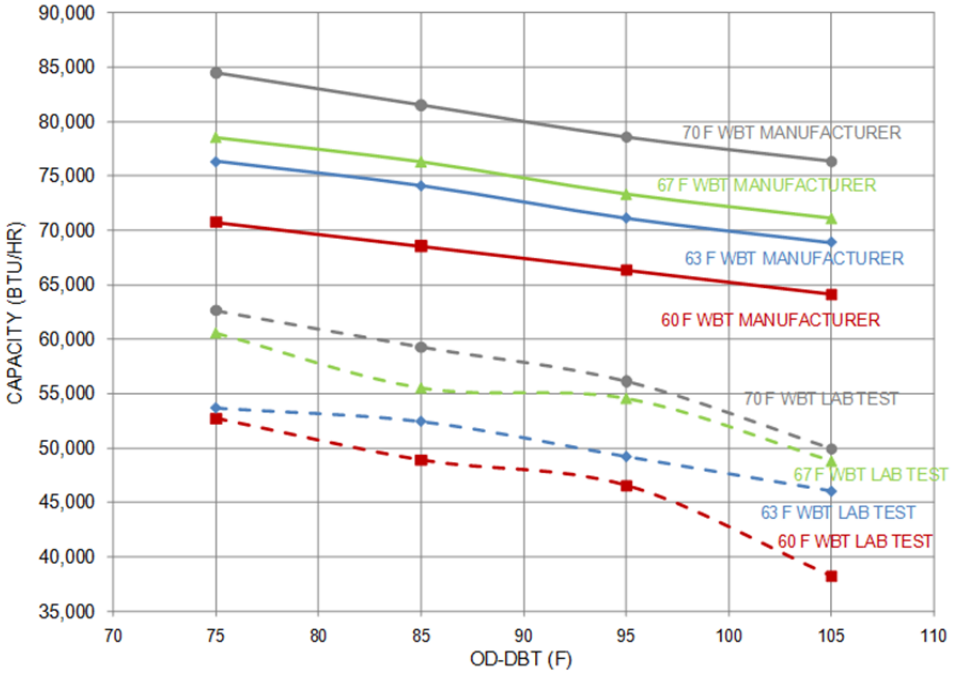

Figure 4-21 Mitsuibishi: Cooling Capacity, Varying OD-DBT and RA-WBT

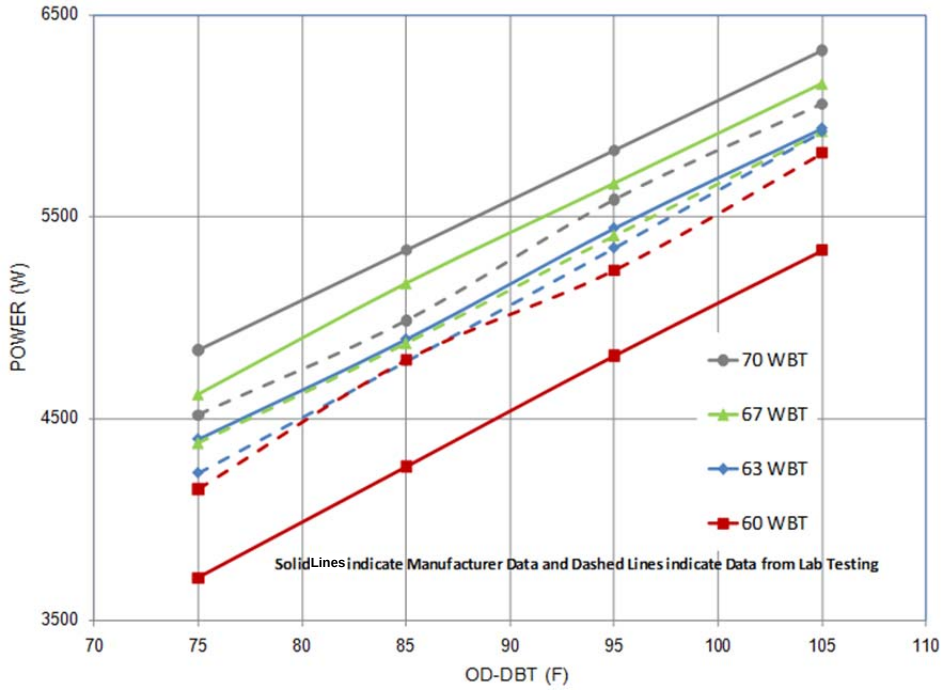

Figure 4-22 Mitsuibishi: Cooling Mode Power Draw, Varying OD-DBT and RA-WBT

4.2.2.2 Percent Indoor Units Running in Cooling Mode

The system test results for four, three, two and one indoor units in cooling mode are shown in Figure 4-23. The system was tested at an outdoor condition of 95°F DBT and 80°F RA-DBT / 67°F RA-WBT. The cooling capacity provided by the aggregate system decreases as the units are turned 'OFF'.

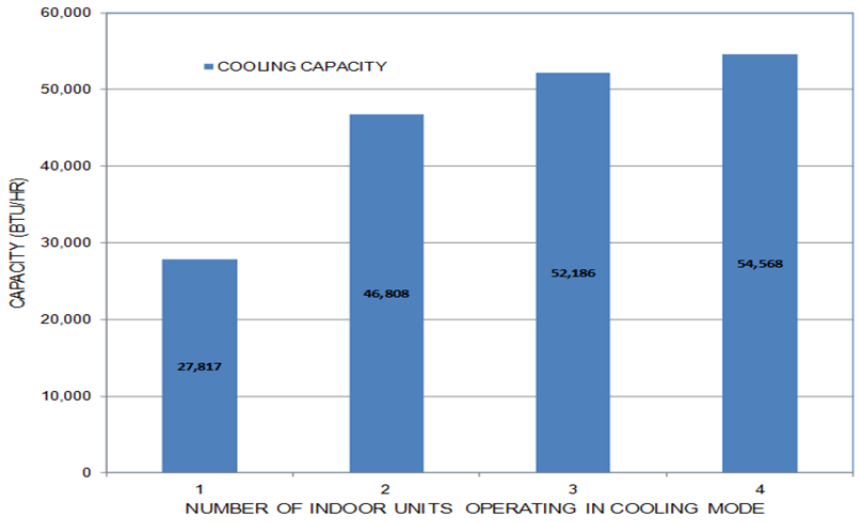

Figure 4-23 Mitsuibishi: Measured Capacity versus Number of Operating Indoor Units

During the transition from 4 to 3 to 2 units, the compressor power draw remains fairly constant until the second IDU is disabled (right to left) as shown in Figure 4-24. The operating parameter that changes during this transition is the suction pressure. The suction pressure is controlled to a set pressure of 103 psig by the system. The compressor is running full speed until only one indoor unit is calling for cooling at which point the compressor speed reduces when the required suction pressure can be attained and hence the reduction in power.

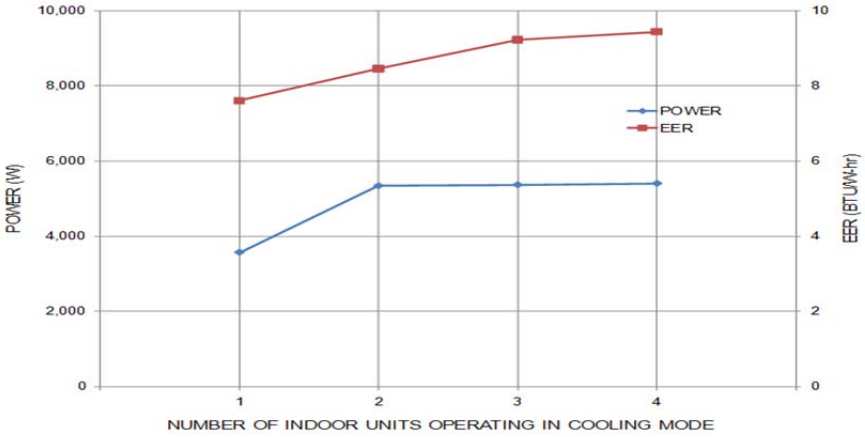

Figure 4-24 Mitsuibishi: Measured Power and EER versus Number of Operating Indoor Units

4.2.2.3 Heating Performance Mapping – Test Results

Figure 4-25 shows the heating capacity measurements at various outdoor WBT and varying indoor RAT. The lab data follows the manufacturer's trend until a certain point. In the case of 70°F RAT, the manufacturer's data shows that after a certain upper limit on the OD-WBT (37°F WBT), the capacity does not increase. However, in lab tests the capacity increased linearly with increase in OD-WBT. For the period where the capacity increases with increasing WBT, the measured data follows the trends with a 15% lower capacity. This too may be a result of the test methodology and further testing may prove or disprove these results.

Figure 4-26 and Figure 4-27 show the power draw and the COP in heating mode. The power draw trends are different from the manufacturer published data. From manufacturer's data, the power draw increases until about 38°F WBT and then decreases. The measured data shows a different characteristic in which the power draw actually decreases right around the 38°F WBT mark and then increases again as the WBT increases. The COP values are not published by the manufacturer. Figure 4-27 shows linearly increasing trend in predicted COP.

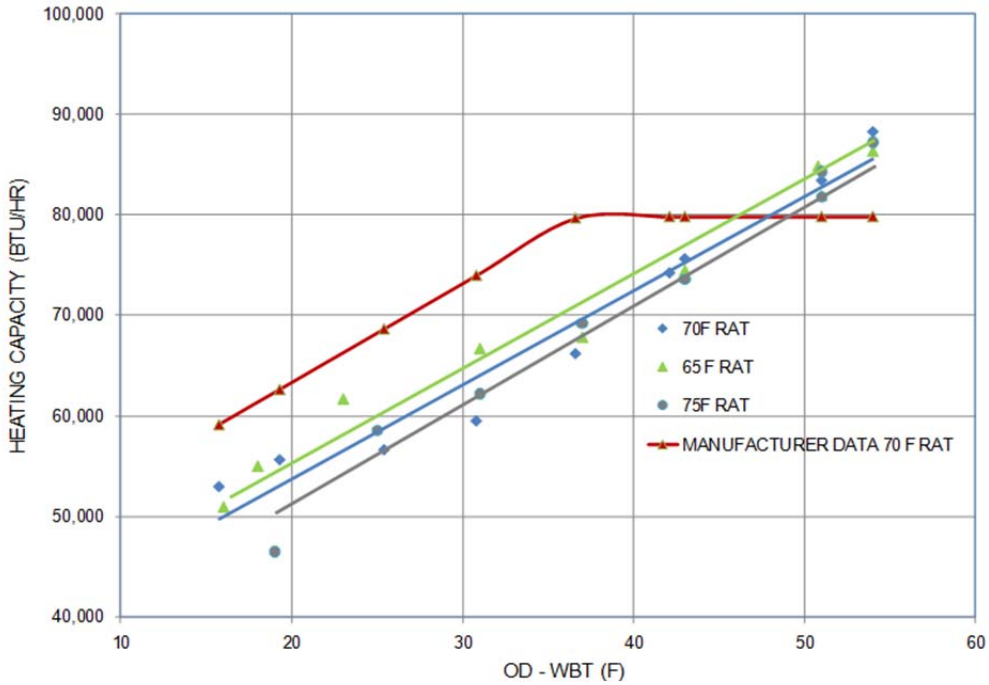

Figure 4-25 Mitsuibishi: Heating Capacity, Varying OD-WBT and RA-DBT

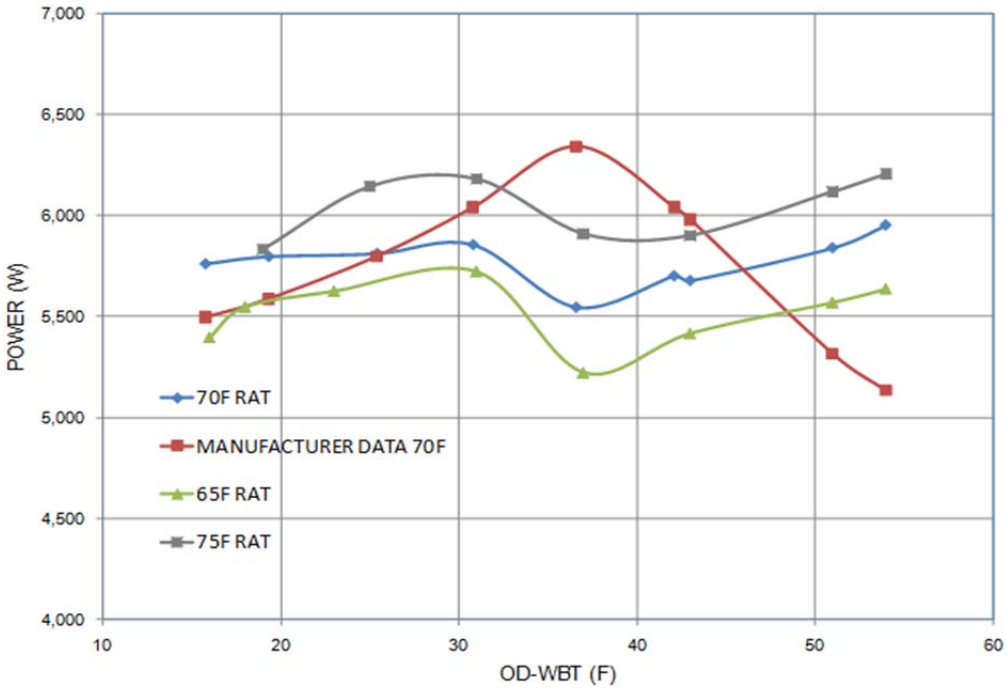

Figure 4-26 Mitsuibishi: Heating Mode Power Draw, Varying OD-WBT and RA-DBT

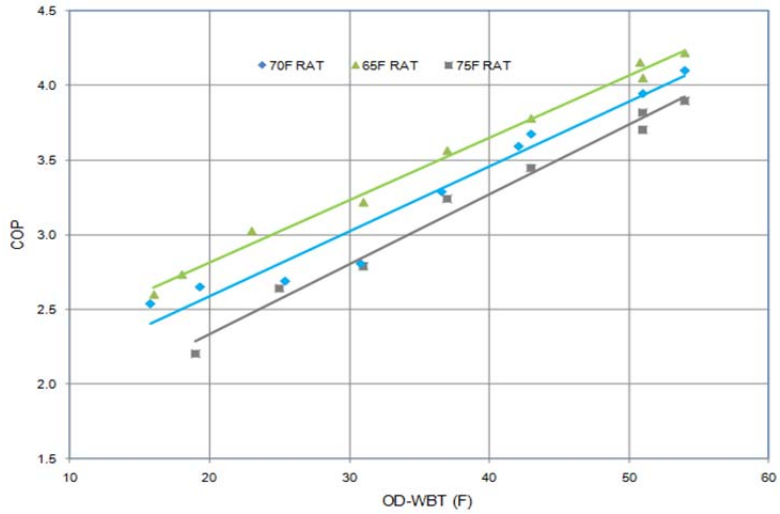

Figure 4-27 Mitsuibishi: Heating Mode COP, Varying OD-WBT and RA-DBT

4.2.2.4 Percent Indoor Units Running in Heating Mode

The systems test results for four, three, two and one indoor units in heating mode are shown in Figure 4-28. The total capacity increases with increasing number of indoor units running. The individual capacity of each unit decreases as the number of units running increases. Figure 4-29 shows the measured power and COP for the same data points as in Figure 4-28.

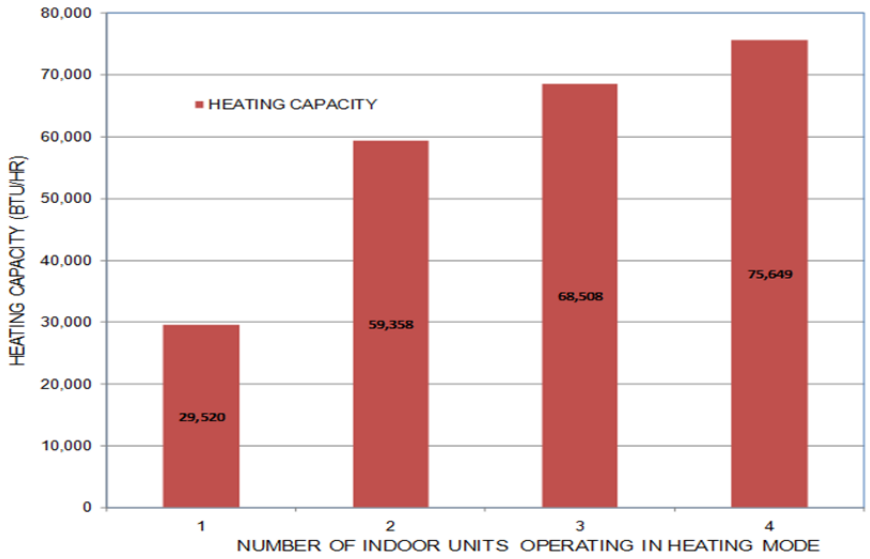

Figure 4-28 Mitsuibishi: Measured Heating Capacity Against Number of Indoor Units Running

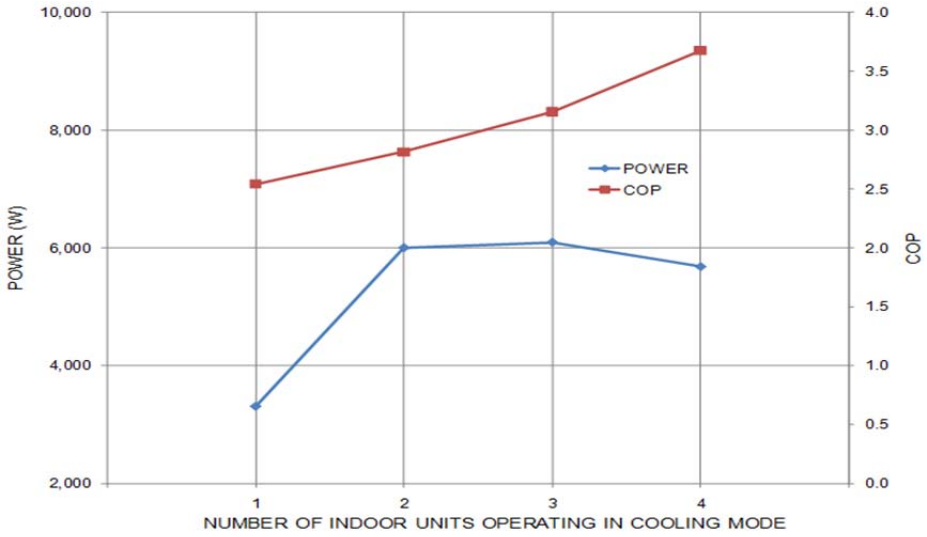

Figure 4-29 Mitsuibishi: Measured Power and COP versus Number of Operating Indoor Units

4.2.2.5 Broader Comparison of Measured Data with Manufacturers Data

The following two figures show measured heating and cooling performance (e.g. Lab in figures) along with manufacturer's published performance data (i.e., Man. in figures). In these figures, fan power/heat was not included in the measured capacity or power data. Both heating and cooling capacity are reduced compared to the manufacturers published data while power measurements show much agreement with the manufacturer's reported performance. The manufacturer was on-site during testing and suspected an issue with sensor hardware after reviewing these results. It is believed that the method of test is the reason for the differences measured in the laboratory. It was intended that the selected test

method show the full-load available capacity and power consumption, however, and to be fair to manufacturers, it is probably rare that VRF systems would encounter this type of over-load condition in the field (i.e., thermostat was buried which means the VRF system's control algorithm may have responded with an unlikely control scenario). The slopes of the measured and manufacturers reported performance data do appear to be similar except in heating mode where the capacity plateau at higher outdoor wet-bulb temperatures is never achieved. A similar difference in the slope of the power consumption in heating mode is also apparent.

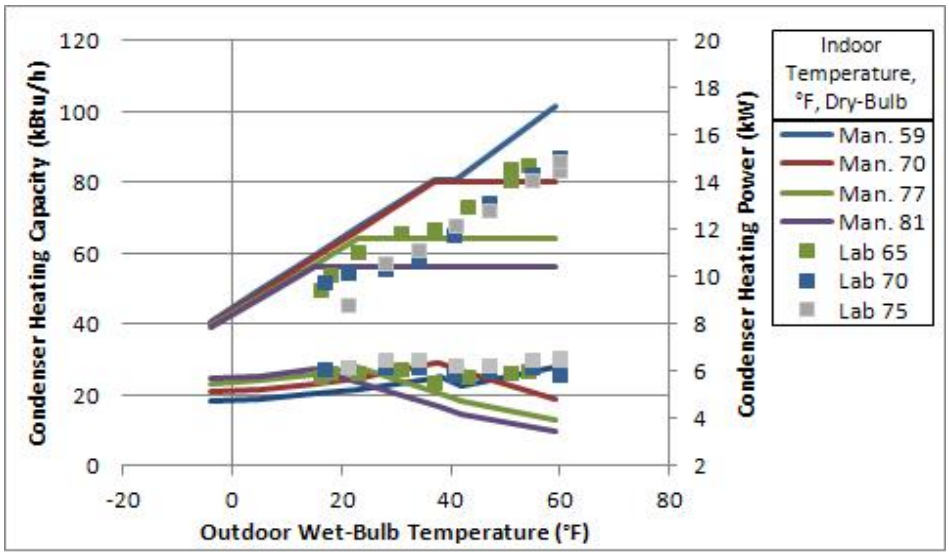

Figure 4-30 Mitsubishi: Heating Mode Comparison to Manufacturers Data

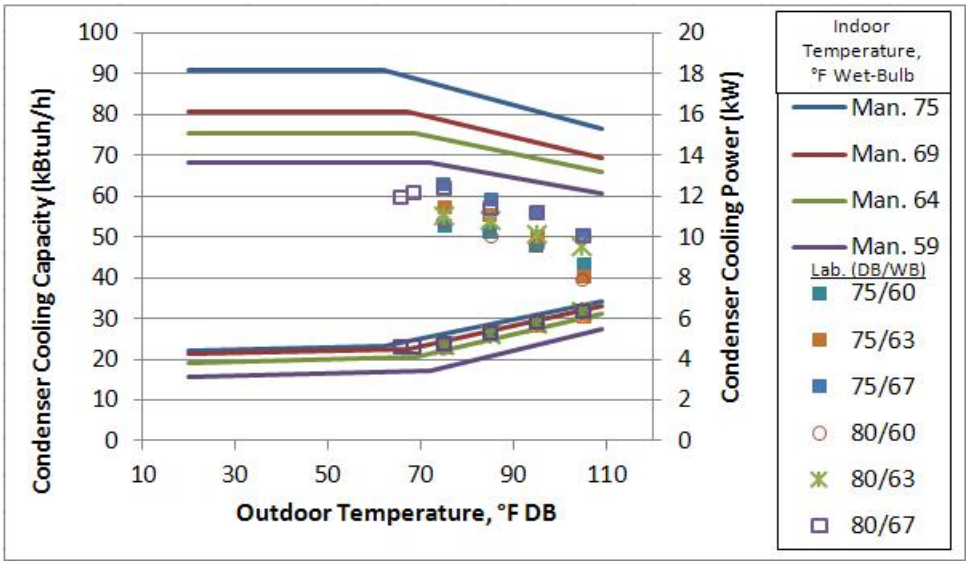

Figure 4-31 Mitsubishi: Cooling Mode Comparison to Manufacturers Data

4.2.2.6 Effect of Switching Operating Modes on Capacity and Power

Figure 4-32 shows the effect of changing modes on capacity. In the '3 COOL/1 HEAT' mode the outdoor unit runs in a cooling mode and in '1 COOL/3 HEAT' mode the outdoor unit runs in a heating mode. The plot shows that as the units are turned to heating mode, the heating capacity starts increasing and the cooling capacity starts decreasing. The data point with all 4 units in heating mode is at 60ºF outdoor temperature instead of 65ºF.

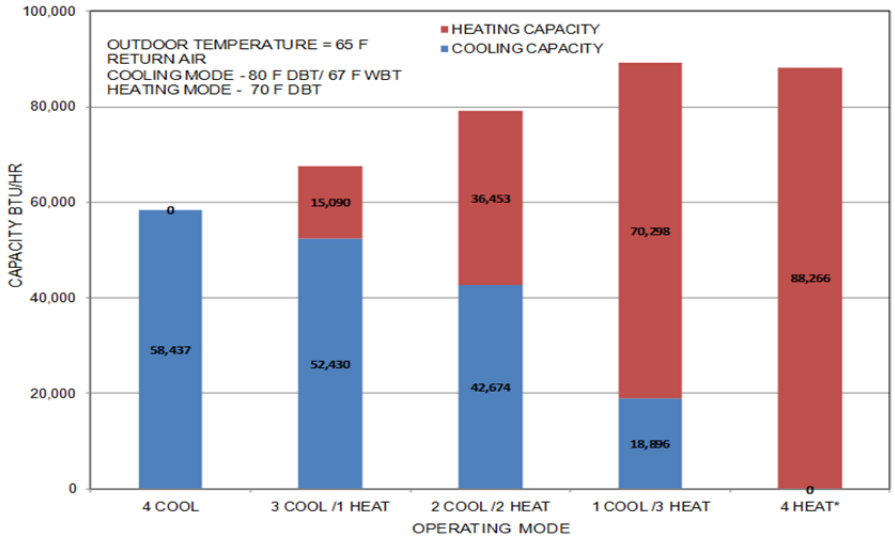

Figure 4-32 Mitsuibishi: Measured Capacity for Changing Operating Modes (65°F, *60°F-ODB)

The measured power draw and EER of the system operating at various conditions is shown in Figure 4-33. The power draw is dependent on the operating mode of the outdoor unit. The system running in 4 cool mode (i.e. cooling only mode) has a higher EER than the 3 cool /1 heat mode due to lower power draw. Once the unit is switched to 3 cool/1 heat mode the power draw increases and the EER decreases. A more in-depth discussion of this efficiency decrease is found in the Task 4 final report (Raustad, 2012a). In 2 cool/ 2 heat mode the outdoor unit is still operating in the cooling mode. The EER is higher because of the increased capacity. In 3-heat/1-cool mode the outdoor unit operates in heating mode and the outdoor heat exchanger acts as an evaporator. Like the 2 cool / 2 heat configuration, higher capacity increases the system EER.

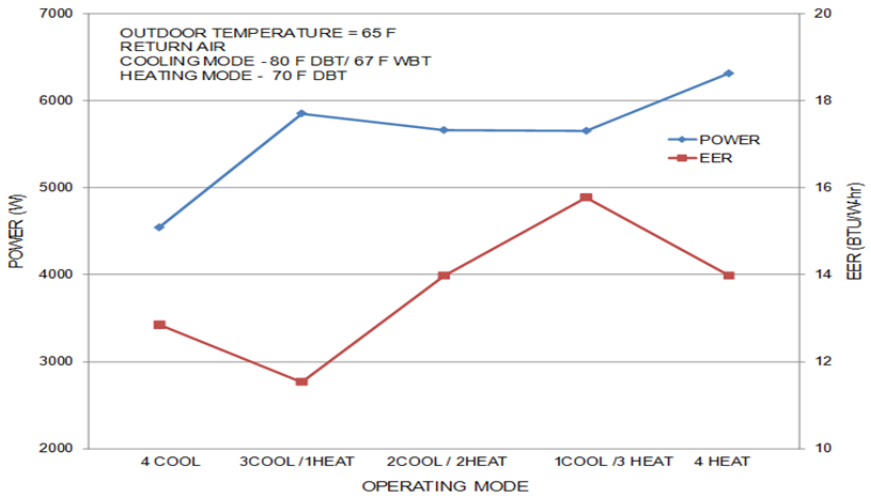

Figure 4-33 Mitsuibishi: Measured Power and EER for Changing Operating Modes (65°F)

Figure 4-34 shows measured capacity similar to Figure 4-32 except at a higher outdoor temperature of 75°F. The data point for 4 heat mode is not available at 75°F because the system cannot operate in heating only mode beyond 73°F. Figure 4-35 shows measured power and EER for simultaneous cooling and heating mode at 75°F outdoor temperature. Again in this case the trends are similar to the 65°F case. The effect of increasing power when switched from cooling only to simultaneous heating and cooling mode was studied at various temperatures to verify the behavior.

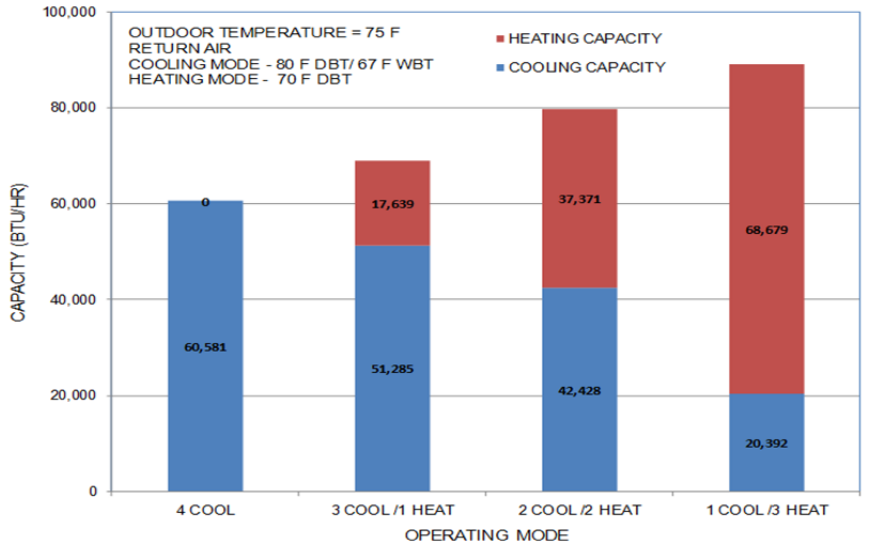

Figure 4-34 Mitsuibishi: Measured Capacity for Changing Operating Modes (75°F)

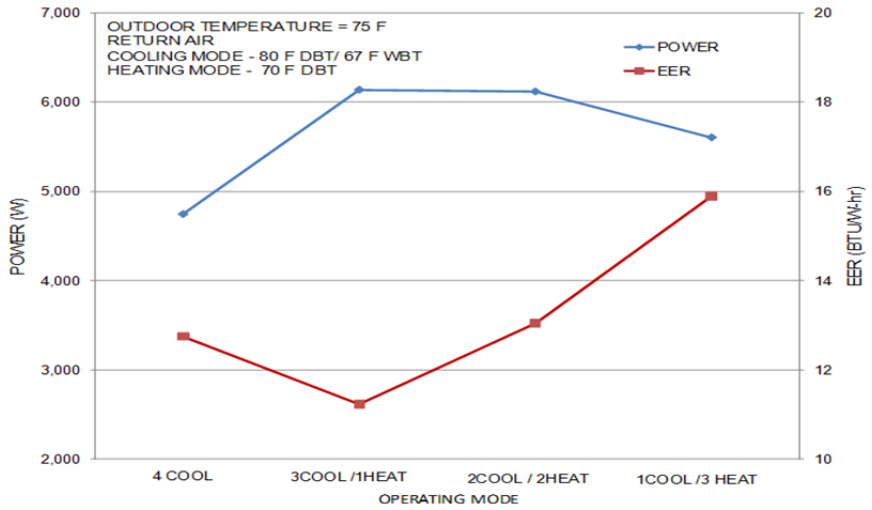

Figure 4-35 Mitsuibishi: Measured Power and EER for Changing Operating Modes (75°F)

Figure 4-36 shows power draw with return air at 80°F DBT/60°F WBT in cooling mode and 70°F DBT in heating mode for varying outdoor temperatures and operating modes. The trend is similar though the power draw difference decreases with increasing outdoor temperature. The effect is much more prominent at milder ambient conditions and is important because the use of SCH mode might be greater during milder conditions.

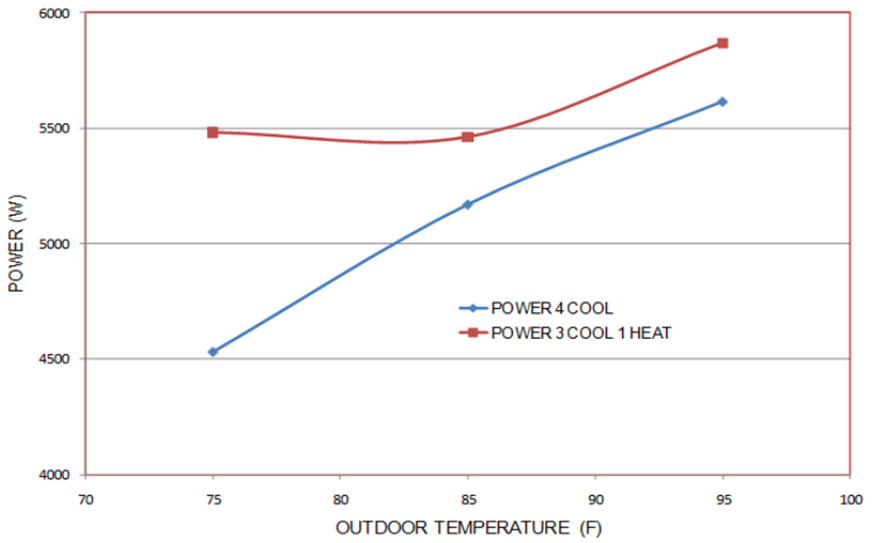

Figure 4-36 Mitsuibishi: Power Draw for Three Different Outdoor Air Temperatures

Outdoor temperature effect on capacity is studied in simultaneous cooling and heating mode to determine if trends seen in cooling only mode and heating only mode are applicable in SCH mode. In 2 cool/2 heat (Figure 4-37) and 3 cool/1 heat mode (Figure 4-38) the cooling capacity remains constant across the temperature range (from 65°F to 95°F). In these two cases the outdoor unit is operating in

cooling mode and is utilizing the indoor units as condensers with little support from the outdoor heat exchanger. Since the return air on the units in heating mode is fixed at 70°F, the outdoor temperature doesn't have a significant impact on the capacity. In 1 cool/3 heat (Figure 4-39) a similar behavior is observed. The condensing pressure is determined by the return air in heating mode. The evaporator is the unit in cooling mode and the outdoor heat exchanger which is seeing varying outdoor temperatures. The influence of the outdoor temperature is reduced to the percentage of the condensing / evaporating capacity utilized by the outdoor heat exchanger. Figure 4-40 shows the effect of outdoor temperature on power draw when operating in SCH mode. The compressor has the same target pressures as in heating and cooling mode and hence the power is not affected a lot. The variations in power are due to the outdoor unit fan adjusting speed to reach setpoint.

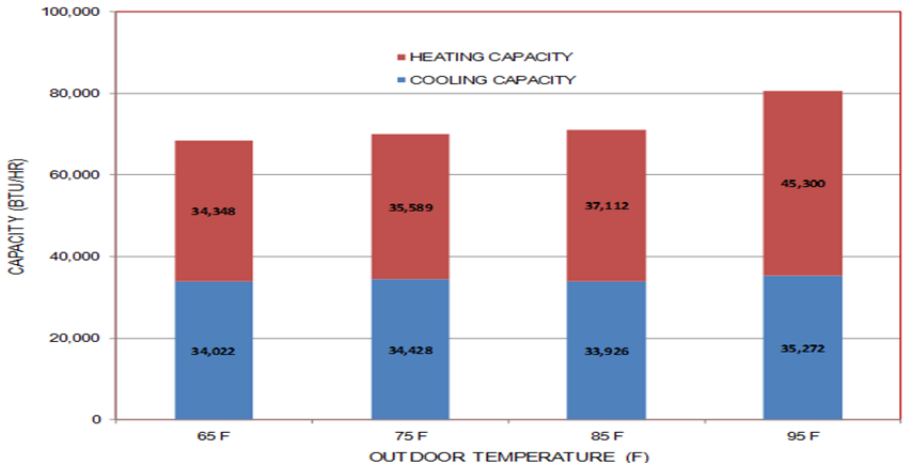

Figure 4-37 Mitsuibishi: Effect of Outdoor Air Temperature on Capacity (2 Cool/2 Heat)

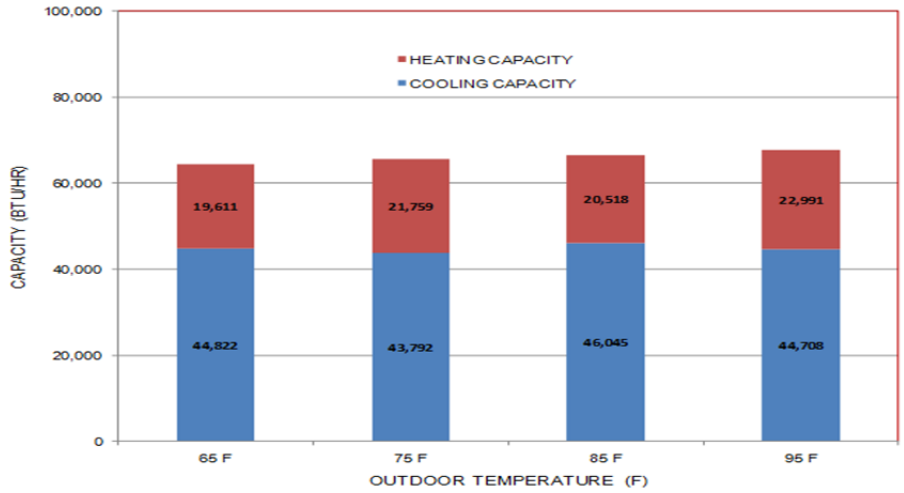

Figure 4-38 Mitsuibishi: Effect of Outdoor Air Temperature on Capacity (3 Cool/1 Heat)

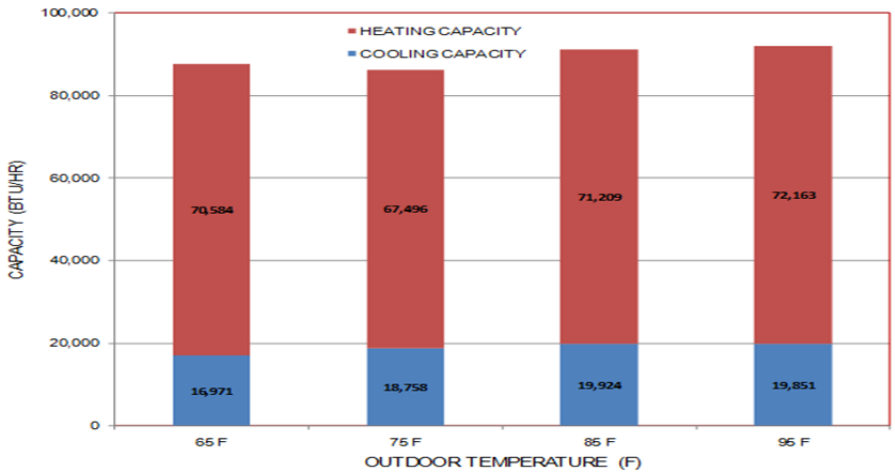

Figure 4-39 Mitsuibishi: Effect of Outdoor Air Temperature on Capacity (1 Cool/3 Heat)

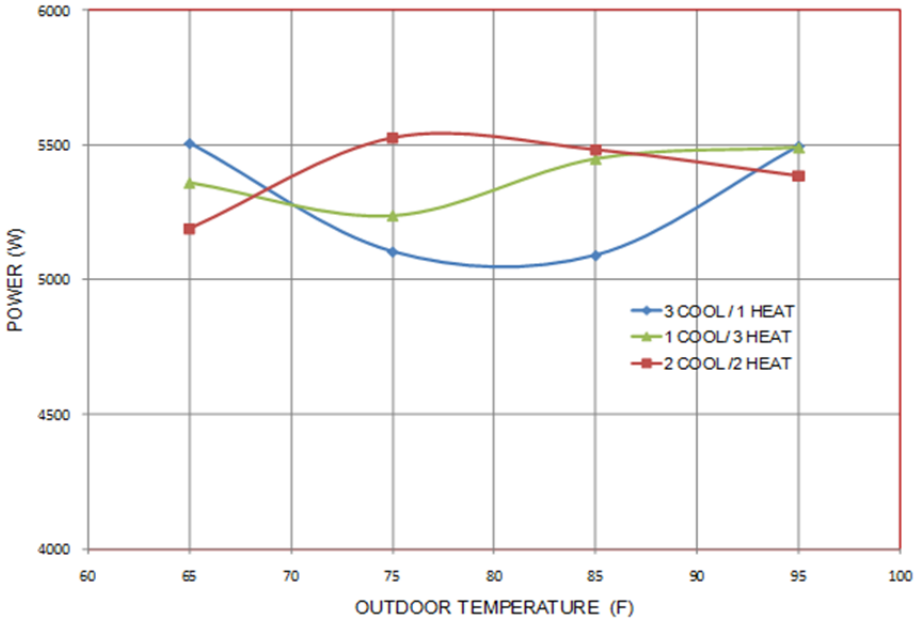

Figure 4-40 Mitsuibishi: Effect of Outdoor Air Temperature on Power in SCH Mode

4.3 Discussion and Conclusion

Two Variable Refrigerant Flow (VRF) heat pumps were tested at the Electric Power Research Institute's (EPRI) Knoxville, TN laboratory. These VRF systems were not tested in accordance with the Standard method of test as described by ANSI/AHRI Standard 1230. Instead, these systems were tested in an attempt to measure full-load performance as if these systems were field installed. Although every attempt was made to accurately measure actual performance, the results in this document may not necessarily reflect actual operation. Future testing will ultimately determine actual field performance.

The selected method of test was the air enthalpy method with fixed operating conditions using a buried thermostat set point temperature. As the results show, the performance measured did not agree with manufacturer's published performance data. It is believed that this specific method of test is not appropriate for testing advanced variable-speed heating and cooling equipment and that alternate test methods should be investigated to determine the most appropriate, or a more appropriate, test method for variable-speed HVAC system types. Project participants have suggested that a calorimetric test method may more accurately represent performance and allow the control algorithms to better respond to imposed loads. One method currently being investigated through other funding sources is to impose a fixed load (both sensible and latent) on the system and allow that system to operate according to the internal control algorithm. If the system operation does not provide the desired operating conditions, minor adjustments to the fixed loads could push the operating conditions toward the desired state point. It is anticipated that this method of test may be more representative of the VRF system operation in the field.

The ANSI/AHRI Standard 1230 test procedure measures system performance at fixed compressor speeds, with other internal modulating devices also fixed and set as determined by the manufacturer. The ANSI/AHRI Standard 1230 test procedure provides a metric by which all manufacturers can be compared. Conversely, the actual response of the system, including the system response as determined by the internal control algorithm, was of most interest in this study. A preliminary test, unrelated to Standard 1230, was performed where the thermostat set point temperature was varied to investigate the change in system performance as shown in Figure 4-41. For this test, the operating conditions were fixed (i.e,. air inlet/outlet T and RH) and the system was then enabled and allowed to operate. The lowest thermostat temperature set point provided the highest system capacity, albeit at a lower efficiency. For this reason, the buried thermostat approach was chosen as the favored test method to determine full-load capacity. The intent of this choice was to measure full-load system performance as if the unit were field installed (i.e., no compressor speed override was used).

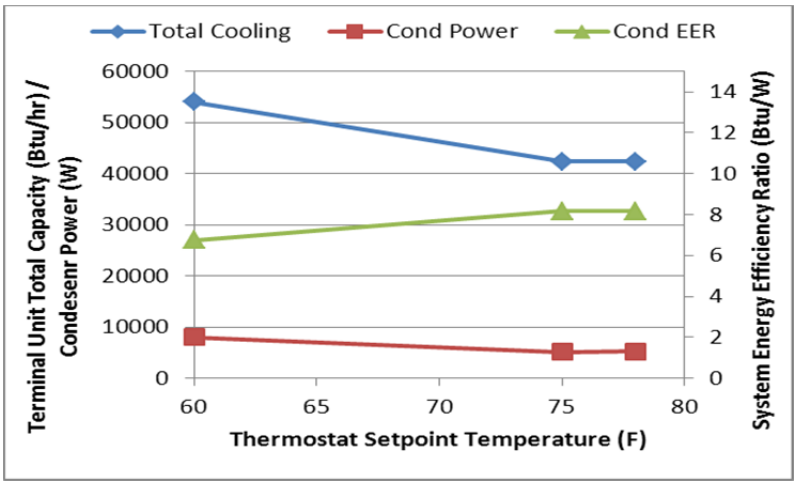

Figure 4-41 Effect of Thermostat Setpoint Temperature on System Performance

Manufacturers argue that the control algorithm cannot respond to fixed inlet conditions (i.e., the control algorithm cannot adjust performance without feedback), which is a valid argument regardless of the use of a fixed compressor speed during the ANSI/AHRI Standard 1230 test procedure. Although the measured capacity was greatest at the lowest thermostat setpoint temperature, the system efficiency may have been higher had the system's control algorithm been allowed to adjust system performance. Power and EER in Figure 4-41 represent only the measured condenser power.

As the thermostat temperature set point approaches the inlet air dry-bulb temperature (80F), the on-board controls sense the load is reduced and hence capacity is also reduced and the efficiency improves. Since the intent of the testing was to measure the full-load performance, setting the thermostat to an extreme seemed to be the most reliable. However, the system efficiency appeared to suffer as a result. For this reason, it is believed that an alternative method of test be used to more accurately measure VRF system performance. One such method of test would be to impose a fixed load on the VRF system and allow the return air conditions to vary as the VRF system adjusted performance and/or cycled to meet the imposed load. This is exactly how the system operates in the field with the only difference being the size of the laboratory with respect to the actual building. The load could be varied to provide both part-load and full-load performance information.

Results from this type of test would provide a more representative indication of field performance and also provide a means for each manufacturers control algorithm to be included in the results. Researchers are investigating a "load based method of test" procedure that would allow more accurate performance measurements for both constant-speed and variable-speed compression systems. Preliminary laboratory testing using this new method of test has occurred but it is still too early in the test method development process to discuss the results of these tests in any detail.

5. Development of a VRF System Heat Recovery Computer Model

5.1 VRF Heat Recovery Computer Model

A VRF heat pump model was added to Energyplus V6.0.0.037. This model was limited to heating only or cooling only operation mode since it was unknown at that time how the heat recovery operation mode behaves. Thus this laboratory based performance study was conducted to understand how the heat recovery operation mode performs and differs from the heat pump mode. The VRF heat recovery model was then formulated based on observations made using laboratory measured performance. The heat recovery model was added to EnergyPlus version V7.2. The details of the VRF heat recovery computer model are described in Task 5 final report (Raustad, 2012b). Issues found with the original heat pump model are shown in Appendix A. The following figures are the foundation for the VRF heat recovery computer model.

Two VRF systems were tested in the laboratory and noticeably different performance was observed when operating in heat recovery mode. Figure 5-1 shows a laboratory test of the VRF system installed at the EPRI facility where 3 terminal units were operating in cooling mode, and a 4th terminal unit, which had been off, was turned on in heating mode. This test measured the impact on total cooling capacity of the previously operating terminal units and the resulting change in power when heat recovery was active. It is evident that cooling capacity and operating power changes were observed. For this specific test, the available cooling capacity decreased by 5.5% and the operating condenser power increased by 14%. The anticipated performance of the computer model is also graphically presented as dotted lines.

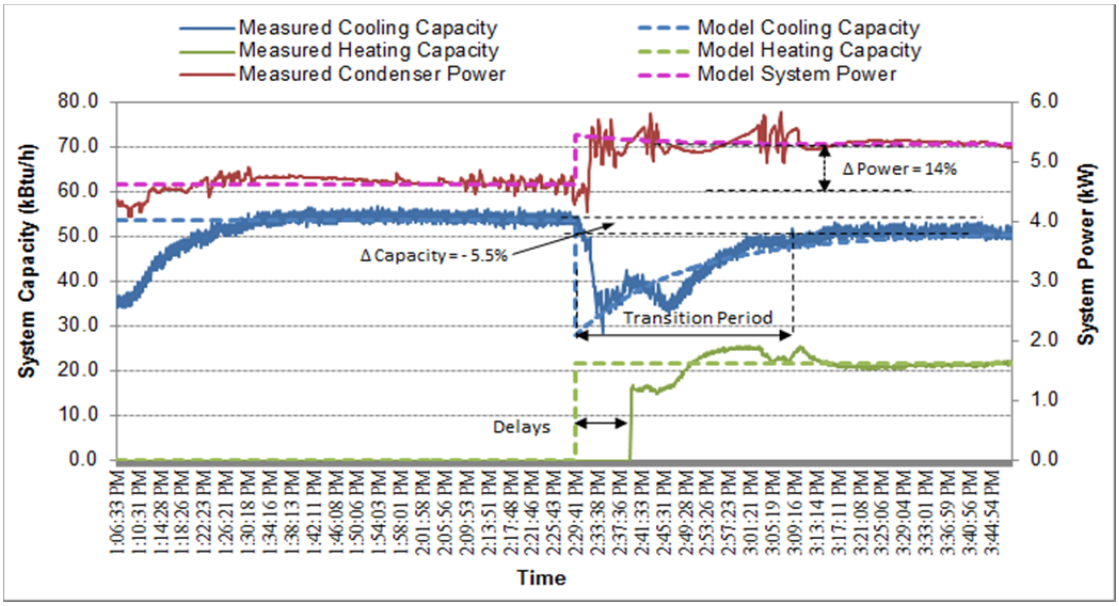

Figure 5-1 Measured Performance in Cooling Only and Heat Recovery Modes

Figure 5-2 shows another laboratory test of a VRF system installed at the EPRI facility where 3 indoor units were operating in heating mode, and a 4th indoor unit, which had been off, was turned on in cooling mode. This test measured the impact on heating capacity of the previously operating terminal units and the resulting change in power when heat recovery was active. In heating operation mode the heating capacity increased by 12.3% and electric power increased by 8.8%. The anticipated performance of the computer model is also graphically presented as dotted lines.

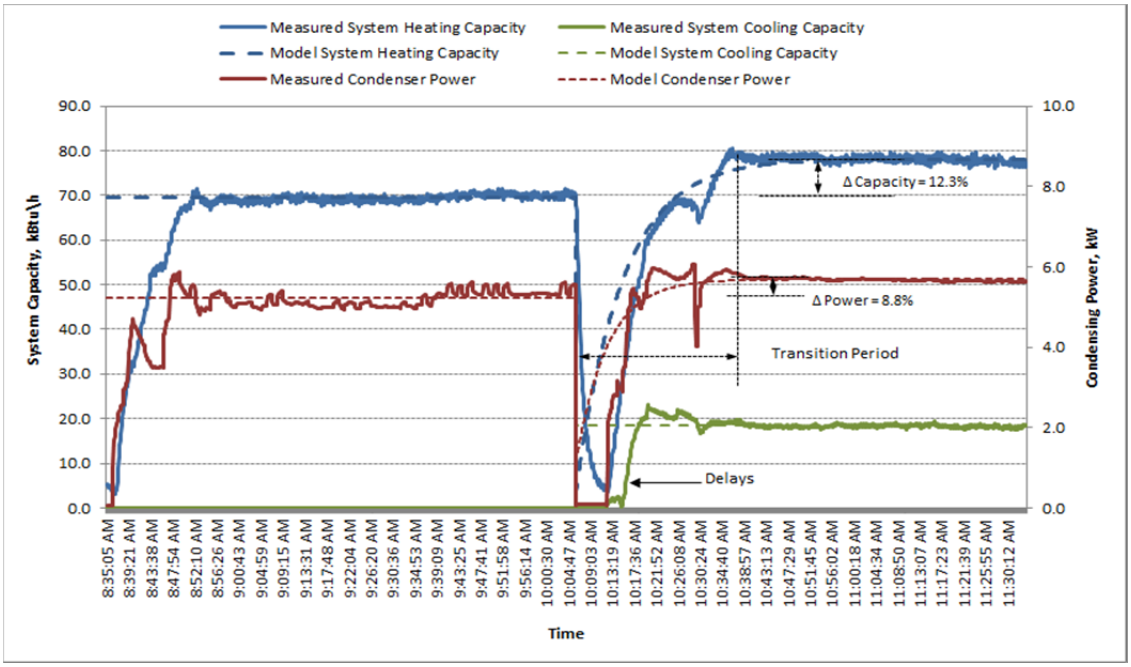

Figure 5-2 Measuring Performance in Heating Only and Heat Recovery Modes

This change in performance was previously suspected, which is the reason the heat recovery model was not included during the development of the original VRF heat pump model. More detailed testing of this system reveals this same trend at various operating conditions. Although limited data was collected in simultaneous heating and cooling mode, the data collected shows a consistent trend. One other observation made is the time involved in reaching steady-state operation when the system switches from cooling only or heating only operation, to simultaneous cooling and heating operation. For the test represented in Figure 5-1, data was collected for a total of 2 hours and 42 minutes. The portion of the test where heat recovery mode was active was approximately 1 hour and 20 minutes. Given this time series, the transition period (the time from when the system switched over to heat recovery mode to when steady-state performance was evident) lasted for about 45 minutes (Raustad, 2012b). This is a relatively long period of time in a computer simulation given that in EnergyPlus the minimum simulation time step is 1 minute. Similar delays and transition period were observed when the VRF system switched from heating only mode to heat recovery mode as shown in Figure 5-2. To accurately model this system type, and the resulting impact on zone conditions, the transition period may be modeled. For this reason, a time

constant was included to account for the time required for the system to recover from the capacity (and similarly power) degradation measured during transition period to a steady state value.

Figure 5-3 shows VRF system laboratory data for cooling only mode (solid characters) and heat recovery mode (simultaneous cooling and heating (SCH), dotted characters). Only the cooling performance is shown. The percentages in the figure refer to the number of terminal units operating for cooling only operation, and the number of terminal units operating in cooling mode (e.g., 4 of 4 equals 100%) where the remaining terminal units are operating in heating mode for heat recovery operation. Using the limited laboratory data, the available cooling capacity fraction used to model heat recovery mode is approximately 0.91 and the cooling electric power fraction is approximately 1.14. It is apparent from this figure that the cooling performance changes when heat recovery mode is active. In the bi-quadratic equation (Eq-31), only coefficient "a" should be used until more complete data sets exist. Full characterization of the heat recovery mode of operation requires further studies. In future laboratory testing it would be necessary to determine performance of the heat recovery operating mode as a function of the indoor and outdoor conditions and part-load operation. Laboratory testing will eventually provide more data and better estimates of performance in heat recovery mode. Of importance is the fact the measured data follow the same trends shown by manufacturers and that the manufacturers data can be used to create normalized performance curves used for simulating VRF systems.

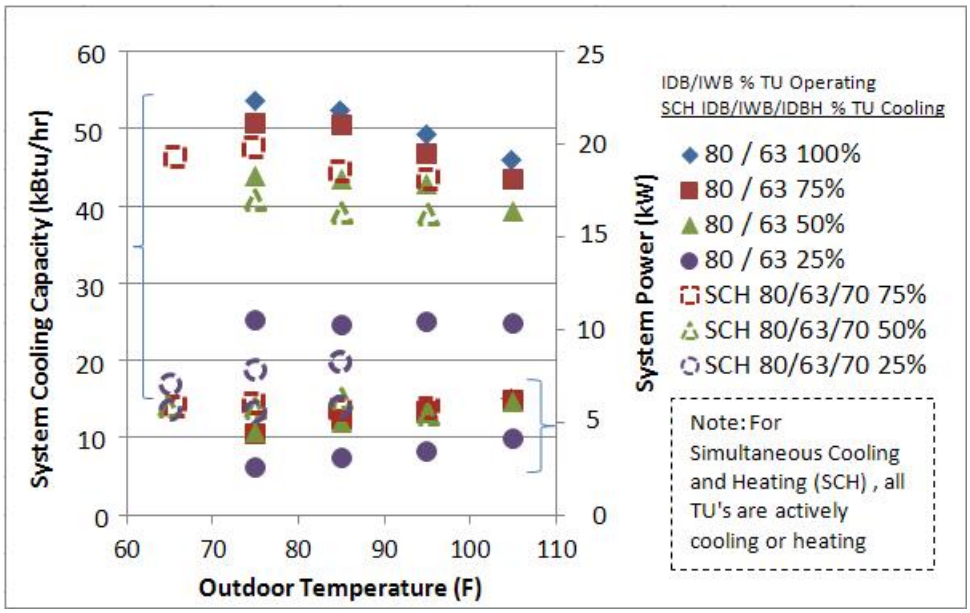

Figure 5-3 Comparing cooling only performance to heat recovery mode

Based on observed performance trends the VRF heat recovery model was formulated using the VRF heat pump model with new terms added to account for the change in performance when simultaneous heating and cooling is active. The new terms adjust the heat pump operating mode capacity and power

and provide a means to model the transition period if desired. Since the VRF heat pump already has performance curves for capacity and energy input ratio, new inputs for Heat Recovery Capacity Modifier and Heat Recovery Electric Power Modifier were added. These new heat recovery performance curves define the fractional change in performance from the existing (heat pump) performance to when heat recovery is active. Since the outdoor unit operates in either cooling or heating mode, there will be one set of performance curves each for cooling and heating operating modes. A total of 14 new inputs were added to the existing VRF heat pump object. Two inputs are included to limit the outdoor temperature range where heat recovery mode is allowed. Four groups of 3 inputs (12 total) model the change in performance when heat recovery mode is active. Of these 12 performance inputs, only 4 are critical to the steady-state computer model. The remaining 8 of 12 inputs are optional and account for the transient period when the system changes from a cooling only or heating only to heat recovery mode.

In heat recovery mode, the VRF system can simultaneously cool and heat multiple zones. The VRF system selects an operating mode according to the dominant load as reported by the zone coil(s). The calculation of the dominant load is based on the master thermostat priority control selection and may either be based on individual coil loads, the number of zones requiring cooling or heating, the master thermostat zone load, or an operating mode schedule. The VRF system will operate in cooling mode, and provide heating to zones with a heating load, when the dominant load among all zone terminal units is cooling. The VRF system will operate in heating mode, and absorb heat from zones with a cooling load, when the dominant load among all zone terminal units is heating. The VRF system is then modeled to determine any impact it might have on the zone terminal units (i.e., capacity limitations due to oversized terminal units, operating limitations due to allowable operating temperature range, impacts of defrost operation, changes in performance when heat recovery mode is active, etc.). The following sections provide a brief description of the performance calculations for cooling dominant and heating dominant heat recovery operating modes and are based on observations made during lab testing (see Section 5.1).

5.1.1 Heat Recovery Mode Cooling Capacity

The existing VRF heat pump computer model simulates capacity in cooling mode as a function of indoor air wet-bulb and outdoor air temperature (CAPFT). The combination ratio (CR) term accounts for differences in installed indoor terminal unit capacity with respect to the system capacity. The combination ratio is defined as the ratio of indoor terminal unit rated cooling capacity to outdoor condenser rated cooling capacity. The VRF heat pump model capacity calculation is described in detail in Task 2 final report (Raustad, 2011) and the available cooling capacity is given by Eq-30:

$$\dot{Q}_{hp,\,total,cool} = \dot{Q}_{hp,cool,\,ref} \cdot CAPFT_{hp,\,cool} \cdot CR_{cool,\,correction} \qquad (30)$$

When operating in heat recovery mode, the heat pump's available cooling capacity is typically different than the available capacity when operating in cooling only mode. The change in available cooling

capacity when the system is in heat recovery mode is accounted for using a Heat Recovery Cooling Capacity Modifier (HRCapMod). This modifier is based on a bi-quadratic equation with indoor and outdoor temperatures used as independent variables and is given by Eq-31:

$$HRCapMod_{hr,cooling} = a + b\overline{T}_{wb,ID} + c\cdot\overline{T}^{2}_{wb,ID} + d\cdot T_{db,OD} + e\cdot T^{2}_{db,OD} + f\cdot\overline{T}_{wb,ID}\cdot T_{db,OD} \quad (31)$$

This equation can be used to provide a constant modifier for available cooling capacity in heat recovery mode (i.e., only "*a*" coefficient is non-zero) or a modifier that varies with indoor and outdoor conditions. With very limited performance data available at this time, it is recommended that only the coefficient "*a*" term be used. When the VRF system is not operating in heat recovery mode, the modifier is set to 1 and calculation of cooling capacity reverts to Eq. 8. The steady state total cooling capacity in heat recovery operating mode is given by Eq-32 and represents the steady-state operation at the right side of Figure 5.1.

$$\dot{Q}_{hr,cooling,total} = \dot{Q}_{hp,total,cool}\cdot HRCapMod_{hr,cooling} \quad (32)$$

When the heat pump changes operating modes (e.g., from cooling only to heat recovery mode), the transition does not happen immediately as shown in Figure 5-1. During this transient period the available cooling capacity can change significantly. The performance of the system during the initial start of heat recovery mode can be modeled using a constant fractional input and a time constant to account for transient recovery. At the start of the transition period, only a fraction (k_{cool}) of the steady-state capacity in heat recovery mode is available. The transient period is modeled using an exponential capacity recovery model. The heat recovery mode cooling capacity time constant ($\tau_{cap,\ cool}$) identifies the time needed to recover to 99% of the steady-state value. The remaining capacity is recovered over a period of 5 time constants ($\tau_{cap,\ cool}$). The available total cooling capacity in heat recovery mode is given by Eq-33 (see Figure 5.1):

$$\dot{Q}_{hr,avail,cooling,trns} = k_{cool}\cdot\dot{Q}_{hr,total,cooling} + \left(1-k_{cool}\right)\cdot\dot{Q}_{hr,total,cooling}\cdot\left(1-e^{\left(-\frac{t}{\tau_{cap,cool}}\right)}\right) \quad (33)$$

The operating part-load ratio (*PLR*) of the VRF system is calculated by Eq-34:

$$PLR = \dot{Q}_{cooling,total} \Big/ \dot{Q}_{hr,avail,cooling,trns} \quad (34)$$

5.1.2 Heat Recovery Mode Cooling Power

The system electric power in the heat recovery operating mode calculation procedure was formulated based on a similar concept used for available capacity. The change in total electric power when the system is in heat recovery mode is accounted for using a Heat Recovery Cooling Electric Power Modifier

(HRPowerMod). This modifier is the ratio of the electric power expected when heat recovery mode is active to that of the heat pump operating mode at steady-state operation (e.g., cooling mode). The modifier is based on a bi-quadratic equation with indoor and outdoor temperatures used as the independent variables and is given by Eq-35:

$$HRPowerMod_{hr,cool} = a + b\overline{T}_{wb,ID} + c\cdot\overline{T}^{2}_{wb,ID} + d\cdot T_{db,OD} + e\cdot T^{2}_{db,OD} + f\cdot\overline{T}_{wb,ID}\cdot T_{db,OD} \qquad (35)$$

This equation can be used to provide a constant modifier for cooling electric power input in heat recovery mode (i.e., only "*a*" coefficient is non-zero) or a modifier that varies with indoor and outdoor conditions. With very limited performance data available at this time, it is recommended that only the coefficient "*a*" term be used. When the VRF system is not operating in heat recovery mode, the modifier is set to 1 and calculation of cooling power reverts to Eq. 17. The steady state cooling electric power in heat recovery mode is given by Eq-36 and represents the steady-state operation at the right side of Figure 5.1.

$$P_{hr,cool} = P_{hp,cool}\cdot HRPowerMod_{HR,cool} \qquad (36)$$

In heat recovery mode the transient period cooling electric power has the steady state term and a transient term and is given by Eq-37 (see Figure 5.1):

$$P_{hr,cool,trns} = k_{e,cool}\cdot P_{hr,cool,total} + \left(1-k_{e,cool}\right)\cdot P_{hr,cool,total}\cdot\left(1-e^{\left(-\frac{t}{\tau_{e,cool}}\right)}\right) \qquad (37)$$

Capacity and electric power modifying parameters used to model the transition period of heat recovery operation mode of VRF system are provided in Table 5-1.

Table 5-1 Heat Recover Operation Mode Constants

Heat Recovery Modifier Parameters	Capacity	Electric Power
k_{cool}	0.55	1.03
τ_{cool}	0.30	0.20
k_{heat}	0.05	0.20
τ_{heat}	0.15	0.10

Setting the "*k*" terms to 1.0 turns off the transient effects during the transition period. This implies that when the VRF system switches from heat pump to heat recovery mode, the system reaches a steady state condition instantaneously. Since this mode change is limited, modeling or not modeling this aspect of performance is not expected to result in noticable differences in simulated energy performance.

5.1.3 Heat Recovery Mode Heating Capacity

When operating in heat recovery mode, the heat pump's available heating capacity is typically different than the available capacity when operating in heating only mode. This modifier is used to adjust the available heating capacity using a factor when heat recovery is active. The modifier is based on a bi-quadratic equation with indoor and outdoor temperatures used as the independent variables and is given by Eq-38:

$$HRCapMod_{HR,heat} = a + b\overline{T}_{db,ID} + c \cdot \overline{T}^{2}_{db,ID} + d \cdot T_{OD} + e \cdot T^{2}_{OD} + f \cdot \overline{T}_{db,ID} \cdot T_{OD} \quad (38)$$

This equation can be used to provide a constant modifier for available heating capacity in heat recovery mode (i.e., only "*a*" coefficient is non-zero) or a modifier that varies with indoor and outdoor conditions. With very limited performance data available at this time, it is recommended that only the coefficient "*a*" term be used. When the VRF system is not operating in heat recovery mode, the modifier is set to 1 and calculation of heating capacity reverts to Eq. 18. The available heating capacity in heat recovery mode is given by Eq-39 and represents the steady-state operation at the right side of Figure 5.2.

$$\dot{Q}_{hr,heat} = \dot{Q}_{hp,heat} \cdot HRCapMod_{hr,heat} \quad (39)$$

In heat recovery mode the transient period heating capacity is calculated using similar formulation as in the cooling mode and is given by Eq-40 (see Figure 5.2):

$$\dot{Q}_{hr,heat,trns} = k_{heat} \cdot \dot{Q}_{hr,heat} + \left(1 - k_{heat}\right) \cdot \dot{Q}_{hr,heat} \cdot \left(1 - e^{\left(-\frac{t}{\tau_{cap,heat}}\right)}\right) \quad (40)$$

This exponential model used for modeling the transition period can be turned off by setting the initial heat recovery heating capacity fraction to 1.0.

5.1.4 Heat Recovery Mode Heating Power

When operating in heat recovery mode, equations similar to those used for available heating capacity are used to model operating electric power. The change in total heating electric power when the system is in heat recovery mode is accounted for using a Heat Recovery Heating Electric Power Modifier (HRPowerMod). This modifier is the ratio of the heating electric power expected when heat recovery mode is active to that of the heat pump operating mode at a steady-state condition. The modifier is based on a bi-quadratic equation with indoor and outdoor temperatures used as the independent variables and is given by Eq. 41:

$$HRPowerMod_{hr,heat} = a + b\overline{T}_{db,ID} + c \cdot \overline{T}^{2}_{db,ID} + d \cdot T_{OD} + e \cdot T^{2}_{OD} + f \cdot \overline{T}_{db,ID} \cdot T_{OD} \quad (41)$$

This equation can be used to provide a constant modifier for heating electric consumption rate in heat recovery mode (i.e., only "*a*" coefficient is non-zero) or a modifier that varies with indoor and outdoor conditions. With very limited performance data available at this time, it is recommended that only the coefficient "*a*" term be used. When the VRF system is not operating in heat recovery mode, the modifier is set to 1 and calculation of heating power reverts to Eq. 19. The steady-state heating electric power in heat recovery mode is given by Eq. 42 and represents the steady-state operation at the right side of Figure 5.2.

$$P_{hr,heat} = P_{hp,heat} \cdot HRPowerMod_{hr,heat} \quad (42)$$

In heat recovery mode the transient period heating electric power is calculated using a similar formulation as described for cooling mode and is given by Eq. 43 (see Figure 5.2):

$$P_{hr,heat,trns} = k_{e,heat} \cdot P_{hr,heat} + \left(1 - k_{e,heat}\right) \cdot P_{hr,heat} \cdot \left(1 - e^{\left(-\frac{t}{\tau_{e,heat}}\right)}\right) \quad (43)$$

5.2 Defrost Adjustment Factors

Frost can form on the outdoor coil when the conditions are favorable for water vapor to condense and freeze. Thus, the need to periodically defrost this coil has a significant impact on heating capacity and energy use by the DX heating system. This VRF computer model uses a timed or on-demand reverse-cycle or resistive defrost algorithm. If the outdoor air dry-bulb temperature is below the specified maximum temperature for defrost operation, then the model calculates adjustment factors for heating capacity and input power due to frost formation. This method of accounting for the impacts of frosting/defrost was taken from the model used in DOE-2.1E (ESTSC 2001, Miller and Jaster 1985). A detailed description of the EnergyPlus defrost model is provided in Task 5 final report (Raustad, 2012b) and in the EnergyPlus engineering reference (US Department of Energy, 2011).

6 Field Testing Two VRF Systems

6.1 Introduction

VRF systems have been gaining small market penetration in the U.S., but there remains a need for verified performance data and accurate performance modeling for multi-zone VRF heat pumps and VRF heat recovery systems to quantify their efficiency and enable further market penetration. The objective of part of this project is to describe VRF system field performance. The energy use and demand characteristics of the VRF systems was monitored and recorded over a period of at least six months by EPRI and the measured data was delivered to UCf/FSEC. Some of these data sets were used for the EnergyPlus VRF computer model validation (see Chapter 9). A detailed description of the field test is provided in the Task 6 final report (Raustad, 2012c). A two pipe VRF Heat Recovery (VRF-HR) system was installed to condition part of an EPRI lab facility in Knoxville, TN. The VRF-HR system was manufactured by Mitsubishi Electric. The outdoor unit was a nominal six ton unit connected to four – two ton indoor low static ducted units. The combination ratio (ratio of total indoor cooling capacity to outdoor unit cooling capacity) for this system was 133.3%. The system was installed in the last week of April 2012 with weekly data being provided to the Florida Solar Energy Center (FSEC) every week. As an additional data set, not necessarily a required data set, internal data from the system was also recorded using special Mitsubishi hardware and software but the data recorded was not continuous due to hardware and software issues. Also a two-pipe VRF Heat Pump (VRF-HP) system was installed in Alabama and monitored for electric power draw and energy consumption as a function of indoor and outdoor air conditions. The system has a nominal 24 ton outdoor unit with 28 tons of connected indoor units. The combination ratio is 1.16. Eight classrooms are served by the VRF system, each of which has 3.5 tons of capacity from two ceiling cassettes of 2.0 tons and 1.5 tons capacity. The system was instrumented for automatic data acquisition with sensor readings once per minute. Data was collected and stored on an EPRI server.

6.2 VRF Field Monitoring – Site 1

The selected site for monitoring one VRF- HR system was a part of EPRI laboratory in Knoxville, Tennessee. The selected site is a part of EPRI's building 2 laboratory space designated as a HVAC and electric vehicle laboratory. Figure 6-1 shows the EPRI building with an outline of the space being conditioned by the installed VRF-HR system. The south-east facing side of the building is the front side whereas the north-west facing side is the back side. The building is a single story building ideally suitable for a tenant that needs warehouse facilities. The roof is 15'8" high and is a standard silver metal roof with 4" R-13 fiber glass insulation. The conditioned zone for this site has only one exterior filled concrete block wall which is the back side of the building. The conditioned space has a total of seven openings into

adjacent zones (two garage doors, two double doors and three single doors). The floor is a poured concrete slab. The conditioned space has lighting loads, lab equipment and computers.

Figure 6-1 VRF Field Site 1 – EPRI Lab, Building 2, Knoxville, Tennessee

6.2.1 VRF-HR Installed and Instrumentation

The VRF-HR system installed for this site had one outdoor unit and four indoor units. The branch selector (BS) box is installed in the conditioned space in the HVAC laboratory area. The standard communication setup used in various EPRI field sites is used for monitoring the VRF-HR system. Electrical measurements (power and energy consumption) of the outdoor unit and indoor units (all four combined) were recorded. Return and supply air temperatures and relative humidity for each individual indoor unit were also recorded. The outdoor temperature and relative humidity is measured and recorded.

6.2.2 Field Monitoring Results – Site 1

The VRF-HR system was monitored for eight months from May 1st 2012 until December 31st 2012. The entire monitoring period was divided into two parts: all four indoor units operating and only two indoor units operating. The two indoor units operating period was selected because of the nature of load on the units installed in the HVAC laboratory. The HVAC lab, when testing different equipment, would impose a cooling or heating load on the indoor units in that part of the lab. To eliminate the impact of such loads on the operation of the VRF system, the two units in that part of the lab were switched OFF (using thermostats) between September 19th and December 14th 2012. For indoor units that were ON, thermostats were set at 70°F and in auto fan mode. In auto fan mode the system determines whether it needs to provide heating or cooling to a particular zone.

Figure 6-2 shows the monthly energy consumption during the months the system was monitored. The monthly energy consumption is high during the months May through July and dropped off in the later part of the year. The drop off can be attributed to two indoor units being shut off during those months. The indoor units during the months of May, June, and July that were ON were always operating in cooling mode. The increasing energy consumption can be attributed to the number of Cooling Degree Days (base 65°F) plotted in Figure 6-3. The outdoor unit power tends to follow the Cooling Degree Days during the May through August timeframe. The September and December months' data is difficult to analyze due to the indoor units being shut off during part of the periods. The data in months of October and November is exclusively with only two indoor units operating. In the months of October and November combined the system ran for 508 hours in cooling mode and 79 hours in heating mode. There were very few instances when the system was operating in mixed mode.

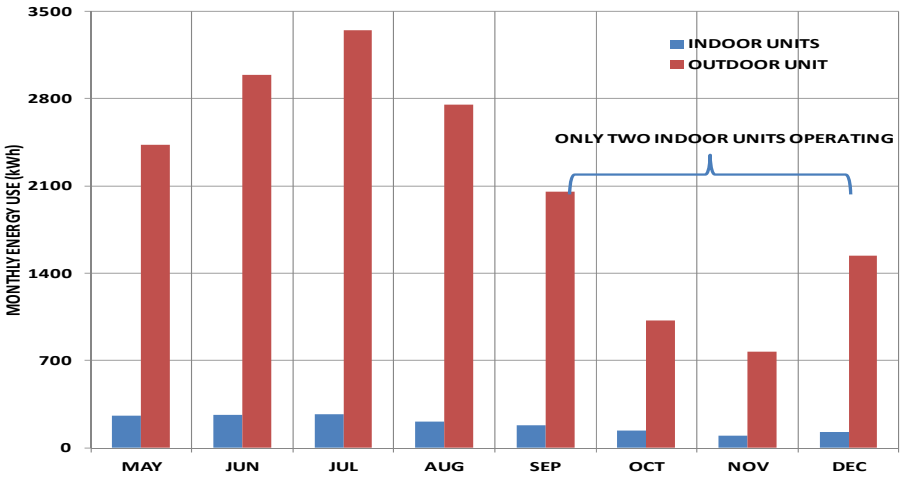

Figure 6-2 Monthly Measured Energy Consumption

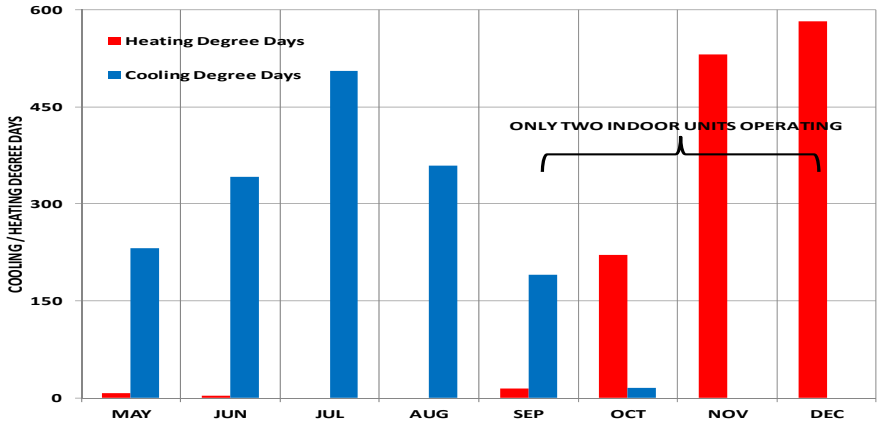

Figure 6-3 Cooling and Heating Degree Days During Test Period

Figure 6-4 and Figure 6-5 show VRF system performance on a hot and cold day during the test period when all four units were enabled. Each figure shows 6 individual plots; Plot 1) outdoor conditions (°F/%), Plot 2 – Plot 5) fan coil #1 - #4 measured air-side performance (e.g. return air [RAT1] temperature and relative humidity [RARH1] °F/% with supply air denoted as SA) and capacity kBTU/hr, and Plot 6) indoor fan (IDF) and outdoor unit condenser (ODC) power (P, kW) and energy (E, kWh), total system capacity (kBTU/hr), and condenser refrigerant suction temperature (°C). Time was recorded in coordinated universal time (UTC). Numeric data show daily average or summations. Fan coil units 1 and 2 were installed in the laboratory and at times were turned off since lab testing influenced operational performance of these units. Fan coil units 3 and 4 were installed in an open-floor plan research area next to the laboratory.

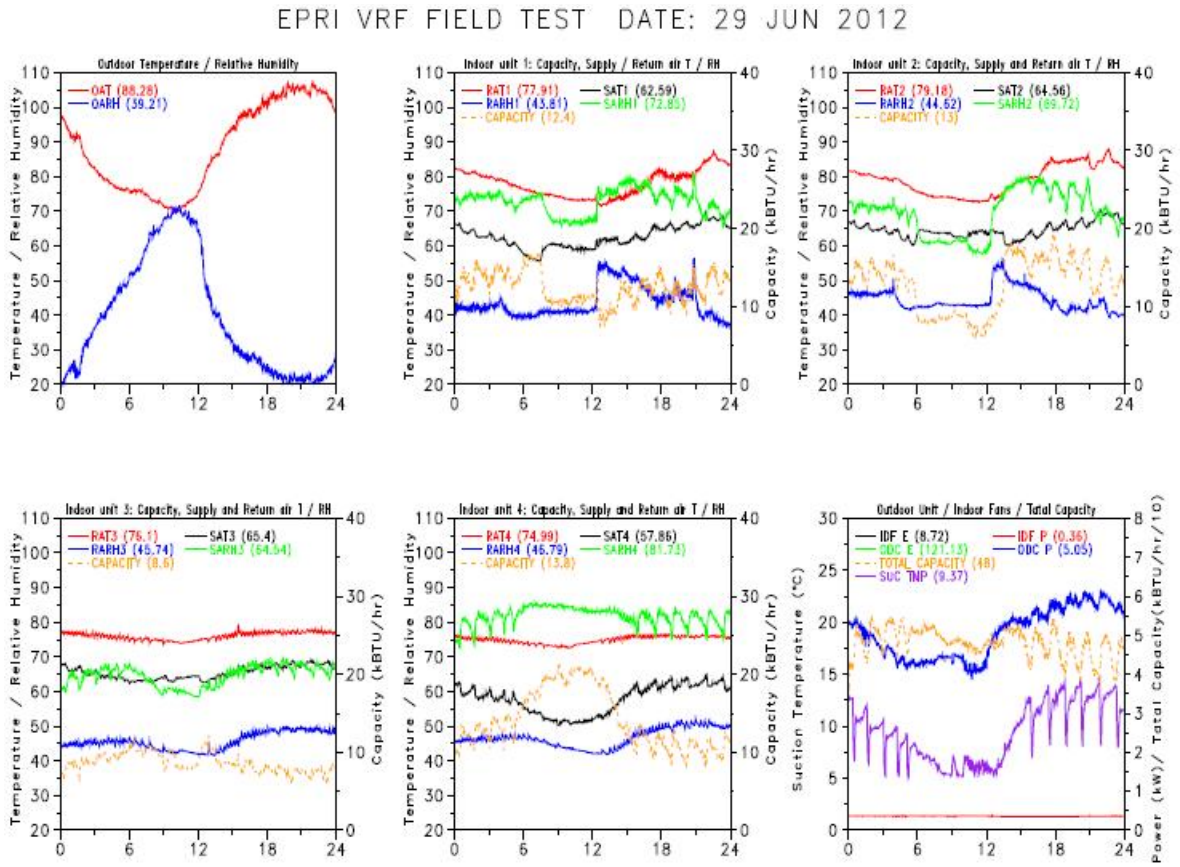

Figure 6-4 VRF System Performance on a Hot Summer Day

Of interest is the lower right plot where capacity and power are plotted using the y2-axis and capacity is divided by 10 (i.e., capacity shown here is 38-54 kBTU/hr). This means that when the outdoor unit condenser power (ODC P, blue line) is higher than the total capacity (yellow line), the EER is less than 10. When the yellow line is higher than the blue, the EER is greater than 10. For example at around 7:00 UTC, the EER is approximately 12 and between 20:00 – 24:00 UTC, the EER averages at approximately 7.5. During the winter day shown in Figure 6-, the fan coil units are cycling to meet the load and operate in both heating and cooling mode at different times of the day. Low efficiency was also measured for

heating operation. Since the unit operate in heating mode the entire day, even when the system was providing cooling, the suction temperature averaged around 63 C and was divided by 10 only in Figure 6-5. Interestingly, a reasonable cooling efficiency (~10) was attained on this cold winter day.

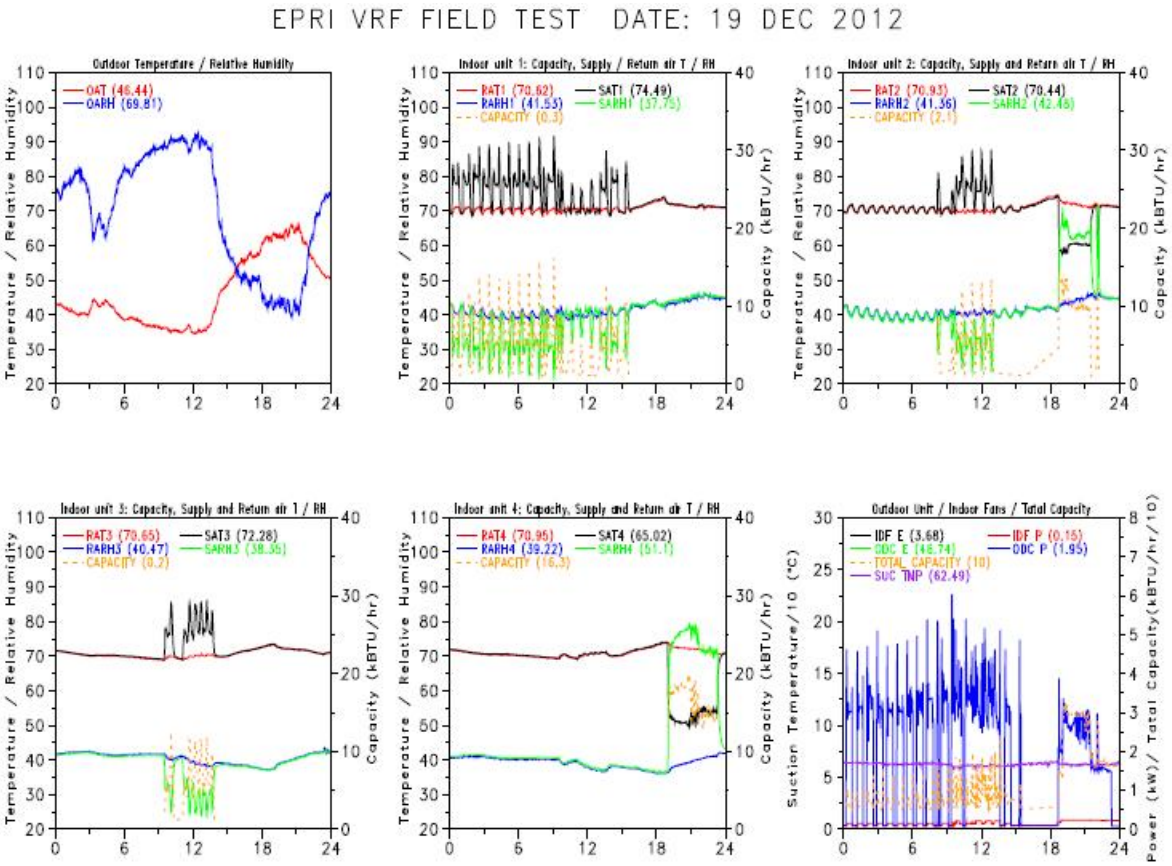

Figure 6-5 VRF System Performance on a Cold Winter Day

The efficiency of the VRF system was found to be less than expected. For a moderate day on September 3, 2012, the measured data is shown in Figure 6-6. Temperature is shown in degrees Fahrenheit unless otherwise noted. On this day, fan coil units 1 and 2 were turned off to investigate part-load performance. Outdoor conditions are shown in the upper left figure, with fan coil units 1 – 4 shown individually in subsequent plots. The final plot in the lower right shows measured power, cooling capacity, and suction temperature measured in degrees Celcius. The fan coil unit return air temperature for unit 3 and 4 were very near the thermostat temperature set point and these units were operating at less than their total rated cooling capacity. Note that the operating fan coil units do modulate capacity to some degree. At this time, the VRF system was operating at an assumed part-load ratio of less than 0.5.

Notice the measured system EER is very near 10 the entire day even though the system was operating with only 2 fan coil units enabled. The efficiency measured on these representative days are fairly typical of measurements throughout the data collection period.

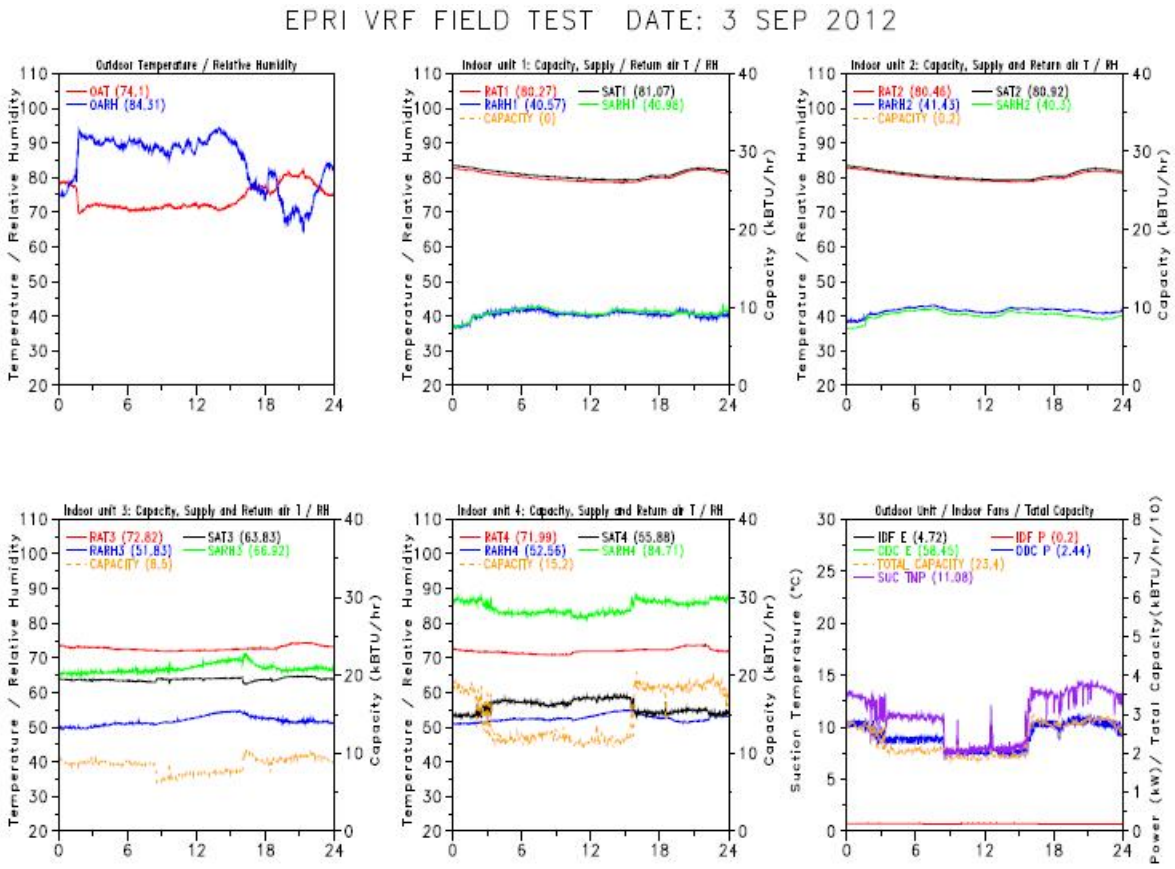

Figure 6-6 VRF System Measured Data on a Moderate Summer Day.

6.3 VRF Field Monitoring – Site 2

The second field site for VRF monitoring is a school building in the hot and humid climate of Mobile, Alabama. Figure 6-7 shows the building that was monitored for VRF system performance. The building is a part of a school and has 14 classrooms, restrooms and storage. The total area of the building is approximately 20,850 square feet of which half the area is served by the VRF system (10,425 square feet). Each of eight classrooms is served by two ceiling cassettes providing 3.5 tons of combined capacity. The total indoor unit capacity is 28 tons and the outdoor unit nominal capacity is 24 tons resulting in a combination ratio of 1.16. The ceiling cassette unit installed in one the classrooms. Prior to this retrofit, each classroom was served with a 3.5 tons split-system heat pump and was its own zone. The building is a single story structure with a metal roof. The walls are filled cinder block walls. The floor is a poured concrete slab. A drop ceiling in all the occupied zones separates the conditioned space from the unconditioned space (attic). The attic space is used to run the communication cables and the refrigerant lines. The school is occupied year round roughly from 7:30 am to 5 pm. Each classroom has about 20 students.

Figure 6-7 VRF Field Site 2 –Faith Academy, Mobile, Alabama

6.3.1 Field Monitoring Results – Site 2

The energy used by the VRF system as well as a side-by-side comparison with a corresponding baseline building (not part of this project) is presented. Measured data show that the VRF system used 17,890 kWh energy over the year compared to 32,250 kWh used by the baseline system. This results in a 45% energy consumption reduction over one year. Figure 6-8 shows the monthly breakdown of energy consumption for both the VRF system and the baseline system. Figure 6-9 shows a representative summer day of operation for both the VRF and the baseline system. Both the units began operating in the early morning hours and reached peak power in between 2 pm - 3pm. The peak demand reduction was 9.6kW (24.9kW for baseline and 15.3 kW for the VRF system). Figure 6-10 shows the power draw from VRF system and the baseline system on a representative cold weather day. Both units do not operate during overnight hours. Due to night time setback the space was cooled down to about 63°F during this particular test day. The VRF unit operates for some time in the morning and then later on in the afternoon. The morning operation was in the heating mode whereas the afternoon operation was in cooling mode, indicating that the internal heat gain is sufficient to offset the heating requirement. No explanation was provided as to why the baseline unit did not also operate in the morning (e.g., scheduling?).

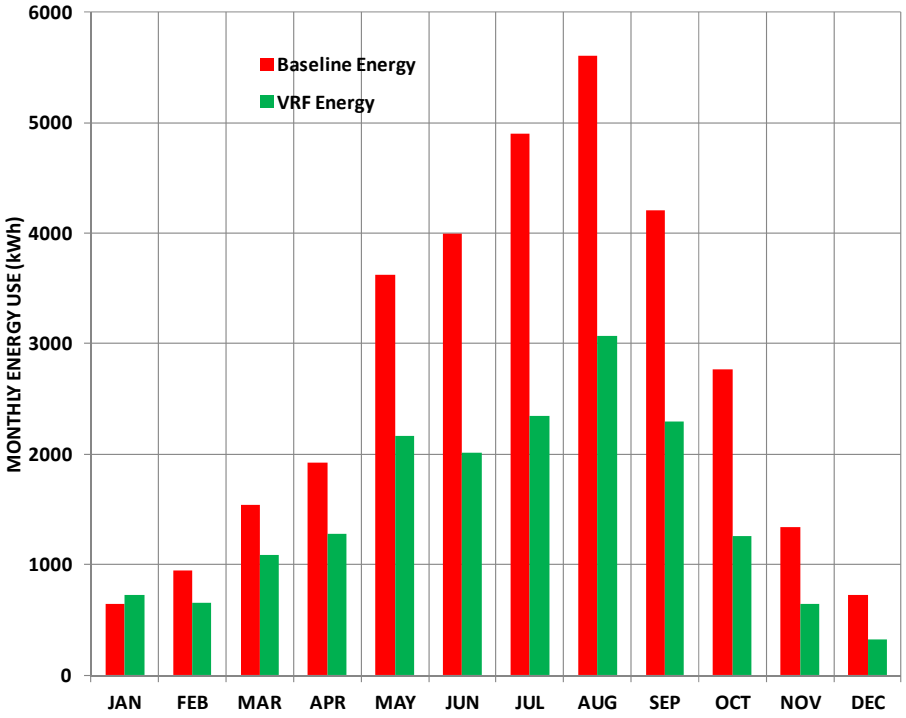

Figure 6-8 Monthly Breakdown of Energy Consumption for VRF and Baseline System

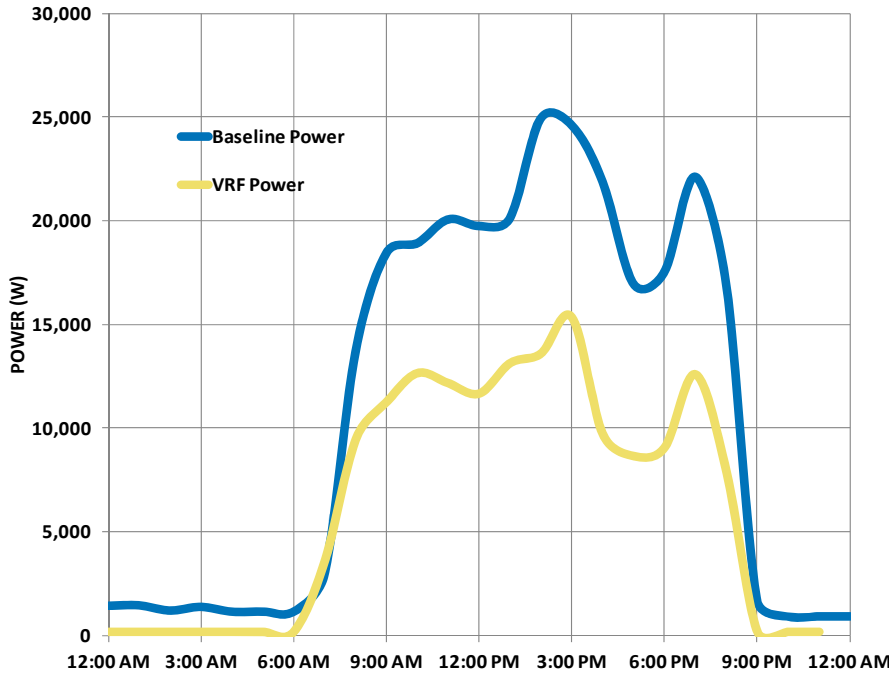

Figure 6-9 Power Draw for VRF and Baseline System on a Warm Weekday

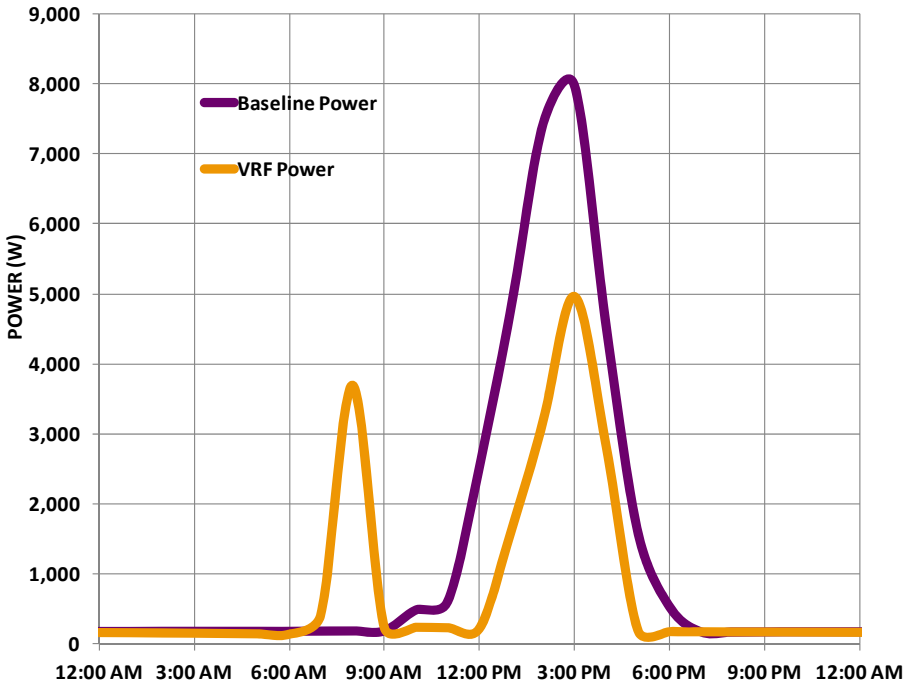

Figure 6-10 Power Draw of VRF System and Baseline System on a Cold Winter Day

6.4 Discussion and Conclusion

Two sets of VRF system field performance data were collected. Only the field data collected from EPRI laboratory facility was used for the VRF computer model validation. The data set used for VRF computer model validation included electric power draw and energy consumption of the indoor units and the outdoor unit, and temperatures and relative humidities of the indoor and outdoor air. The validation procedure and results are discussed in Chapter 8 of this report. Replacing the Mobile, Alabama school class room split system heat pump with VRF system shows a significant energy and demand savings. The energy savings potential reported was calculated by comparing the baseline annual energy consumption to the VRF retrofit annual energy consumption assuming that the data was measured under similar indoor conditions. There is no monitored and measured data collected for the previous system installed prior to the VRF installation and hence, it is not possible to provide a comparison of energy savings in the same building nor a breakdown of the contributors to the energy savings. The majority of savings is believed to be due an improvement in system efficiency. In addition to the possible difference in the system efficiency between the split system and the VRF system, a possible reduction in fan power may have also contributed to the energy savings. Variable speed operation of the VRF system also contributes to energy savings by reducing cycling losses at part-load operation. More details of system specification and operation would be needed to accurately assess field performance of these systems at this site.

7. Implementing a VRF System Heat Recovery Model In EnergyPlus

7.1 Introduction

There are two common types of variable refrigerant flow heat pump systems: cooling only or heating only air-conditioning systems (a.k.a. heat pump), or heat recovery systems that allow simultaneous cooling and heating. This chapter discusses how the VRF heat pump computer model in EnergyPlus was expanded to include heat recovery mode. The EnergyPlus heat pump and heat recovery operating mode computer models are described in detail in chapter 2 and chapter 4, respectively. The variable refrigerant flow model currently supports air-, evaporatively-, or water-cooled condenser equipment. When the heat pump does not operate to reclaim waste heat, the VRF system can only operate in either cooling *or* heating mode. Based on the master thermostat priority control selection, the operating mode is determined by polling the appropriate zone(s) served by the VRF system. When the system is operating in cooling mode, the cooling coils will be enabled only in the terminal units where zone cooling is required. When the system is operating in heating mode, the heating coils will be enabled only in the terminal units where zone heating is required. Supply air fans will continue to operate if the zone terminal unit's fan operating mode is set to continuous fan. When the heat pump does operate to reclaim waste heat, the VRF system can simultaneously cool and heat multiple zones. The heat pump will select an operating mode according to the dominant load as reported by the zone thermostat(s). Calculation of the dominant load is based on the master thermostat priority control selection and may either be based on individual zone loads, the number of zones requiring cooling or heating, the master thermostat zone load, or an operating mode schedule. The VRF system will operate in cooling mode, and provide waste heat to zones that require heating, when the dominant load among all zone terminal units is cooling. The heat pump will operate in heating mode, and extract heat from zones which require cooling, when the dominant load among all zone terminal units is heating. The VRF model inputs were modified to allow the user to enable Heat Recovery mode. The model input for Heat Pump Waste Heat Recovery was changed to allow the choice "Yes". If Yes is selected, heat recovery is enabled and the heat pump can independently cool and heat different zones. If No is selected, the heat pump is only able to cool or heat for any given time step. Additionally, the choices for condenser type were expanded to include water-cooled systems.

7.2 Transition from Cooling Only mode to Heat Recovery mode

When the VRF system transitions from cooling only operation to heat recovery operation, this transition takes some finite amount of time. During the transition period the available cooling capacity can change significantly. Figure 5-1 illustrates the transition between cooling only mode and heat recovery mode. For this test, the VRF system was turned on and was allowed to reach steady-state operation. Three of the four indoor terminal units were operating in cooling mode. When the fourth terminal unit was

enabled in heating mode, the transition from cooling only mode to heat recovery mode took approximately 45 minutes (Raustad, 2012d). During this time, the available cooling was significantly reduced and recovered over time. When the system again reached steady-state operation, the available cooling capacity and power consumption are noticeably different. Although computer models do not typically model this type of transient performance, efforts to model this aspect of performance were included in the VRF heat recovery model. The initial heat recovery cooling capacity fraction and heat recovery cooling capacity time constant are used to model this transition period. The initial heat recovery cooling capacity fraction identifies the fraction of available cooling mode capacity at the start of the transition period, the heat recovery cooling capacity time constant identifies the time needed to recover to 99% of the steady-state value. This exponential model used to represent the transition period and can be turned off by setting the initial heat recovery cooling capacity fraction to 1.

The heat pump total available cooling capacity should be greater than or equal to the total cooling capacity requested by the zone terminal units. When the total operating capacity of all terminal unit's is greater than the available operating capacity of the heat pump condenser, one or more of the terminal unit's operating capacity is reduced to the point where the sum of the indoor terminal unit demand request plus piping losses is equal to the total available cooling capacity of the outdoor condenser. A maximum terminal unit cooling capacity limit is used to restrict the cooling capacity of each indoor terminal unit. The capacity limit is equivalent to a maximum allowed operating capacity for each zone terminal unit. This limit is used to conserve energy between multiple indoor terminal units and a single outdoor condensing unit. When multiple terminal units are operating, the terminal units near their maximum capacity are more likely to be capacity limited than those terminal units operating well below their available capacity. The assumption here is that terminal units that are not capacity limited can provide more refrigerant to meet the same load. When the model finds that there is no terminal unit capacity limit, this variable is set to a large number (i.e., 1.0E+20) indicating that no limit exists. When the heat pump's part-load ratio is less than 1 (i.e., the total capacity of all terminal unit's is less than the available capacity of the heat pump condenser), the heat pump's part-load ratio is compared to the minimum heat pump part-load ratio. If the heat pump's part-load ratio is less than the minimum heat pump part-load ratio, the heat pump will cycle on and off to meet the cooling load. A cycling correction factor is used to account for startup losses of the compression system.

7.2.1 Heat Recovery Cooling Based Modifiers

When operating in heat recovery mode, the heat pump's available cooling capacity is typically different than the available capacity when operating in cooling only mode. A modifier is used to adjust the available cooling capacity when heat recovery is active. This modifier is based on a bi-quadratic equation with indoor and outdoor temperatures used as the independent terms given by Eq-31. This equation can be used to provide a constant modifier difference for available cooling capacity in heat recovery mode or a modifier term that varies with indoor and outdoor conditions. With very limited performance data

available at this time, it is recommended that only a constant modifier term be used. When the VRF system is not operating in heat recovery mode, this modifier is set to 1. The available cooling capacity in heat recovery mode is given by Eq-33. When operating in cooling based heat recovery mode, equations similar to those used for available cooling capacity are used to model cooling electric power input. A biquadratic electric power modifier curve (Eq-35) is used to modify the heat pump steady state cooling electric power. This equation is used to provide a constant modifier for cooling electric power use in heat recovery mode or a modifier that varies with indoor and outdoor conditions. The cooling electric power in heat recovery mode is calculated using Eq-37. The details of the calculation procedure is described in Chapter 5.

7.2.2 Heat Recovery Heating Based Modifiers

Calculations of the heat pump's heating performance is nearly identical to the calculations for cooling operation. A heat recovery heating capacity modifier was created to account for the effects of heat recovery mode. When operating in heat recovery mode, the heat pump's available heating capacity is typically different than the available capacity when operating in heating only mode. A modifier is used to adjust the available heating capacity when heat recovery is active. This modifier is based on a bi-quadratic equation with indoor and outdoor temperatures used as the independent terms (Eq-38). This equation can be used to provide a constant modifier for available heating capacity in heat recovery mode or a modifier that varies with indoor and outdoor conditions. The available heating capacity in heat recovery mode is given by Eq-39. The heating electric power in heat recovery mode is calculated using Eq-43.

7.2.3 Operating Coefficient of Performance

Similar to the rated cooling and heating COP, the operating COP identifies the overall system efficiency. The operating COP includes fan power, auxiliary electric power and other parasitic electric use associated with the operation of the VRF system. The numerator represents the total cooling and heating coil capacities where piping losses have been accounted for. If heat recovery is not used, only one of the terms in the numerator is non-zero. When heat recovery is used, both of these terms are non-zero, therefore, the operating COP includes recovered energy. The denominator includes the electric power of all system components. For water-cooled VRF systems, the plant pump power is not included.

$$COP_{opr} = \frac{\left(\dot{Q}_{TUs,cooling} + \dot{Q}_{TUs,heating}\right)}{\left(P_{hr} + P_{Crankase} + P_{EvapCooler} + P_{defrost} + P_{TUs,fan} + P_{TUs,auxiliary}\right)} \quad (44)$$

8 Compare Field Demonstration Energy Use to Computer Simulations

8.1 Introduction

Variable Refrigerant Flow (VRF) heat pumps are often regarded as energy efficient air-conditioning systems which offer energy savings potential as well as a reduction in peak electric demand (see Figure 6-9 and 6-10) while providing improved individual zone control. One of the key advantages of VRF systems is the elimination or minimization of duct losses and a reduction in duct space requirements. However, there is limited data available to show their actual performance in the field. Since VRF systems are increasingly gaining market share (Goetzler, 2007) in the US, it is highly desirable to have actual field performance data of these systems. This task is an effort made in this direction to monitor VRF system performance over an extended period of time at the EPRI test facility. Furthermore, due to increasing demand by the energy modeling community, an empirical VRF systems model was implemented in the building simulation program EnergyPlus (Raustad, 2013). This chapter describes the test condition and facility, presents validation methodology and discusses the results. The validation describes the accuracy of the VRF heat pump computer model in predicting field measured electric energy consumption. The validation procedure and the results are documented by Sharma and Raustad (2013) in Task 8 final report.

8.2 VRF System

A Mitsubishi PURY-P72THMU VRF system was installed in the Electric Power Research Institute (EPRI) test facility at Knoxville, TN. The specifications of the installed VRF system are shown in Table 8-1. The table contains system parameters as obtained from the manufacturer's catalog data and also as measured in the EPRI lab. Measured system parameters are shown in parenthesis. For the simulation study of the installed VRF system in EnergyPlus, lab measured parameters were used.

Table 8-1 VRF System Specification of the unit tested

System Parameter	Description
Nominal Cooling Capacity	21.1 (18.47) kW [72 (63) kBTU/hr]
Nominal Cooling Power Input	5.55 (6.71) kW [18.9 (22.9) kBTU/hr]
Cooling COP	3.8 (2.75) W/W [13 (9.4) BTU/W-hr]
Nominal Heating Capacity	23.4 (25.39) kW [79.8 (86.6) kBTU/hr]
Nominal Heating Power Input	6.04 (6.47) kW [20.6 (22) kBTU/hr]
Heating COP	3.87 (3.92) W/W [13.2 (13.4) BTU/W-hr]
Minimum Outdoor Temperature in Cooling Mode	-5.0 °C [23 °F]
Maximum Outdoor Temperature in Cooling Mode	43.0 °C [109.4 °F]
Minimum Outdoor Temperature in Heating Mode	-21.0 °C [-5.8 °F]
Maximum Outdoor Temperature in Heating Mode	35.0 °C [95 °F]
Terminal Unit Rated Total Cooling Capacity	6000.0 W [20.47 kBTU/hr]
Terminal Unit cooling SHR	0.79866
Terminal Unit Rated Total Heating Capacity	6782.0 W [23.13 kBTU/hr]
Terminal Unit Rated Air Flow rate (Cooling/Heating)	0.333 (m3/s) [705 CFM]

The rated performance parameters measured in the lab and performance curves generated from manufacturers catalogue data (Mitsubishi catalog) were used to create the EnergyPlus simulation model input. The building geometry configuration inputs, building construction, and other related inputs were based on the design drawing of the EPRI test facility.

8.3 Test Facility and Test Conditions

Field data monitoring of VRF system has been conducted by EPRI in Knoxville, TN, in a single-story building shown in Figure 8-1. This building consists of an office space, workout room, cubicles, lab, and warehouse. The installed VRF system has four terminal units serving the lab and warehouse section of the building. The remaining portions of the buildings were served by separate HVAC systems.

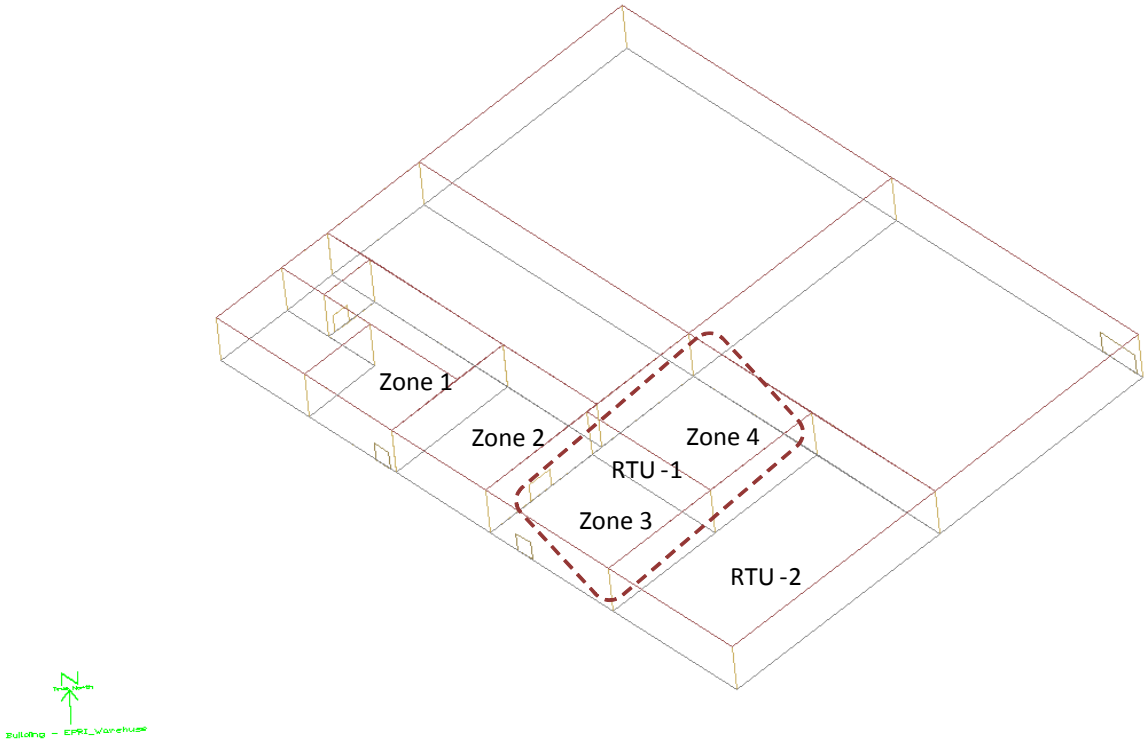

Figure 8-1 Multizone building for VRF field validation

Figure 8-2 shows the location within the lab and warehouse where VRF system terminal units (indoor units) were installed. The lab space was partitioned into two thermal zones, Zone1 and Zone2, using a fictitious wall for modeling purposes. Similarly, the warehouse space was partitioned into two thermal zones, Zone3 and Zone4, using a fictitious wall. Thermal zones, Zone1, Zone2, Zone3, and Zone4, are served by terminal units TU1, TU2, TU3 and TU4, respectively. The two terminal units, TU3 and TU4 at the left side of Figure 8-2 are located in the warehouse and serve part of the warehouse that was previously served by a 5-ton rooftop unit (RTU-1) air conditioner. RTU-1 is completely turned off during this study period. The other 5-ton rooftop unit (RTU-2), which serves the remaining portion of the

warehouse (not shown in Figure 8-2 but located far to the left side of first RTU-1) was running on and off during the test period. To emulate the impact of the roof top unit 2 (RTU-2) on the operation of the terminal units serving Zones 3 and 4, additional equipment load was added using the “OtherEquipment” EnergyPlus object with peak cooling load of 3000 W. This peak cooling load is adjusted with an operating schedule to account for hourly variations as described in Task 8 final report (Sharma and Raustad, 2013).

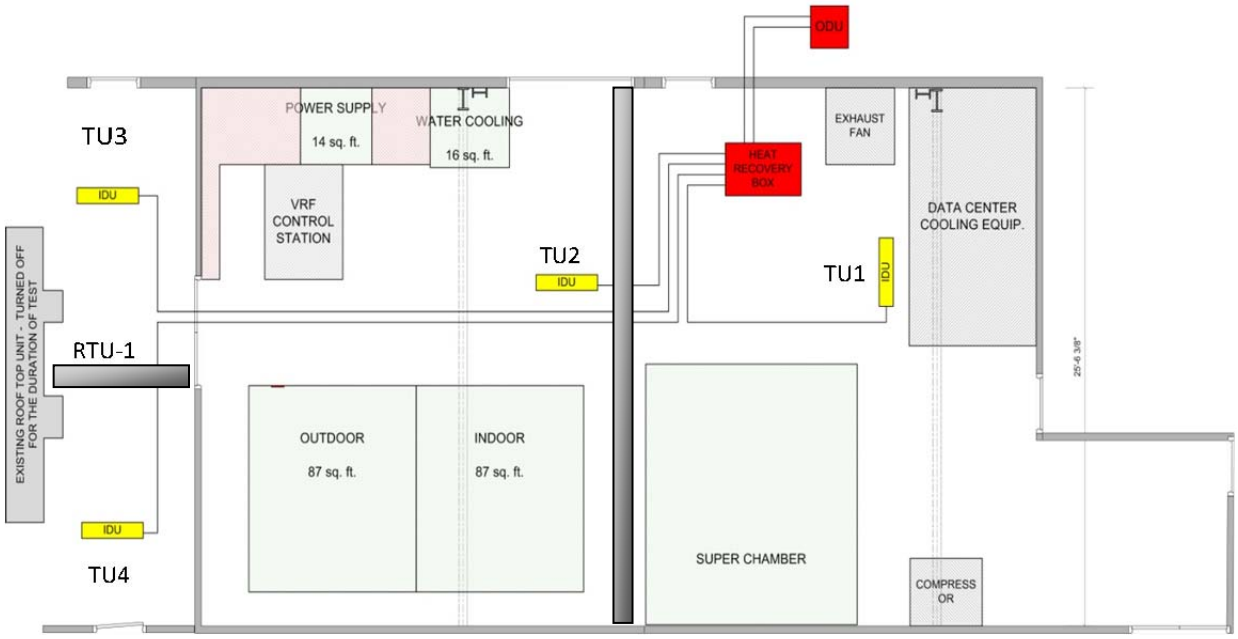

Figure 8-2 Field test of Mitsubishi VRF system in EPRI test site

8.4 Measured Field Data

EPRI has monitored and recorded electric power and energy consumption of the indoor and outdoor units including the indoor and outdoor air conditions. The following variables were measured and recorded by EPRI at the test site:

1) Outdoor temperature and relative humidity
2) Return air temperature and relative humidity at indoor units
3) Supply air temperature and relative humidity at indoor units
4) Indoor unit and BS Box power and energy consumption
5) Outdoor unit (compressor and condenser fan) power and energy consumption

The operating schedule of the various HVAC equipment and components, occupancy, internal heat gains, infiltration, lighting, thermostat setpoint, infiltration levels, and thermo-physical properties of the construction materials that were input to the simulation model are listed in Task 8 final report (Sharma and Raustad, 2013).

8.5 Validation Methodology and Simulation

Performance curves defining the installed VRF system at the EPRI test facility were created from manufacturer's catalog data. The performance curves created along with lab-measured rated performance parameters were used to model the VRF system in EnergyPlus. The building model input geometry and construction data were created from design and detailed drawings of the test facility provided by EPRI. The VRF system installed at the test facility had four terminal units that served one thermal zone each. Other required building input parameters, such as occupancy, lighting, plug loads, and thermostat set-points, were inputs to the model. These input parameters were determined based on best practices and information provided by EPRI. In the absence of measured wind speed and direction data, infiltration rates were determined based on information from DOE's EnergyPlus reference buildings inputs. The reference building uses a fixed coefficient of flow per unit exterior surface area and a fixed correction term for temperature to estimate infiltration rate. The initial infiltration value was adjusted once to tune the computer model. In the absence of real weather data it is common to use local TMY weather. In this case a custom weather data was created by replacing the outdoor dry-bulb temperature, and relative humidity of the Knoxville, TN TMY weather data (Station 723260) with measured values. A weather converter auxiliary utility program that is distributed with EnergyPlus was used (US Department of Energy. 2012c). This was done to facilitate a better approximation of the outdoor environment of the building in the simulation model.

During field measurement it was found that the return air dry-bulb temperature entering the indoor coils were different from the zone temperature measured near the thermostat. A room air model was added to the simulation model inputs to account for room air temperature variation within the zone. Room air model objects in EnergyPlus can be used to model temperature distribution of room air within the zone. These models allow EnergyPlus to take into account natural/forced thermal stratification during surface heat transfer and air system heat balance calculations. Of note is that these models have limited modeling capability in the sense that they cannot model every conceivable air flow that might occur within a zone. Such models are too computationally intensive for a building simulation engine. In this project, a user defined room air model is used which explicitly defines temperature patterns that are to be applied to modify the mean air temperature within a thermal zone. This object is coupled with the EnergyPlus RoomAir:TemperaturePattern:ConstantGradient object, which is used to model room air with a fixed temperature gradient in the vertical direction. Detailed information about this object can be found in EnergyPlus Input Output reference document (US Department of Energy. 2012a).

After the EnergyPlus model input was created, detailed simulations were run, and EnergyPlus outputs were compared against field measured data. The measured data comparison includes the total daily electric energy consumption of indoor and outdoor units. The predicted (simulated) total electric power includes the VRF outdoor unit, terminal unit fan power, and terminal unit parasitic electric power. The

predicted VRF outdoor unit electric power includes electricity used by the compressor and condenser fan. The parasitic electric power includes electricity used by the zone terminal unit's controls, or other associated devices.

8.6 Comparative Results

Figure 8-3 illustrates field measured and model predicted daily total electric energy consumption. Terminal Units 1 and 2 were turned off during field testing from 15th September 2012 until 14th December 2012. Also shown on the same plot are the daily average return air dry-bulb temperature of zones which had terminal units operating and daily average outdoor air dry-bulb temperature. From the graph it is clear that the "average" zone temperatures are mostly maintained near the set-point temperature of 72°F (22.22°C) and then gradually fell to 70°F (21.1°C) during winter months. Daily fluctuations in zone temperature were apparent when reviewing hourly data. Figure 8-4 shows the predicted and measured monthly total electric energy consumption of the VRF system. Predicted and measured total monthly energy for August and September are within 3%, for October 13% and for November and December, 26% and 30% respectively. Both measured and predicted data follow similar profiles though predicted data diverges from measured data at very low ambient temperature. This is more predominant at lower loads since impacts of the model input uncertainty is more significant at these times. This is reasonable agreement when there are uncertainty in the EnergyPlus model input parameters, such as: internal gain rates, infiltration level, and lack of real weather data solar irradiation, wind speed, and wind direction.

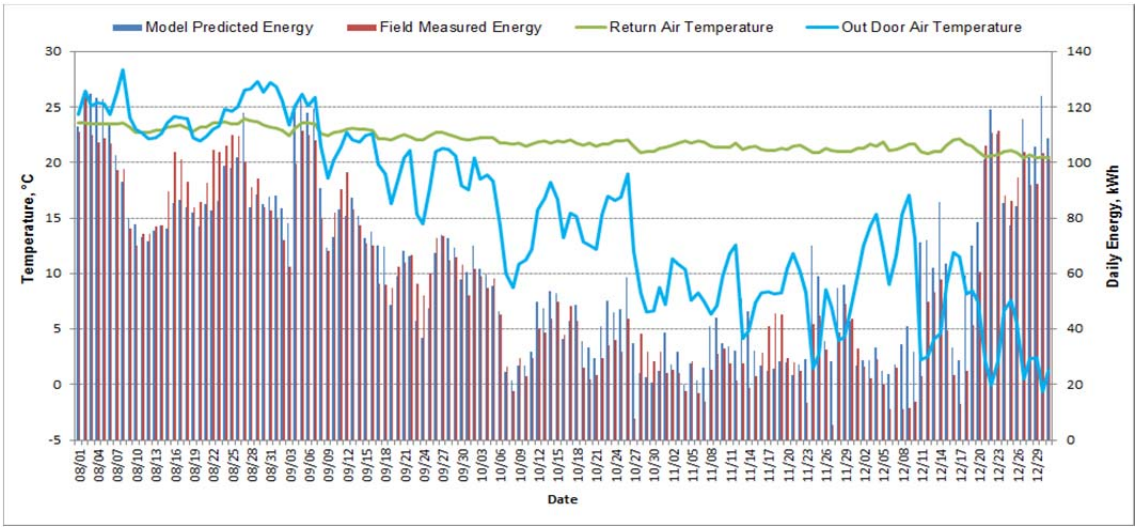

Figure 8-3 Daily Total Electric Energy Use and Daily Average Temperature

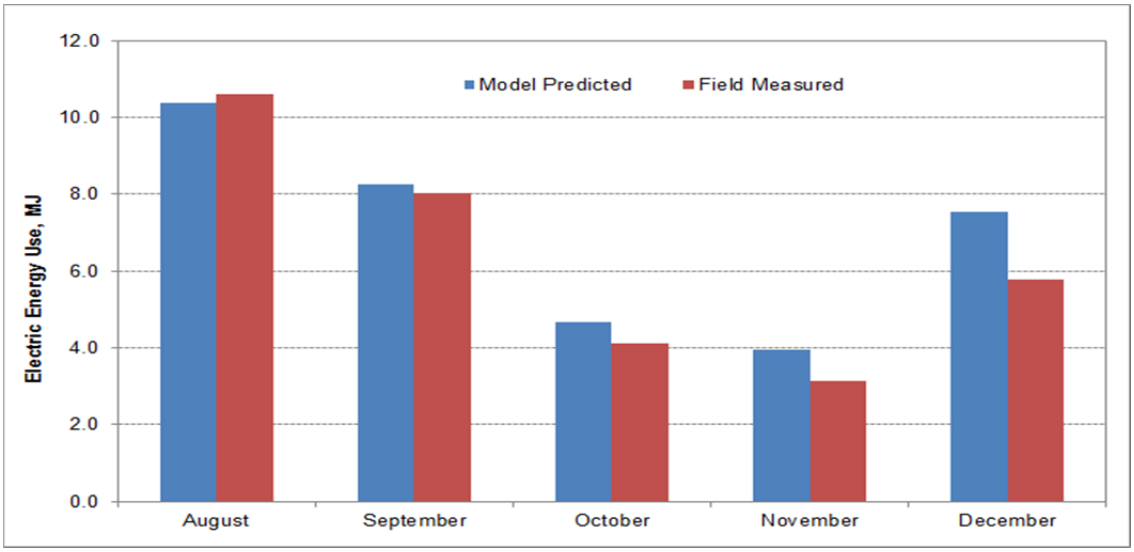

Figure 8-4 Predicted and Measured Monthly Total Electric Energy Use

The variation of daily total electric energy consumption with respect to temperature difference between zone return air and outdoor air is shown in Figure 8-5. Cooling energy consumption decreases as the delta temperature decreases until it reaches a balance point where the heating load starts to pick up and heating energy consumption increases. Figure 8-6 shows field measured and model predicted daily electric energy use. As can be seen in the graph, measured and predicted data are mostly in good agreement (±25%) with some discrepancies at low energy consumption. This discrepancy can be attributed to divergence of measured and predicted energy use in the heating season. The histogram plot in Figure 8-7 shows the distribution of the percent deviation between predicted and measured daily energy consumption. As can be seen in the graph, 72% of measured differences are within the ±25% error band and 79% of measured differences are within the ±35% error band. It can be concluded that the field measured and model predicted daily total electric energy use of the VRF system was found to be in good agreement.

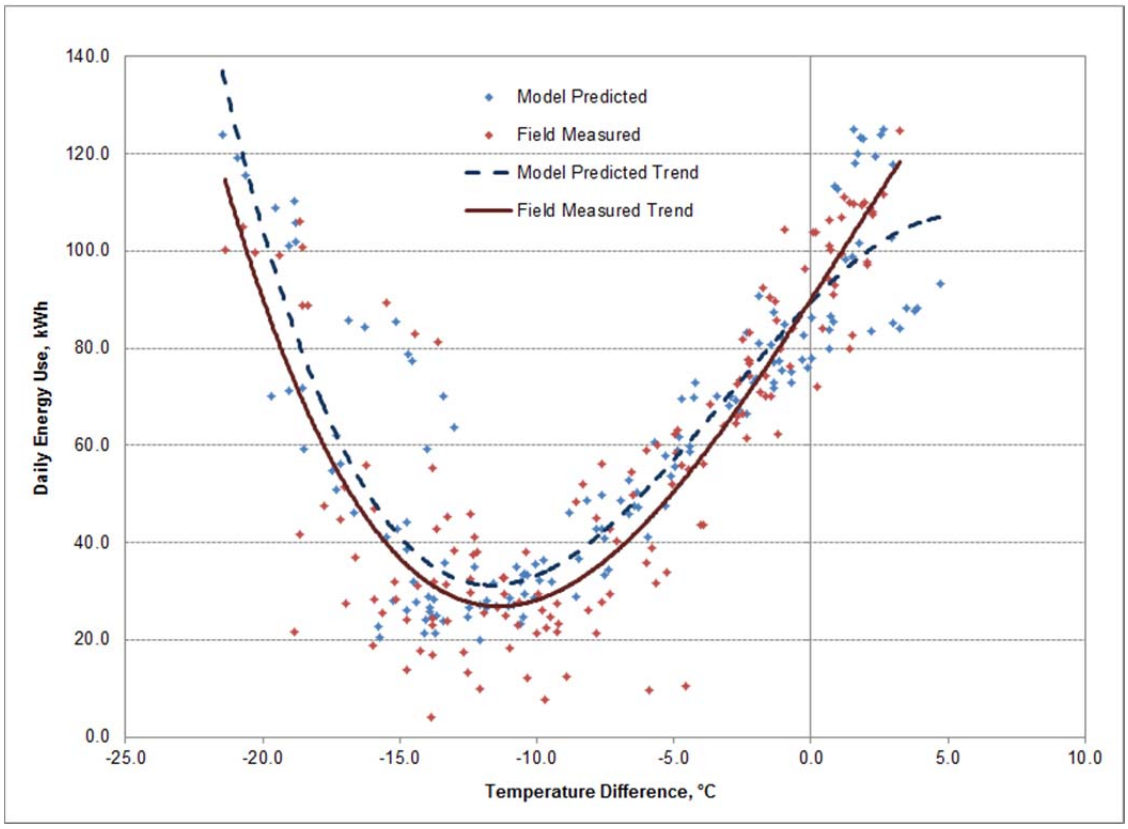

Figure 8-5 Daily Electric Energy Use Against Temperature Difference

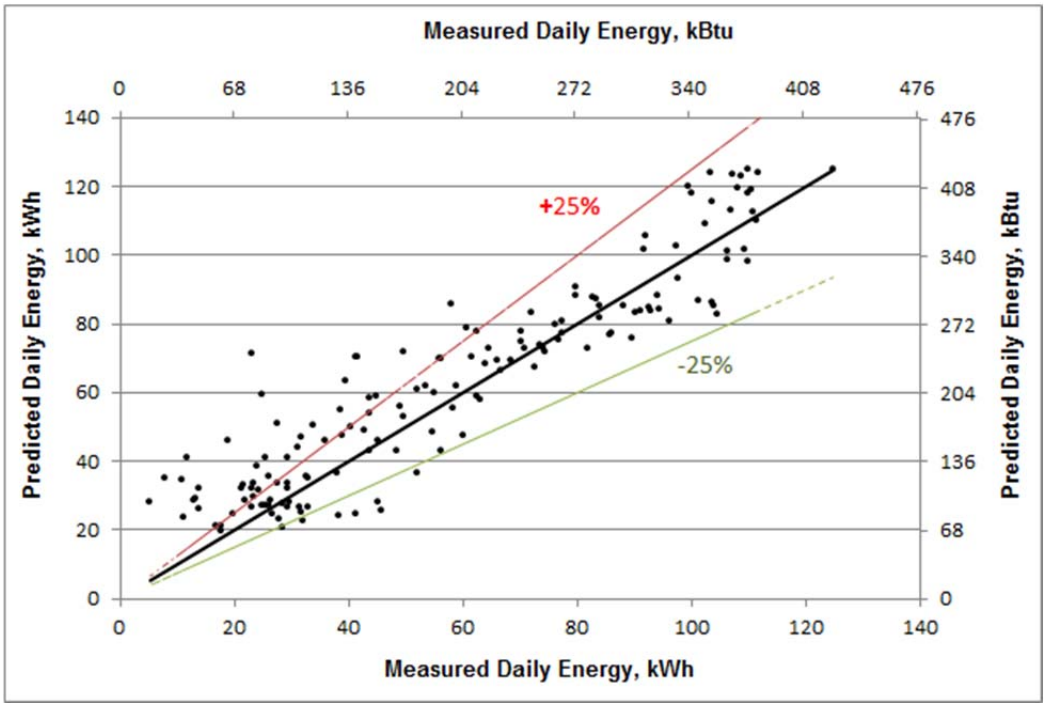

Figure 8-6 Comparison of Predicted and Measured Daily Total Electric Energy Use

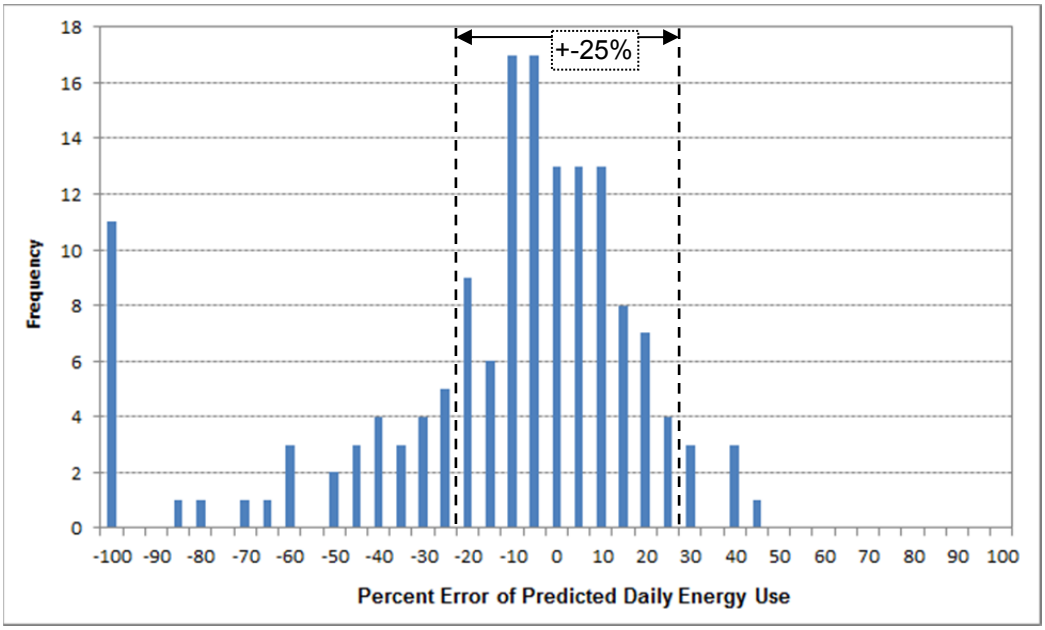

Figure 8-7 Daily Total Electric Energy Use Error Distribution

8.7 Statistical Analysis

In order to evaluate consistency and dependency of measured and simulated data, the sample correlation coefficient (r) is determined as follows:

$$r = \frac{\sum_{i=1}^{n}(X_s - \bar{X}_s)(X_m - \bar{X}_m)}{\sqrt{\sum_{i=1}^{n}(X_s - \bar{X}_s)^2}\sqrt{\sum_{i=1}^{n}(X_m - \bar{X}_m)^2}}$$

The calculated correlation coefficient is presented in Table 8-2. The correlation hypotheses that the predicted results accurately reflect the measured data are verified through a t-test (t = 29.4) with significance level (α) of 5%. The hypotheses of correlation coefficient are accepted.

Table 8-2 Sample correlation of measured and simulated data

Item	Total Power
Sample correlation coefficient (r)	0.93
Coefficient of Variation (Cv)	20%
Sample size	153

Coefficient of variation of root mean square error Cv between measured and simulated data is calculated as follows:

$$C_v = \frac{\sqrt{\frac{\sum_{i=1}^{n}(X_s - X_m)^2}{n}}}{\bar{X}_s}$$

Cv is a normalized measure of the variability of root mean square error between measured and model predicted daily total electric energy consumption. In this case, Cv is calculated as 20% which is a reasonable variability between measured and simulated data given the uncertainty in model inputs (i.e., weather data, internal loads, infiltration, etc.).

8.8 Discussion and Conclusion

In this study, the EnergyPlus VRF heat pump computer model predicted results were compared against field measured data. For the comparison of measured data and simulation outputs, EPRI's field test building was created as an input to the EnergyPlus simulation program. Other inputs to the EnergyPlus model consisted of the VRF system model based on lab-measured rated performance, occupancy of the building, lighting and plug loads, thermostat set-points, etc. The infiltration rates were based on the DOE's EnergyPlus reference building inputs. These infiltration rate levels were adjusted once to tune the computer model to represent the laboratory use conditions and then subsequent field measurements were compared to the simulation results. Other detailed infiltration models could not be used because of the absence of measured wind speed and direction data at the test facility. For increased accuracy in the comparison, a customized weather file was created by replacing the local TMY outdoor temperature and relative humidity with measured data. Findings of the validation can be summarized as follows:

- About 73% of the measured and simulated total daily electric energy are within a ±25% error band, and about 80% of the measured and simulated total daily electric energy are within a ±35% error band.
- The sample correlation coefficient (r) between measured and simulated total daily electric energy is about 0.93, which reflects a high correlation. Coefficient of correlation is verified and the hypotheses are accepted through t-test.
- Variability of normalized room mean square error, i.e., coefficient of variation (Cv), is about 20%, which shows measured and simulated data have small variability.

Some of the important input parameters for the simulation were measured inadequately in this project, hence, a wide range of uncertainty in some of the simulation input parameters was expected. For example, accurate information regarding internal loads, infiltration, solar radiation, etc., would have helped the model to better predict the energy calculation with higher certainty. Future field tests of VRF systems are highly recommended and should focus on sub metering internal loads and using real weather data to demonstrate the accuracy of the model prediction.

9 Parametric Analysis using the EnergyPlus VRF System Model

9.1 Introduction

Variable Refrigerant Flow HVAC systems, although not new, are gaining more popularity in American HVAC markets. For this reason, the Department of Energy (DOE) sponsored this project to incorporate a variable refrigerant flow (VRF) heat pump and heat recovery computer model in DOE's EnergyPlus building simulation software. The VRF computer model is described in detail in the EnergyPlus reference documents (U.S. Department of Energy, 2012b, and Raustad, 2013). As part of this project, the potential benefits of VRF systems were investigated fully through parametric simulation studies. In this chapter, EnergyPlus simulations are discussed and provide a performance comparison between VRF systems and conventional HVAC systems. The conventional systems described here include central variable-air-volume and large rooftop packaged systems. The systems were compared using four different building types and in one representative city from each of the eight U.S. climate zones. The VRF system benefits investigation include: impacts of duct conduction losses, air distribution losses (duct leakage), fan energy use, system efficiency, and simultaneous heating and cooling operation. Most VRF installations require no ducts to supply air except when providing outdoor air or delivering air to common areas. Thus, the VRF system may benefit in first cost and energy cost savings by eliminating all or part of the ducts. Fan energy is another area of potential energy saving for the VRF system. Complete or partial elimination of ducts in VRF systems has a direct consequence of reducing the total external pressure that the supply air fan needs to overcome. VRF systems are also expected to show energy saving as a consequence of variable speed compressor operation. Simultaneous heating and cooling operation is another feature that allows the VRF system to excel in energy efficiency compared to the traditional HVAC systems. However, for the heat recovery operating mode to be efficient compared to heat pump mode there must be a high diversity of cooling and heating loads in a building given the penalty imposed as described in Chapter 5. This study identifies and quantifies the energy saving potential of VRF systems compared to conventional HVAC systems. These simulations also evaluate thermal comfort, potential reduction in CO_2 emissions and the energy cost savings. The details of the parametric analysis is available in Task 9 Final Report (Nigusse et al., 2013)

9.2 Building Models

For each of the four building types listed in Table 9-1 the original reference building model was simulated. A modified reference building model was also created to incorporate building features necessary to compare energy use of VRF systems using ductless terminal units to conventional HVAC system types with ducts installed in unconditioned space. A duct conduction loss model was included for all building types and a duct leakage model was included for the large office building as this is the only

reference building to model a return plenum which is currently an EnergyPlus requirement for modeling duct leakage.

Table 9-1 Building Models Used for Parametric Evaluation of VRF systems

Reference Building	Floor Area ft^2 [m^2]	Number of Floors	Heating Type	Cooling Type	ASHRAE System Type
Small Office	5,500 [511]	1	Fossil fuel Furnace	Packaged DX	PSZ-AC
Large Office	498,588 [46,320]	12	Hot-water fossil fuel Boiler	Chilled Water	VAV with Reheat
Stand Alone Retail	24,962 [2,319]	1	Fossil fuel Furnace	Packaged DX	PSZ-AC
Large Hotel	122,120 [11,345]	6	Hot-water fossil fuel Boiler	Chilled Water	VAV with Reheat

9.3 HVAC Types and Models

In addition to the reference HVAC systems, conventional heat pumps were simulated in the small office and standalone retail building types. The heat pump was included as an alternate system type to compare to conventional DX cooling equipment using a fossil fuel heating system. Supplemental heating and cooling systems were added to the VRF heat pump systems to bring the number of hours the thermostat set point was not met while occupied towards zero when the VRF systems were off due to operational temperature limits. Table 9-2 summarizes the various HVAC systems investigated in this study. Several minor changes were also made to the original reference buildings inputs to include necessary changes to accurately comply with modeling VRF equipment and are designated as the modified reference building [Ref Modified]. The various changes made to the reference building model and the VRF system are described in Task 9 final report (Nigusse et al., 2013).

Table 9-2 Simulation Input Summary

Mnemonic	**Description**
Ref Original	Original DOE reference building
Ref Modified	Modified sizing SAT and economizer controls, added attic space for stand-alone retail
Ref Modified Duct	Supply duct conduction loss model
Ref Modified Duct Leak	Supply duct conduction loss plus leakage model for large office only
Heat Pump	Electric cooling and heating for small office and stand-alone retail
VRF Manu BB	VRF using manufacturers COP with electric baseboard backup
VRF Lab BB	VRF using lab measured COP with electric baseboard backup
VRF Manu UH	VRF using manufactures COP with gas heating backup
VRF Lab UH	VRF using lab measured COP with gas heating backup

Note: Heat pump and VRF systems also use window AC as a backup cooling source

The DOE reference buildings do not model duct conduction losses, which is a crucial contributor to increased HVAC energy use when ducts are installed in the unconditioned space or plenum. The VRF system, which may not require ducts and therefore will minimize duct conduction losses, shows the greatest potential for energy savings compared to conventional systems with ducts installed in the attic or unconditioned space. In order to compare the VRF system to a central air-loop system with ducts installed in the attic, a duct conduction loss model was added to the modified reference models. The modified reference model with a supply-duct conduction loss model is designated as [Ref Modified Duct] as shown in Table 9-2. Sizing factors of the reference systems with ducts were increased to match the increased cooling and heating demand imposed by duct conduction losses. These values were selected in order to maintain the annual unmet setpoint hours of the Ref Modified Duct model to acceptable limits (less than 300 hours) per ASHRAE Standard 90.1 (ASHRAE, 2007). Studies have shown that commercial buildings may require up to 25.0% increase in capacity to overcome duct conduction losses (Fisk et al., 2000). Since EnergyPlus requires a return plenum to model supply air leakage, a duct leakage model was added for the large office building as this is the only reference building to have a return plenum in the model. Thus, for large office, another modified reference model [Ref Modified Duct Leak] was created to expand upon the duct model to include duct leakage. The small office and standalone retail buildings were also modeled using a unitary system heat pump with electric backup heating system. The modified reference duct model [Ref Modified Duct] is the baseline model for comparing with the VRF system.

9.4 Duct Heat Transfer and Leakage Model

The duct impact was investigated by adding a duct heat transfer model to the supply side of an air loop. The duct heat transfer model accounts for sensible conduction losses. The duct conduction loss model is a steady-state model and is based on a user-defined heat exchanger model (Nigusse et al., 2013). This duct model assumes a constant duct UA value and constant plenum zone air temperature. The air-to-air U-value is assumed to be 1.13 $W/m^2 \cdot °C$ (0.20 $Btu/(hr \cdot ft^2 \cdot °F)$). The duct heat transfer area is assumed to be about 24% of the conditioned floor area served by the air loop. Surface area of supply ducts in large commercial buildings can be approximately 30%-40% of building floor area (Fisk et al., 2000, and Parker et al., 1998). The EnergyPlus duct leakage model allows specifying fixed duct leakage fractions before and after the VAV box of the air distribution units. The amount of supply air leakage is directed to the return air plenum. Out of the four DOE reference buildings investigated, only the large office building had a return plenum. Therefore, the duct leakage model was investigated solely in the large office building. Supply air leakage fractions of 4% and 3% upstream and downstream of the VAV box, respectively, were selected for this investigation. The total effective supply air leak equates to 6.9% of the supply air flow rate.

9.5 Model Inputs and Assumptions

The VRF equivalent building models were created upon the modified reference model. The cooling and heating systems were replaced by VRF systems with backup cooling and heating systems. Each VRF system was modeled with the manufacturer's listed coefficient of performance (COP) and laboratory measured COP. In addition, each VRF system was modeled with two backup heating systems: electric baseboard heaters and gas unit heaters. The combination of backup heating systems and COPs results in four VRF system test cases for each of the four building types listed in Table 9-2. The values assumed for efficiency of systems, gas coil efficiency, baseboard heater efficiency, unit heater efficiency, fan pressure rise, fan efficiency, fan motor efficiency, boiler efficiency, gas coil efficiencies and electric coil efficiencies are described in Task 9 final report (Nigusse et al., 2013). Each simulation was run in all eight climate zones in the United States using TMY3 data. The eight climate locations simulated were: Miami, FL, Phoenix, AZ, Los Angeles, CAL, Albuquerque, NM, Chicago, IL, Minneapolis, MN, Duluth, MN, and Fairbanks, AK.

9.6 Parametric Analysis Results

The parametric analysis was intended to demonstrate the usability of the VRF computer model in EnergyPlus. The benefits of VRF systems compared to the conventional systems such as VAV and packaged roof top (RTU) HVAC systems are also shown. The analysis quantifies the energy saving potentials, thermal comfort, carbon equivalent emission reduction and total energy cost savings of VRF systems. The modified reference duct model [Ref Modified Duct] is used as a baseline model to quantify the relative performance of the systems investigated. A positive value indicates energy savings and a negative value shows more energy use (inefficient) compared to the baseline HVAC system model. The energy savings unless and otherwise stated is calculated using Eq-45.

$$EnergySaving = 100 \cdot \frac{Ref\ Modified\ Duct - X\ Model}{Ref\ Modified\ Duct} \quad (45)$$

Where X Model represents the various models listed in Table 9-2. The comparative analysis was conducted on energy use, thermal comfort, carbon equivalent emissions, and energy use cost.

9.6.1 Comparative Energy Use

The energy use analysis looks at the VRF and conventional HVAC systems annual total energy use by building type. In this comparison annual total energy savings, impacts of duct losses, and fan energy savings were analyzed. The analysis was conducted for the four building types: large office, small office, standalone retail, and large hotel buildings and the results for the VRF system using heat recovery are summarized by building type.

9.6.1.1 Large Office Building

The large office building reference HVAC model uses central air VAV systems. A single central air VAV system serves each floor. Each floor, with the exception of the basement, is represented by four perimeter zones and a core zone. Each air loop has a central chilled water cooling coil, a hot water heating coil and air terminal hot water reheat coils serving each zone. Figure 9-1 shows the total energy use of a large office building in the eight climate zones. The large office building VRF system energy savings were estimated for two reference models: one with typical duct installed in a return plenum zone, and the other with leaky ducts in a plenum zone. The former considers duct conduction losses while the latter considers both duct conduction losses and duct air leakage. Table 9-3 summarized the predicted energy savings potentials of VRF system in a large office building.

Table 9-3 Large Office Building VRF System Total Energy Savings Potential

Cities	Savings Over Reference Modified Duct Model, %	Savings Over Reference Modified Duct Leak Model, %
Miami, FL	13.0 - 22.6	21.6 - 30.2
Los Angeles, CA	22.1 - 25.2	29.8 - 32.6
Phoenix, AZ	15.3 - 23.6	24.0 - 31.5
Albuquerque, NM	10.5 - 15.5	19.7 - 24.1
Chicago, IL	23.1 - 26.3	31.2 - 34.1
Minneapolis, MN	24.2 - 27.2	31.3 - 34.0
Duluth, N	26.8 - 28.8	33.7 - 35.5
Fairbanks, AK	24.4 - 28.0	28.7 - 32.0

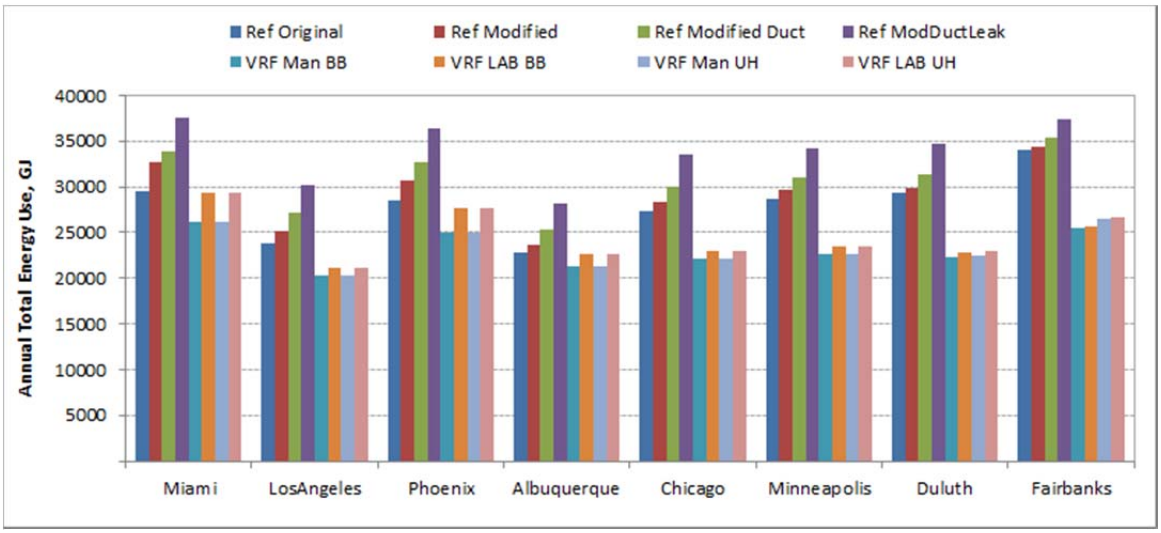

Figure 9-1 Annual Total Energy Use in Large Office Building

The total energy use of the modified reference [Ref Modified] model shows a slight increase compared to the original reference [Ref Original] model due to changes in the model input assumptions

(e.g., design supply air temperatures, economizer controls, etc.). Impacts of such changes are consistent across the eight climate zones. Also the modified reference duct model [Ref Modified Duct] shows a consistent increase in total energy use compared to the modified reference model [Ref Modified] due to duct conduction losses. In the large office building duct conduction losses amounts to 3%-7% of total energy use depending on climate. This is a potential energy saving for VRF systems since it eliminates or minimized the use of ducts. Figure 9-2 shows the VRF system percent energy savings in a large office building. In general, the VRF system shows energy savings compared to the reference modified duct model and the energy savings increase in colder climates. These savings are attributed to the elimination of duct conduction losses, system efficiency differences, and fan energy savings. In Miami, which is a cooling dominated climate, the VRF system total energy savings is due primarily to cooling and the total energy savings are 13.0% for laboratory measured cooling COP and 22.6% for manufacturers cooling COP. Duluth shows annual total energy savings of 29.0%. The reason for increased saving in cold climate in part is due to the difference in efficiency of the heating systems; the reference system uses central hot water system with 78% efficiency and the VRF system has heating COPs of 3.921 and 3.874 for laboratory measured and manufacturer reported values, respectively. The VRF system also uses a backup heating system with 80% efficiency for gas unit heater and 97% efficiency for electric baseboard heater. In heating mode, when the VRF system is active, the VRF may use up to 4.9 times less heating energy depending on the outdoor air temperature. The VRF system in the large office building has a dedicated outdoor air system (DOAS) and the outdoor air system economizer can operate in free cooling mode when the outdoor conditions are favorable. In Los Angeles the amount of outside air used for free cooling sometimes were more than three times the minimum ventilation requirement. In addition to the DOAS variable-speed fan, the VRF system has a constant speed fan for the VRF terminal units and backup cooling and heating system. Given the use of excess economizer ventilation, fan energy use is shown to increase substantially for Los Angeles, moderately for Miami, and marginally for Albuquerque. The remaining five locations show fan energy savings.

In these simulations, the large office VRF DOAS system should have instead been designed for the minimum ventilation requirement only with minimal static pressure rise to realize fan energy savings. Energy lost due to supply air duct leaks in large office buildings has been investigated and can be as high as 6%-12% of the modified reference duct model total energy use depending on location. Had the modified reference duct leak model been the reference for energy saving calculation, the VRF system energy savings potential would have been in the range of 20%-36%.

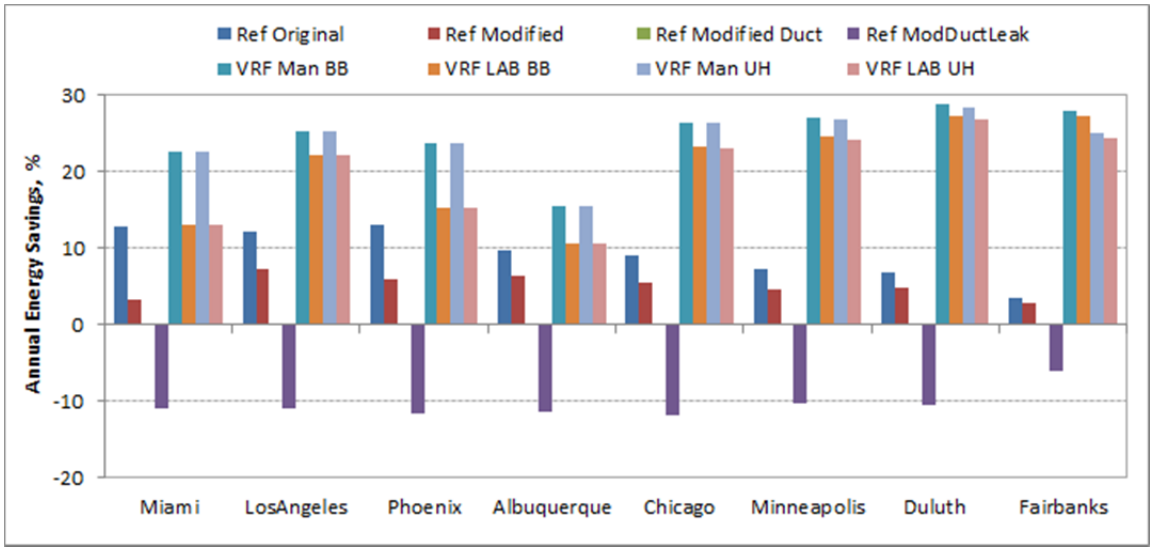

Figure 9-2 Annual Total Energy Savings in Large Office Building

9.6.1.2 Small Office Building

Since the small office reference model does not have return plenum, the duct leakage model cannot be modeled. In the small office reference HVAC models each thermal zone is served with a constant volume system. Similarly, in the heat pump reference model each thermal zone is served with a single packaged heat pump. The VRF and the heat pump systems total energy use show similar trends across all climate zones. The packaged heat pump uses slightly higher energy compared to the VRF in all climates mainly for two reasons: higher fan energy, and a difference in system COP. Table 9-4 summarized the energy saving potential of VRF systems compared to the reference models for a small office building. In Miami and Phoenix, the VRF system with laboratory measured COP shows higher energy use compared to the heat pump HVAC system in part due to differences in the COP.

Table 9-4 Small Office Building VRF System Total Energy Savings Potential

Cities	Savings Over Reference Modified Duct Model, %	Savings Over Heat Pump System Model, %
Miami, FL	3.1 - 12.8	-9.0 - 1.9
Los Angeles, CA	12.7 - 15.4	3.0 - 6.0
Phoenix, AZ	11.0 - 19.1	-8.2 - 1.6
Albuquerque, NM	19.1 - 22.1	1.8 - 5.5
Chicago, IL	24.2 - 27.1	1.8 - 5.5
Minneapolis, MN	27.5 - 30.2	4.5 - 8.1
Duluth, N	30.9 - 32.8	9.3 - 11.8
Fairbanks, AK	32.9 - 35.9	10.4 - 14.4

The small office is a single story building hence the impact of the outside boundary condition on a duct installed in attic space is significant compared to the multi-story commercial buildings. This is evident from the comparison of energy savings potential with the large office building. The modified reference duct model [Ref Modified Duct] shows a consistent increase in total energy use compared to the modified reference model [Ref Modified] due to duct conduction losses as shown in Figure 9-3. Since the small office is a single story building, unlike the large office building, the attic temperature can be significantly higher in summer and lower in winter. Hence, impacts of duct conduction losses amounts to 11% to 20% of total energy use depending on climate. This is more than twice the values predicted for multi-story large office building. Similar to the large office building results, the VRF system in a small office building also shows potential energy savings compared to the reference model and the savings increase for colder climates. In Miami, the percent total energy savings are 3.1% for laboratory measured COP and 12.7% for manufacturer COP as shown in Figure 9-4. The VRF system total energy savings can be as high as 35.9% depending on location and system COP. Due to the difference in efficiency of the heating systems, Fairbanks shows the highest total energy savings (although electric heat pump heating may not typically be used in this cold climate).

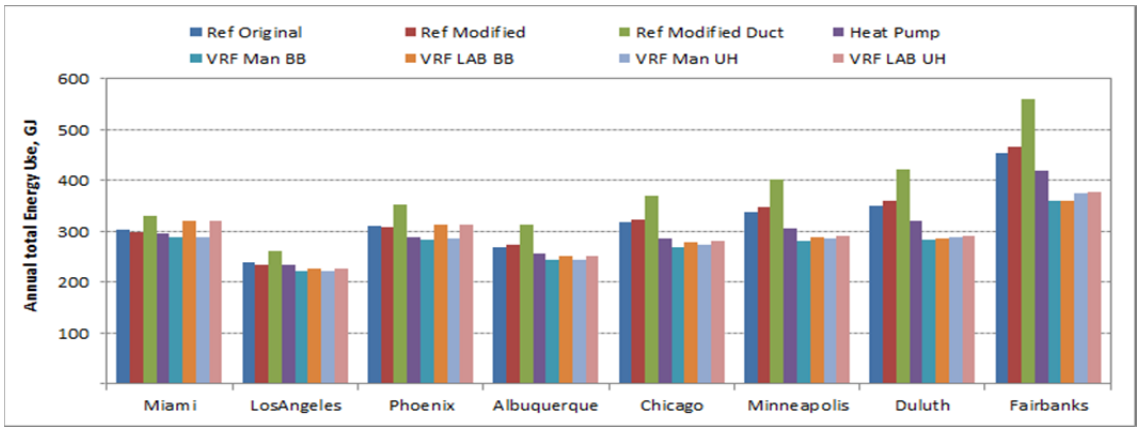

Figure 9-3 Annual Total Energy Use in Small Office Building

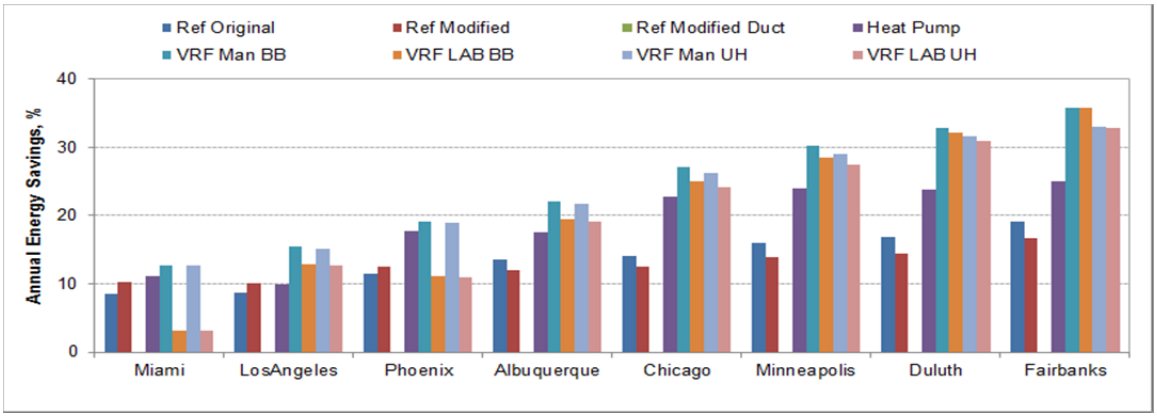

Figure 9-4 Annual Total Energy Savings in Percent for Small Office Building

All HVAC systems in the small office building use a constant volume fan. The VRF system air terminal unit fan needs to overcome the pressure drop across a single coil and hence the pressure rise requirements are small and typically in the range 50-75 Pa depending on the configuration of the terminal units. This pressure rise was selected to represent the measured fan power of approximately 100W measured during the EPRI laboratory tests. The VRF terminal units total pressure rise was increased to 150 Pa to compensate for the additional pressure rise required to deliver a fixed amount of outdoor air for ventilation. Since the VRF air terminal unit fan has a low external static pressure compared to the ducted model, the small office fan energy savings were as high as 84% compared to the modified reference duct model (Nigusse et al., 2013). Similarly the heat pump model can save up to 45% of fan energy compared to the modified reference duct model. The small office heat pump fan energy saving is attributed to increased supply air requirement for the modified reference duct model due to duct conduction loss. The duct condition loss increases the system load and the design supply air flow rates hence proportionally increases the fan energy use of the modified reference duct model.

9.6.1.3 Standalone Retail Building

The original reference standalone retail building did not have an attic or plenum zone thus a 1m high plenum zone was added by modifying the building geometry. This modification allowed the inclusion of a model for duct conduction losses. It was not possible to model duct air leakage losses for lack of a return plenum in the reference building model. Each thermal zone in the standalone retail building is served with a constant volume air loop system. Table 9-5 summarized the energy saving potential of VRF systems compared to the reference HVAC models for a standalone retail building.

Table 9-5 Standalone Retail Building VRF System Total Energy Savings Potential

Cities	Savings Over Reference Modified Duct Model, %	Savings Over Heat Pump System Model, %
Miami, FL	7.9 - 18.7	-0.1 - 11.6
Los Angeles, CA	18.9 - 21.4	10.2 - 13
Phoenix, AZ	15.1 - 22.9	3.4 - 12.2
Albuquerque, NM	24.0 - 28.7	7.1 - 13.0
Chicago, IL	31.3 - 35.7	13.8 - 19.3
Minneapolis, MN	31.8 - 37.6	16.4 - 23.5
Duluth, N	29.4 - 36.1	16.8 - 24.6
Fairbanks, AK	18.9 - 28.7	11.8 - 22.4

The standalone retail modified reference building [Ref Modified] consumes less energy compared to the original reference building as shown in Figure 9-5 due to addition of 1m high attic space which now becomes the new boundary condition for the conditioned space below. This attic space acts as a barrier and reduces the net heat gain or loss of the conditioned thermal zone. Also keep in mind that this building type would not typically include a plenum space. The modified reference duct model [Ref Modified Duct] shows consistent increase in total energy use across all climate zones compared to the modified

reference model [Ref Modified] due to impacts of duct conduction losses. For the standalone-retail building the duct conduction loss increased the total energy use in the range 8%-38% depending on climate. The impact of duct conduction losses in retails buildings is higher than the office buildings in part due to longer operating hours. The standalone retail building VRF system shows potential total energy savings compared to the reference models and the savings increased for colder climates as shown in Figure 9-6. In Miami, the percent total energy savings are 8% and 19% for laboratory measured and manufacturer's published COP values, respectively. Minneapolis shows the highest total energy savings, and the savings can be as high as 38%. The reason for increased energy savings in a cold climate is the difference in efficiency of the heating systems. For the standalone retail building, the modified reference duct model [Ref Modified Duct] fan energy as percent of the total energy use ranges 8%-24% whereas the VRF system fan energy is in the range 1.6%-3.6%. This is mainly due to high central air system fan external static pressure compared to ductless VRF systems. Thus, fan energy savings for VRF system is much higher than conventional HVAC system types. The VRF can save 79% to 88% of the modified reference duct model fan energy.

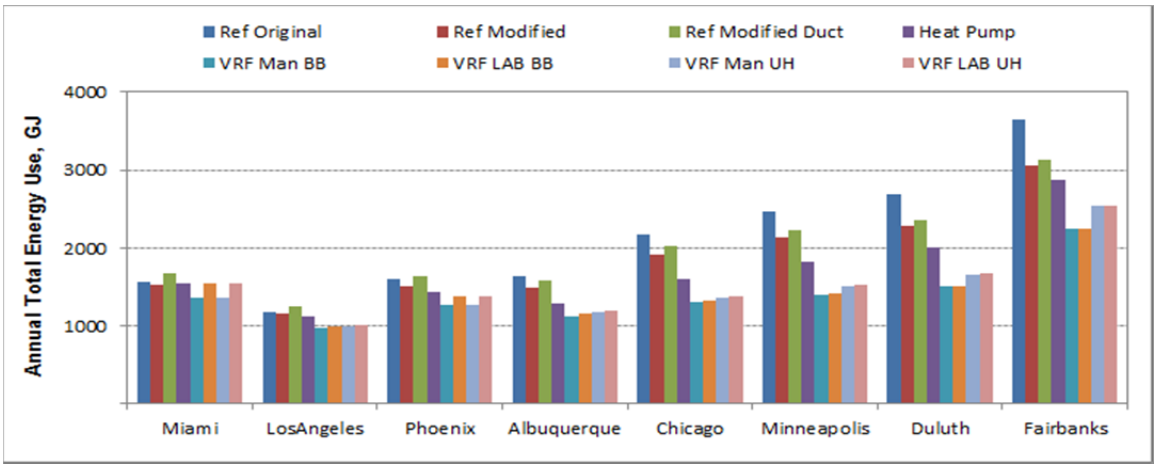

Figure 9-5 Annual Total Energy Use in Standalone Retail Building

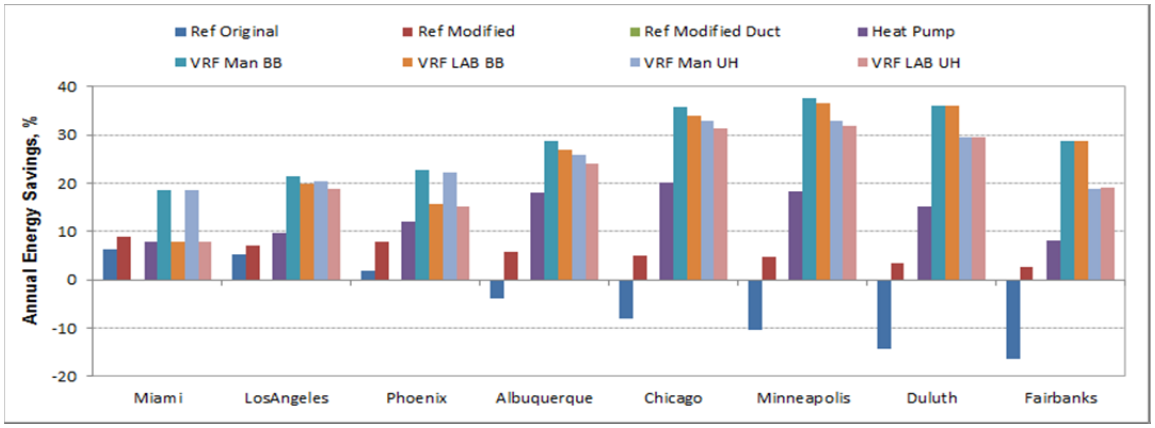

Figure 9-6 Annual Total Energy Savings in Standalone Retail Building

9.6.1.4 Large Hotel Building

The large hotel building reference building model is served with two different HVAC system types: a central VAV system for the common areas such as lobby, banquet, dinning, corridor, kitchen and laundry, with fan coil units used for the guest rooms. The outdoor air requirement of the guest rooms was served by a constant volume dedicated outdoor air system. For the VRF system all zones are served with air terminal units. The VAV system common area was converted into a DOAS for the VRF system with a potential to provide free cooling for the common areas. The constant volume air loop of the guest rooms was modified to provide a fixed amount of outdoor air. Since the large hotel building did not have a plenum zone the duct is assumed to be in the conditioned space. Therefore, energy savings from duct conduction loss is marginal in the large hotel building.

Table 9-6 summarized the VRF system energy savings potential in large hotel building. The modified reference duct model shows marginal energy use differences compared to the modified reference HVAC model since the duct model assumes that ducts are located in the conditioned space. Therefore, for large hotel building total energy savings contributors are primarily reduction of fan energy, and the difference in efficiency.

Table 9-6 Large Hotel Building VRF System Total Energy Savings Potential

Cities	Savings Over Reference Modified Duct Model, %
Miami, FL	-11.6 - -1.3
Los Angeles, CA	2.7 - 6.8
Phoenix, AZ	-8.1 - 0.9
Albuquerque, NM	2.6 - 8.5
Chicago, IL	11.6 - 17.1
Minneapolis, MN	13.4 - 18.9
Duluth, N	15.5 - 20.5
Fairbanks, AK	16.4 - 21.7

In large hotel buildings the VRF system with laboratory measured COP uses 12% more energy in Miami and about 8% more energy in Phoenix whereas VRF with manufacturers COP uses about 1% more energy in Miami, and saves 1% total energy in Phoenix. In cold climates, the VRF with laboratory measured COP in large hotel buildings show annual total energy savings of 12%-21% depending on the backup heating systems, and for manufacturers COP the savings range 14%-22%. The fan energy use as a percent of the total building energy is lower for the VRF system. For the large hotel building the modified reference duct model [Ref Modified Duct] fan energy as percent of the total building energy use ranges 4.4%-8.3% whereas the VRF system ranges 2.1%-3.7% (Nigusse et al., 2013). This is mainly due to the high external fan pressure for central air systems compared to ductless VRF systems. The annual fan energy savings of the VRF system compared to the modified reference duct model fan energy use ranges 54%-63%. The fan energy savings predicted for the large hotel building model amounts to 3%-5% of the total energy use of the modified reference duct HVAC model.

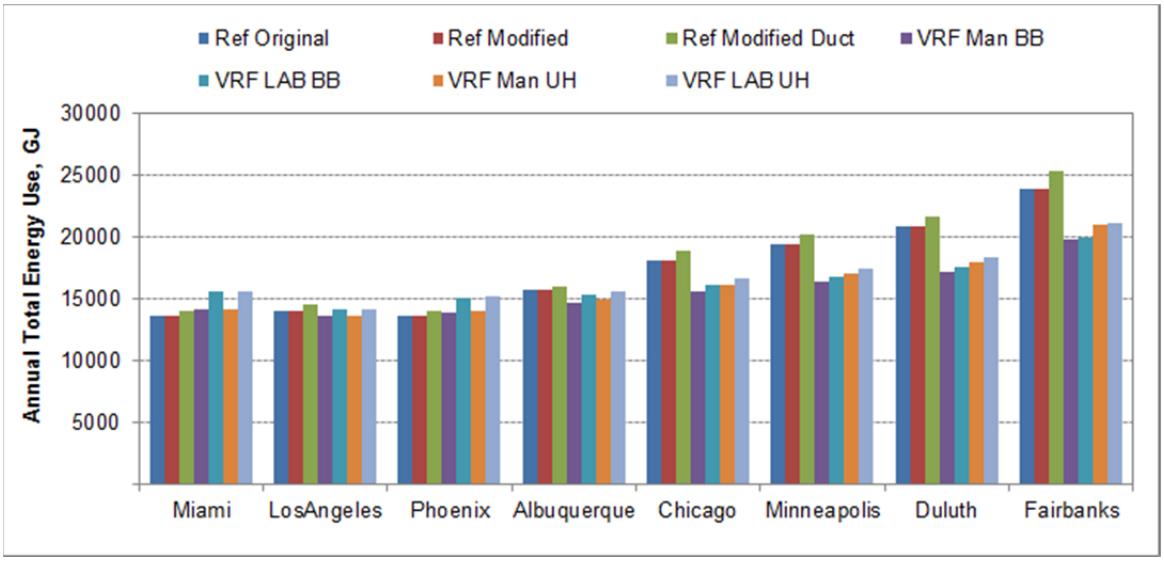

Figure 9-7 Annual Total Energy Use in Large Hotel Building

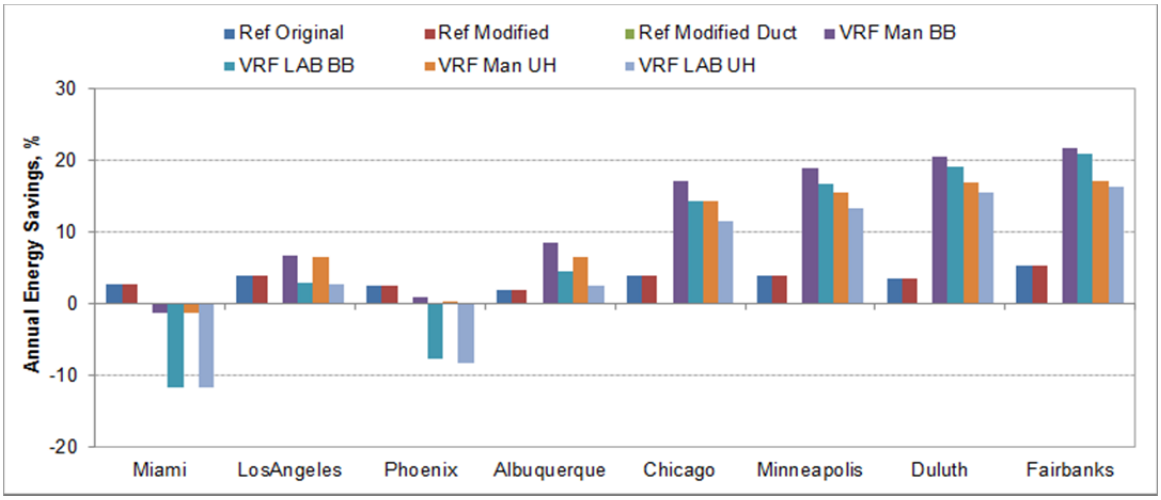

Figure 9-8 Annual Total Energy Savings in Large Hotel Building

9.6.2 Comparative Thermal Comfort

Comparison of annual energy saving potential of the VRF system and the conventional systems needs to be done under identical or equivalent thermal comfort levels. This condition was verified and confirmed by calculating the thermal comfort level of the four building types and HVAC models analyzed. Thermal comfort variables analyzed here include: building average heating and cooling setpoint not met hours while occupied, ASHRAE's thermal sensation scale predicted mean vote (PMV), and the building average relative humidity. Each of these variables were calculated and analyzed. The sizing factors specified in the reference models were increased such that the annual hourly setpoint unmet hours were maintained under 300 as recommended in ANSI/ASHRAE/IESNA Standard 90.1-2007 (ASHRAE, 2007) recommendation. This confirms that the energy use comparisons were made under comparable indoor

thermal comfort levels. ASHRAE's perceived thermal sensation scale is used to report thermal comfort levels. The level of thermal comfort perceived is measured using PMV and the scale ranges between -4.0 to +4.0. The building average indoor relative humidity was also calculated by weighing the individual conditioned zones relative humidity using the zone volume. The building average relative humidity exceeded 65%for the VRF system was higher than the other HVAC system in humid weather climates for all four building types investigated. This is attributed to the difference between the VRF and the regular DX cooling coil model in splitting the total cooling load delivered into the latent and sensible components. The VRF indoor dx cooling coils in general results in higher sensible heat ratio hence higher indoor relative humidity. This modeling aspect may be a result of assuming the VRF terminal unit cooling coil modulates capacity when in reality it may run fully loaded (i.e., a much colder coil surface temperature) and cycle to meet the zone load which would ultimately result in lower zone humidity levels. This specific result, that is the VRF model yields higher indoor humidity, requires further investigation as to the cause. The predicted thermal comfort level results is described by building type as follows.

9.6.2.1 Large Office Building

In all cases, the annual setpoint not met hours was less than 236 hours, and this value is under the maximum threshold of 300 hours required by ANSI/ASHRAE/ISEAN Standard 90.1-2007 for building performance computer models comparison. For some climate zones simulated the unmet hours were zero or near zero. In the cooling season, Albuquerque shows maximum annual unmet hours of 235. This is related to the operation of the DOAS in free cooling mode. Figure 9-9 shows the ASHRAE's perceived thermal sensation scale predicted for large office building. For the large office building and eight locations the Fanger PMV values falls between +0.16 and -0.56. These results imply that the large office occupants in Miami perceive nearly neutral thermal sensation. In the remaining locations occupants may perceive nearly neutral or slightly cool thermal sensation.

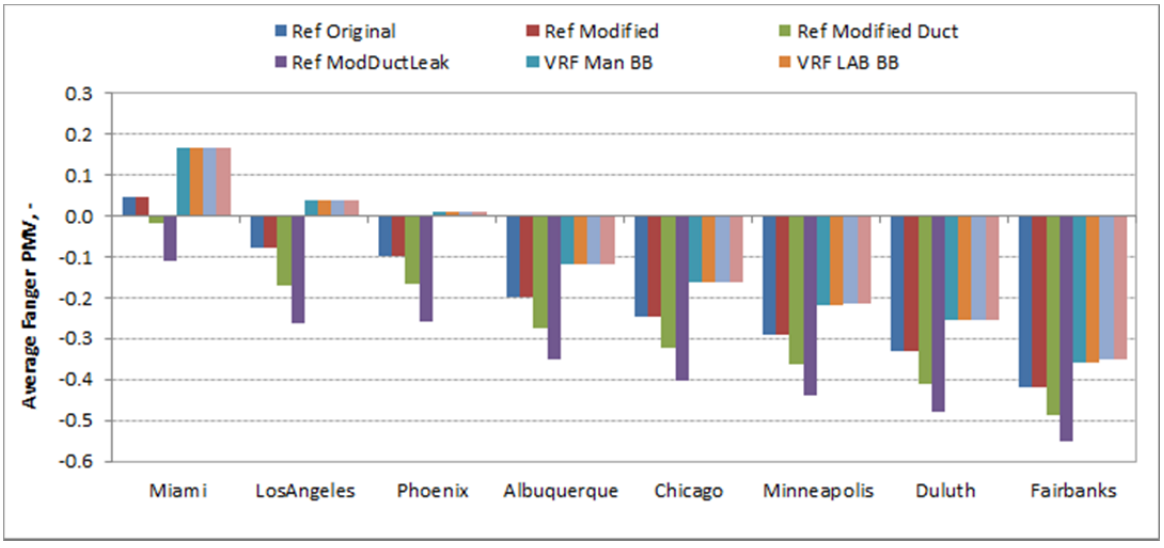

Figure 9-9 Annual Average Fanger PMV Values for Large Office Building

9.6.2.2 Small Office Building

The annual heating temperature set points unmet hours for small office building are well under 100 hours. Annual cooling temperature set points unmet hours are well under 223 hours. The Fanger PMV value calculated for small office falls between +0.14 and -0.58 as shown in Figure 9-10. In Miami occupants in a small office building on average perceive nearly neutral thermal sensation and in the remaining seven climate zones on average occupants feel nearly neutral or slightly cool thermal sensation but with an increasing trend as we go to colder climates. This result is consistent across all HVAC systems investigated.

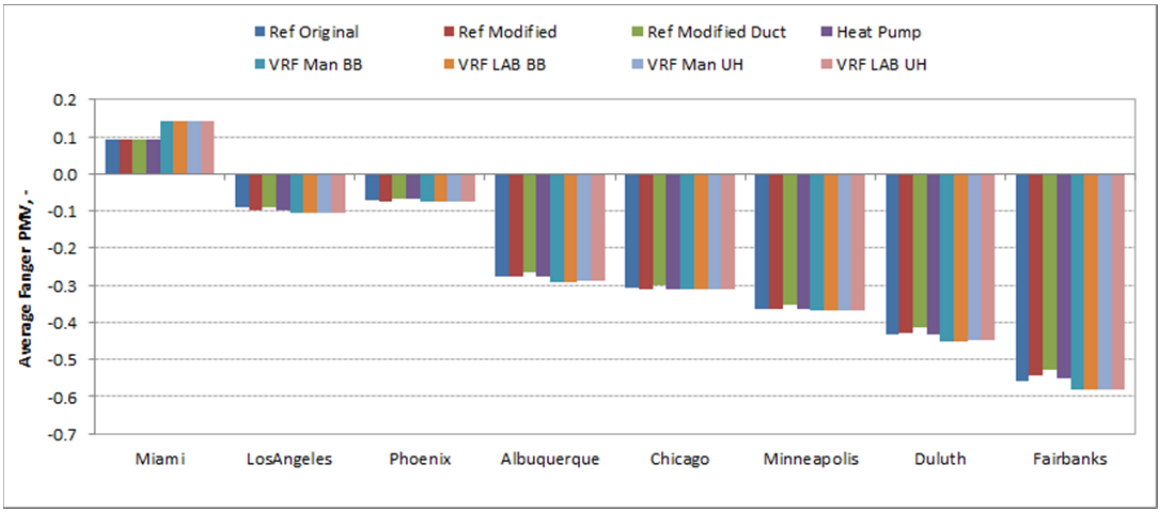

Figure 9-10 Annual Average Fanger PMV Value in Small Office Building

9.6.2.3 Standalone Retail Building

The standalone retail building average indoor air temperatures setpoint unmet hours is well below the maximum limit of 300 hours. The heating setpoint temperature unmet hours is below 113 for all system types across the eight climate zones. The highest heating setpoint unmet hours occurs in Fairbanks. This is probably due to capacity limits when the VRF system is off (e.g. outdoor temperature limits) and the backup heating system could not meet the entire heating load. All the systems in all locations maintained similar indoor air temperature levels acceptable for building performance comparison. ASHRAE's perceived thermal sensation scale, the Fanger PMV value predicted for standalone retail building falls between +0.11 and -0.60 as shown in Figure 9-11. This means that in Miami, on average, occupants perceive close to neutral thermal sensation and for the remaining locations the occupants feel nearly neutral or slightly cool thermal sensation.

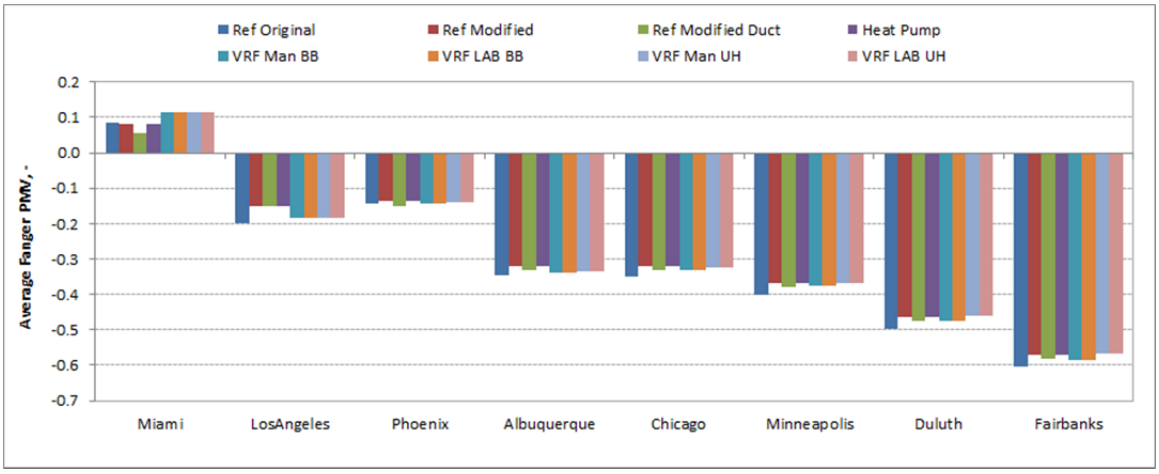

Figure 9-11 Annual Average Fanger PMV Value in Standalone Retail Building

9.6.2.4 Large Hotel Building

The large hotel building average indoor air temperatures heating setpoint temperature unmet hours is below 300 for all system types across the eight climate zones investigated. The highest heating setpoint unmet hours occurs in Fairbanks but it was within acceptable limits. The cooling setpoint temperature unmet hours was acceptable for all HVAC models. For Miami, the cooling setpoint unmet hours for the VRF HVAC model was under 143 and for Phoenix, it was under 181 hours. The PMV value calculated for large hotel falls between +0.80 and -0.50 as shown in Figure 9-12. This means that in warmer climates such as Miami, Los Angeles, and Phoenix, occupants feel slightly warm thermal sensation. In cold climates occupants feel neutral or slightly cool thermal sensation. For the remaining locations on average occupants feel almost neutral thermal sensation.

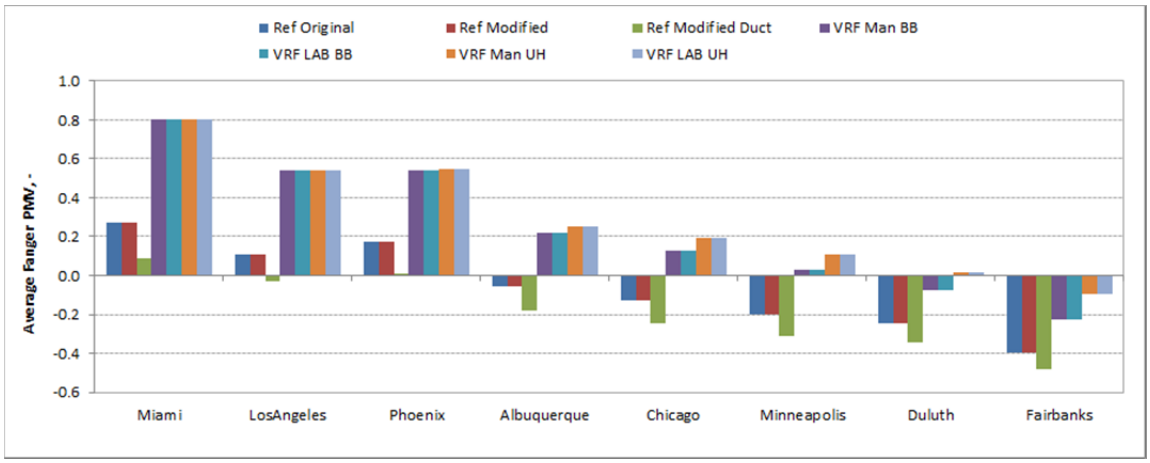

Figure 9-12 Annual Average Fanger PMV Value in Large Hotel Building

9.6.3 Comparative CO2 Emissions

Carbon equivalent emissions for the four building types and the various HVAC systems have been determined. The total emissions depend on the source and emission factors and the magnitude of energy consumption of a particular building. For a given site location these factors depend on energy conversion efficiency and the fuel type. For each of the eight locations investigated the factors were taken from the DOE EnergyPlus reference buildings model (Torcellini et. al., 2008). Carbon equivalent emission factors used here are higher for electricity compared to natural gas. The calculated carbon equivalent emissions are proportional to the total energy for the four building types. But the carbon equivalent emissions reduction is not necessarily directly proportional to the total energy savings because of the differences in fuel type between the reference and VRF HVAC systems. The cooling systems in the reference and the VRF HVAC models are driven by electricity hence for cooling dominated climates the emission reductions are proportional to the energy savings. In heating dominated climates the reference HVAC system uses fossil fuel while the VRF HVAC system uses electricity unless the system is off due to operating temperature limits. Hence, in heating dominated climates the emission reduction may not be proportional to the energy savings due to difference in source and emission factors.

9.6.3.1 Large Office Building

With the exception of the modified reference duct leakage model [Ref Modified Duct Leak], the large office VRF HVAC models show a reduction in annual emissions compared to the modified reference duct building model [Ref Modified Duct] as shown in Figure 9-13. The large office annual emissions reduction varies from 45 tons to 384 tons with location depending on COP of the VRF systems. The reference duct leak model for large office building shows an increase in emissions across all climate zones due to increase energy use attributed to supply air leakage. The VRF system with electric baseboard backup heating system showed an increase in emissions for Fairbanks due to higher source factors for electricity compared to a natural gas backup heating system.

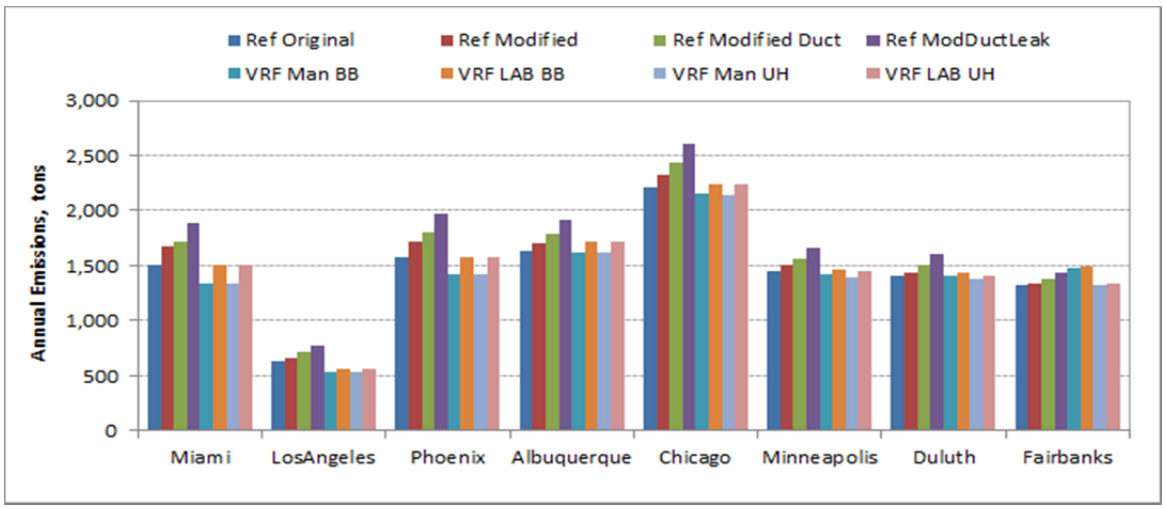

Figure 9-13 Annual Carbon Equivalent Emissions in Large Office Building

9.6.3.2 Small Office Building

The small office VRF HVAC models investigated show a reduction in annual carbon emission relative to the modified reference duct model as shown in Figure 9-14 but the magnitude of emissions reduction varies with location and are dependent on system efficiency. For instance, in Miami, the larger emission reduction difference between the four VRF systems is due to the difference in system efficiency whereas in Fairbanks reduced emission reduction difference is primarily due to the differences in fuel type offsetting the differences in efficiency.

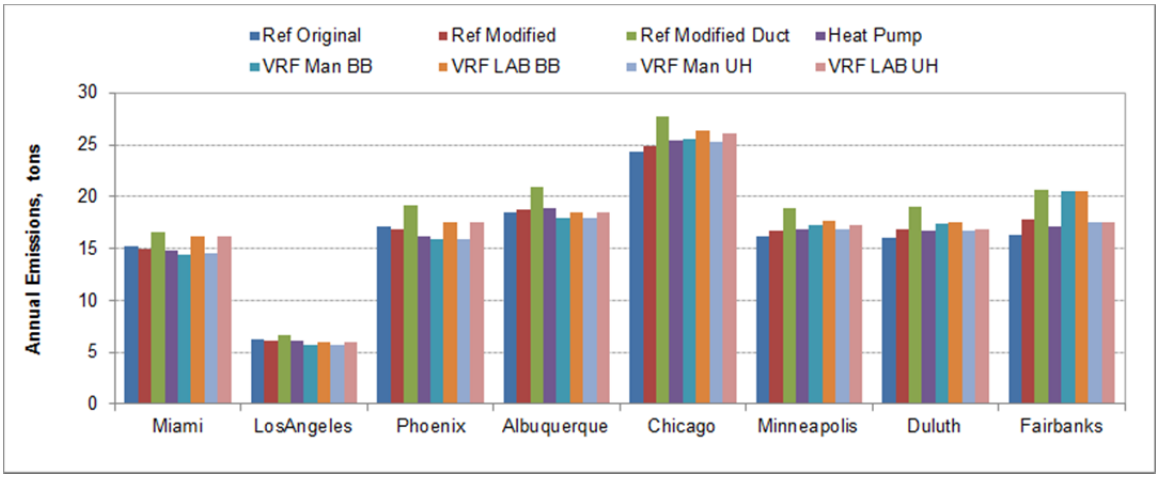

Figure 9-14 Annual Carbon Equivalent Emissions in Small Office Building

9.6.3.3 Standalone Retail Building

The standalone retail building VRF system HVAC model with a gas backup heating system has less emissions relative to the modified reference duct model for all locations as shown in Figure 9-15 whereas the VRF system with electric baseboard backup heater show increased emissions for Duluth and Fairbanks. The standalone retail building VRF system with gas backup heating is the only system type that achieves an annual emission reduction in all eight locations. However, the VRF system shows annual energy savings in all locations for both laboratory and manufacturer COPs. This anomaly is explained by the difference in source and emission factors between the VRF and the reference HVAC systems fuel types.

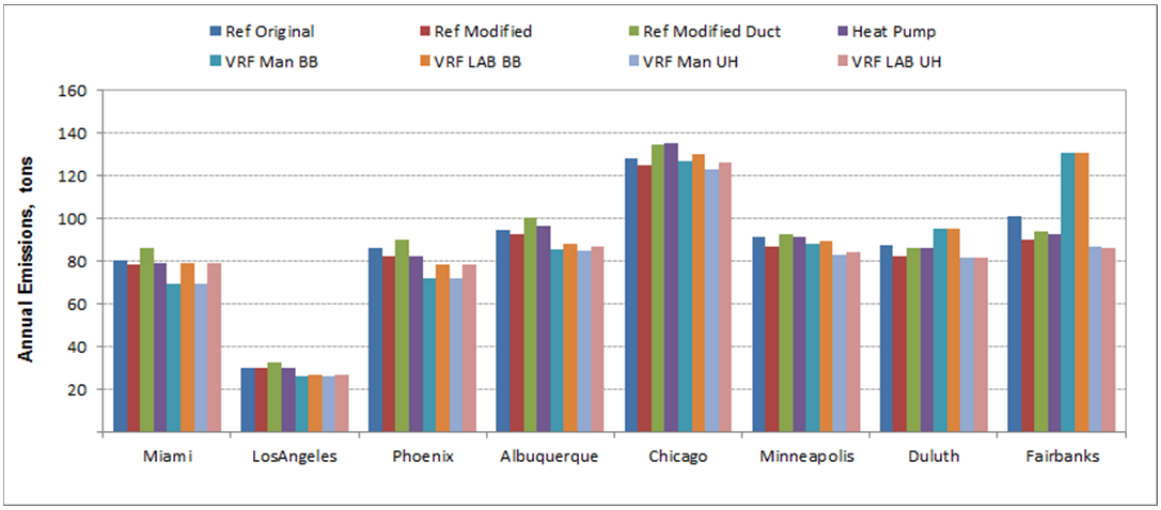

Figure 9-15 Annual Carbon Equivalent Emissions in Standalone Retail Building

9.6.3.4 Large Hotel Building

The large hotel VRF system shows total energy savings for heating dominated cities: Chicago, Minneapolis, Duluth and Fairbanks. The annual total energy percent savings range 7.4%-18.2%. Contrary to the energy savings trend, the large hotel building VRF systems shows mostly an increase in equivalent carbon emissions as shown in Figure 9-16. This increased emission shows a diminishing trend in colder climates due to the difference in efficiency and emission factors between the VRF and reference HVAC systems. The VRF system with laboratory measured COP in hot climates such as Miami and Phoenix show increased emissions due to lower cooling COP. In cold climates the large hotel VRF system with laboratory measured COP and gas backup heating system shows reduction in emissions mainly due to differences in the emission factors of the fuels. The VRF system with manufacturer COP in general shows a reduction in emissions for all locations except Miami and Phoenix.

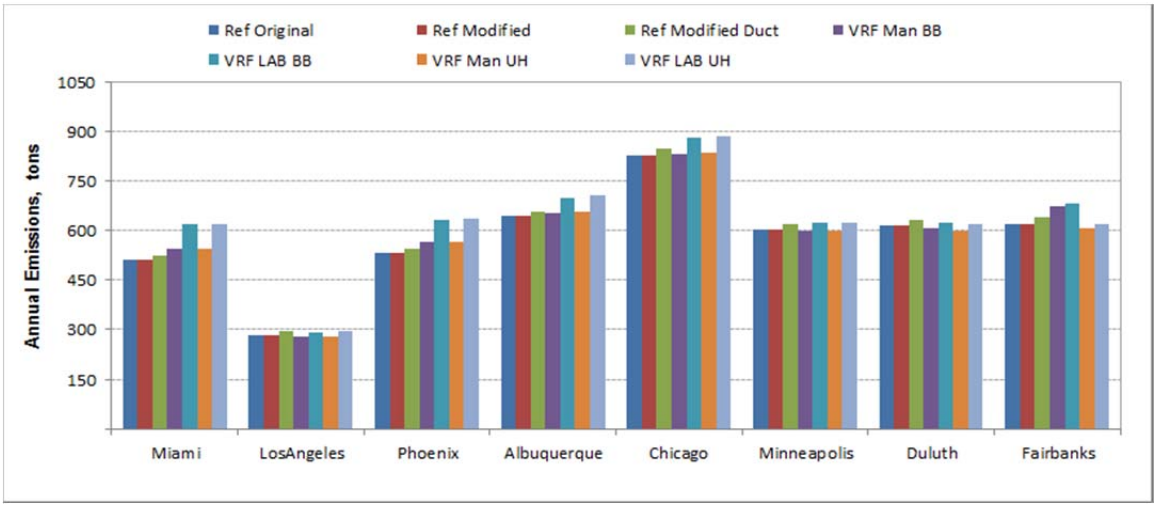

Figure 9-16 Annual Carbon Equivalent Emissions in Large Hotel Building

9.6.4 Comparative Energy Costs

The energy cost comparison was based solely on the cost of the total energy use. The total energy use refers to the sum of the total electric and gas energy uses. The total energy cost is the sum of the electric and gas annual energy costs. The electric and gas costs are based on the energy prices taken from the DOE EnergyPlus reference buildings model (Torcellini et al., 2008). The comparative analyses were made using normalized total energy cost and the normalized cost savings. The normalized energy costs were calculated using building total conditioned floor area.

9.6.4.1 Large Office Building

Figure 9-17 shows the annual normalized total energy costs for the large office building. The large office VRF HVAC system shows total energy costs savings for all locations except Fairbanks. Fairbanks is a heating dominated climate and the VRF system is mostly off due to operating temperature limits and the heating demand is provided by the backup heating system. The VRF system with a gas unit heater backup system shows 1.0 $\$/m^2$ increase in normalized energy cost whereas the electric baseboard backup heating system shows 4.7$\$/m^2$ increase due to high cost of electricity compared to natural gas. This implies that the energy cost saving from gas use outweighs the energy cost savings due to high efficiency of the VRF system when part of the heating demand is provided by the backup heating system. This is one of the reasons that heat pumps and VRF systems are not competitive in cold climates. Extending the operating limits and improving the efficiency of VRF systems and heat pumps in cold climate areas are of interest in current research.

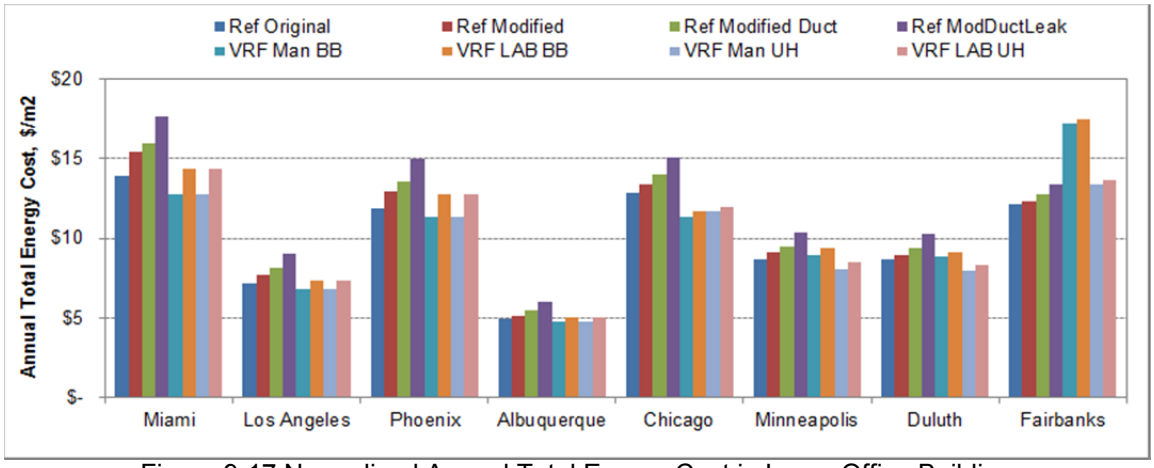

Figure 9-17 Normalized Annual Total Energy Cost in Large Office Building

9.6.4.2 Small Office Building

Figure 9-18 shows the annual normalized total energy cost for the small office building. The small office VRF HVAC system shows energy costs savings for all climate zones investigated except Fairbanks. Fairbanks is a heating dominated climate and the VRF system is mostly off due to operating temperature limits and the heating demand is provided by a backup heating system. The VRF system with a gas unit heater backup system shows moderate cost savings whereas the baseboard electric heaters backup

shows increased energy cost due to high cost of electricity. Again this is one of the reasons that heat pumps and VRF systems are not competitive in cold climates as depicted in the large office building analysis.

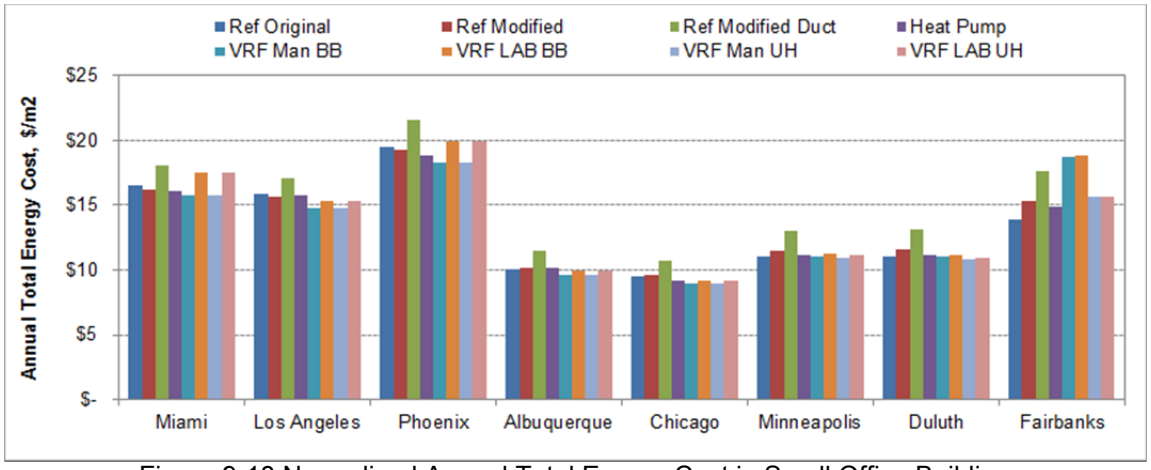

Figure 9-18 Normalized Annual Total Energy Cost in Small Office Building

9.6.4.3 Standalone Retail Building

Figure 9-19 shows the annual normalized total energy cost for a standalone retail building. The total energy cost for a VRF system with gas backup heating system is less than the total energy cost of the modified reference for all climates while the VRF system with electric backup heating system is less than that of the modified reference duct model and packaged heat pump HVAC model for all climates but Chicago, Duluth and Fairbanks. For hot and warm climates the VRF system with lab measured COP compared to the packaged heat pump shows marginal cost savings. The high energy cost of the VRF system with an electric baseboard backup heater in Fairbanks is in part due to the operational limits of the VRF system where the backup heating systems ran a majority of the time. The result for Fairbanks is a good example of why cold climates use fossil fuel heating systems. At this time, the cost of fossil fuel is approximately one-half that of electricity.

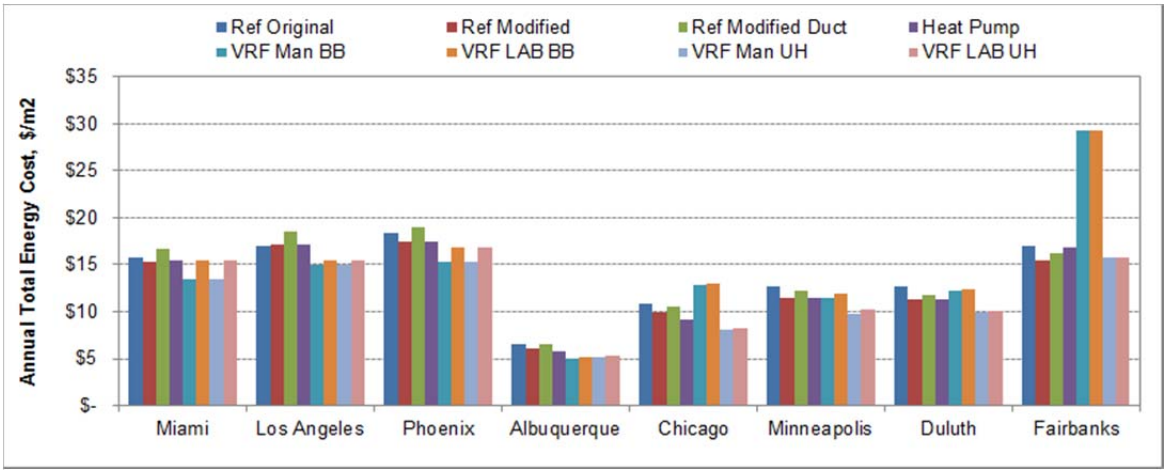

Figure 9-19 Normalized Annual Total Energy Cost in Standalone Retail Building

9.6.4.4 Large Hotel Building

Figure 9-20 shows the annual normalized total energy cost for large hotel building. The total energy costs for a VRF system shows sensitivity to system COP. In hot and warm climates the VRF total energy cost was higher by up to 16.8% for laboratory measured COP and by 6.6% for manufacturer's rated COP. In moderate climates such as Los Angeles, the VRF energy cost was lower by 1.5% for laboratory measured COP and higher by 5.5% for manufacturers COP. For cool and cold climates except Fairbanks, a VRF system showed less total energy cost compared to the modified reference HVAC model. Chicago also showed a marginal increase in total energy cost for the VRF system with laboratory measured COP and a gas backup heating system. The VRF system in Fairbanks showed 3%-28% increase in total energy cost depending on the backup heating system and system COP.

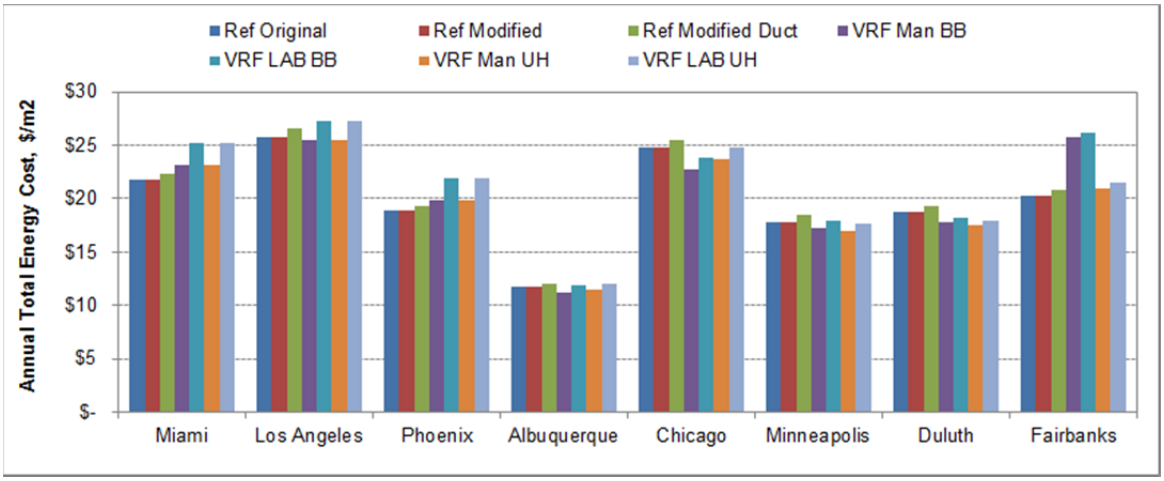

Figure 9-20 Normalized Annual Total Energy Cost in Large Hotel Building

9.7 Discussion and Conclusion

The parametric run analysis demonstrates the modeling capabilities of the DOE EnergyPlus VRF HVAC model and also shows advantages of VRF systems compared to a conventional HVAC system. These benefits include: elimination of air distribution inefficiencies (duct condition losses and supply air leakage), reduced fan energy consumption, and impacts of system efficiency. The relative importance of these variables depends on the building type. For instance, impacts of conduction losses on annual total energy use is significant in single story buildings such as the small office and standalone retail building due to high attic temperatures. VRF systems may require no or less duct work hence the duct conduction and duct leakage losses contributes directly to total energy savings for VRF systems. Elimination of straight duct sections and fittings reduces the static pressure rise requirement of the supply air fan substantially and results in more than 50% annual fan electric energy savings depending on the duct requirements. One of the distinct features of VRF systems is simultaneous cooling and heating operation capabilities. This operation mode is economical only when the additional electric energy required when switching from cooling only mode to simultaneous cooling and heating operation mode costs less than

energy cost saving from the heat recovered. In general energy savings from simultaneous cooling and heating operation of the VRF systems was not significant since there was no substantial cooling and heating load diversity in the buildings investigated in this study. The various energy savings potential of the VRF system compared to conventional HVAC systems determined using parametric analysis are summarized by building type as follows.

On an annual basis, VRF systems show lower energy use than the reference systems typically used in large office building as shown in Figure 9-1. For cooling dominated climates, the savings achieved is in the range 11%-25% of annual total energy use. For heating dominated climates, however, the VRF system annual total energy savings range 26%-29% for gas backup unit heaters and 23%-27% for electric baseboard backup heaters. The VRF system total energy savings in large office buildings is due to the elimination of ducts and difference in efficiency. Higher savings in colder climates is primarily attributed to difference in efficiency between the VRF and the reference HVAC models. Duct conduction loss in large office buildings contributes to 3%-7% total energy saving for VRF. Considering buildings with leaky ducts, the savings may increase by 6% to 12% depending on climate zone.

The small office building VRF system shows greater savings over the reference HVAC model. For hot and warm climates, the small office total energy savings ranges 3%-19% for the laboratory measured COP and 13%-22% for the manufacturer's rated COP. Cooler climates show even greater savings, with 24% to 36% savings over the modified reference with duct model. The total energy savings due to the elimination of ducts in a small office building amounts to 10%-17%. Higher savings were observed in the small office building compared to the large office mainly due to high conduction losses due to very hot in summer and very cold in winter attic space temperature in a single story building. The annual fan energy savings in a small office building ranges 13%-16% of the total energy use of the modified reference duct model. VRF systems showed less energy savings over the conventional heat pump system. In Miami, the laboratory measured COP VRF system used more energy than the packaged heat pump to due to its low cooling COP compared to packaged heat pump system. In cooler climates, energy savings showed only slight savings for all climates except Duluth and Fairbanks, which showed savings of 9%-14%. The total energy savings in a small office building is mainly attributed to elimination of ducts, difference in efficiency and fan energy reduction.

The standalone retail building shows greater savings of the VRF system over the modified duct model and moderate savings over the heat pump system. The laboratory measured COP VRF system achieves savings of 8%-32% over the typical attic duct system and up to 17% savings over the heat pump system. The manufacturer's rated COP system achieves 19%-38% savings over modified duct model and 12%-25% savings over the heat pump system. The total energy savings due to the elimination of ducts in the standalone retail buildings amounts to 3%-9% and the annual fan energy savings range 7%-21% of the

total energy use of the modified reference duct model. The VRF system shows higher energy saving potential in a standalone retail building compared to the small office building in part due to extended operating hours.

Since the large hotel building model does not have a plenum zone the duct was assumed to be installed in conditioned space. This results in marginal conduction losses hence elimination of ducts for VRF has no significant effect on energy savings potential. The fan energy savings of the VRF system compared to the modified reference duct model fan energy ranges 54%-63%. These fan energy savings in a large hotel building amounts to 3%-5% of the annual total energy use of the modified reference duct HVAC model. The large hotel shows significant savings of VRF over the reference building only for colder climates. For hot climates such as Miami and Phoenix, the VRF with laboratory measured COP model is consuming more energy than the reference HVAC model. Whereas the manufacturer's rated COP VRF system model uses within 1% of the reference HVAC model energy. These locations are cooling dominated climates and the cooling COP is lower than the reference HVAC COP, hence the fan energy savings cannot offset the higher cooling energy consumption for the lower COP VRF system. The VRF system in cooler climates, show 12%-22% total energy savings over the reference modified duct model depending on location, efficiency and backup heating system.

Similar thermal comfort levels were predicted among the various HVAC systems. However, the VRF system shows significant hours for building average relative humidity exceeded 65% for all four building types in humid climates such as Miami, Florida. This issue is a direct consequence of the difference in the DX cooling coil model between the VRF and the regular DX coil models. The VRF DX cooling coil model in general yields higher operating sensible heat ratio, which results in higher indoor relative humidity. This high indoor relative humidity requires further investigation to determine the cause. The VRF system has shown annual total energy savings in all building types and all climate zones investigated but those savings don't necessarily directly translate into emissions reduction and energy cost savings due to differences in source and emission factors that emanate from differences in fuel type and associated efficiency of the VRF and the reference HVAC systems.

10 References

ASHRAE. 2007. Energy Standard for Buildings Except Low-Rise Residential Buildings. ANSI/ASHRAE/IESNA Standard 90.1 2007. ASHRAE, Inc. 1791 Tullie Circle NE, Atlanta, GA 30329.

Aynur, T. N., Y. Hwang, and R. Radermacher. 2009. Simulation comparison of VAV and VRF air conditioning systems in an existing building for the cooling season. *Energy and Buildings* 41: 1143–1150.

Aynur, T. N. 2010. Variable refrigerant flow systems: A review. *Energy and Buildings* 42: 1106–1112.

Dyer, Mark June 2006. "Approaching 20 years of VRF in the UK," Modern Building Services, http://www.modbs.co.uk/news/fullstory.php/aid/2127/Approaching_20_years_of_VRF_in_the_UK.html.

Energy Science and Technology Software Center (ESTSC). 2001. DOE-2.1E Version 110 (source code). Oak Ridge, TN.

Fisk, W.J.; Delp, W.W.; Diamond, R.C.; Dickerhoff, D.J.; Levinson, R.M.; Modera, M.P.; Nematollahi, M.; Wang, D. (2000). Duct systems in large commercial buildings: physical characterization, air leakage and heat conduction gains. Energy and Buildings (32): 109-119.

Goetzler, W., K.W. Roth, and J. Brodrick. 2004. Variable Flow and Volume Refrigerant System. *ASHRAE Journal:* 46(1): 164–165.

Goetzler, W. 2007. Variable Refrigerant Flow System. *ASHRAE Journal*: 49(4): 24–31.

Li, Y. Ming, and J. Yi Wu. 2010. Energy simulation and analysis of the heat recovery variable refrigerant flow system in winter. *Energy and Buildings* 42: 1093–1099.

Miller, R.L. and Jaster, H. 1985. Performance of Air-Source Heat Pumps. EM-4226. Palo Alto, CA: Electric Power Research Institute.

Nigusse, B.A. and R. Raustad. 2012. Modeling Variable Refrigerant Flow Heat Pump and Heat Recovery Equipment in EnergyPlus: Task 3.0 – Validation of the VRF AC Heat Pump Model Using Manufacturers Performance Data. Task 3.0 Final Report. Cocoa, FL. Florida Solar Energy Center. FSEC-CR-1961-12.

Nigusse, B., R. Raustad, Verification of a VRF Heat Pump Computer Model in EnergyPlus. ASHRAE Transactions, volume 119, Part 2:101-117. DE-13-010.

Nigusse, B., C. Sharma, R. Raustad, and J. Cummings. 2013. Modeling Variable Refrigerant Flow Heat Pump and Heat Recovery Equipment in EnergyPlus: Task 9.0 - Parametric Analysis using the EnergyPlus VRF AC System Model. Task 9.0 Final Report. Cocoa, FL. Florida Solar Energy Center. FSEC-CR-1967-13.

Parker, D.S., Dunlop, J.P., Sherwin, J.R., Barkaszi, Jr., S.F., Anello, M.P., Durand, S., Metzger, D., and Sonne, J.K. (1998). "Field Evaluation of Efficient Building Technology with Photovoltaic Power Production in New Florida Residential Housing." Report No. FSEC-CR-1044-98, Florida Solar Energy Center, Cocoa, FL.

Raustad, R. 2011. Modeling Variable Refrigerant Flow Heat Pump and Heat Recovery Equipment in EnergyPlus: Task 2.0 – Implementing a VRF AC Heat Pump Model in U.S. DOE's EnergyPlus Software Tool. Task 2.0 Final Report. Cocoa, FL. Florida Solar Energy Center. FSEC-CR-1960-11.

Raustad, R. Creating Performance Curves for Variable Refrigerant Flow Heat Pumps in EnergyPlus. *Florida Solar Energy Center*, Report: FSEC-CR-1910-12, March, 2012.

Raustad, R. 2012a. Modeling Variable Refrigerant Flow Heat Pump and Heat Recovery Equipment in EnergyPlus: Task 4.0 – Independent Lab Testing of Two VRF AC Systems in Heat Pump and Heat Recovery Mode. Task 4.0 Final Report. Cocoa, FL. Florida Solar Energy Center. FSECCR-1962-12.

Raustad, R. 2012b. Modeling Variable Refrigerant Flow Heat Pump and Heat Recovery Equipment in EnergyPlus: Task 5.0 – Development of a VRF AC System Heat Recovery Computer Model. Task 5.0 Final Report. Cocoa, FL. Florida Solar Energy Center. FSEC-CR-1963-12.

Raustad, R. 2012c. Modeling Variable Refrigerant Flow Heat Pump and Heat Recovery Equipment in EnergyPlus: Task 6.0 – Field Testing Two VRF AC Systems. Task 6.0 Final Report. Florida Solar Energy Center. FSEC-CR-1964-12.

Raustad, R. 2012d. Modeling Variable Refrigerant Flow Heat Pump and Heat Recovery Equipment in EnergyPlus: Task 7.0 – Implementing a VRF AC System Heat Recovery Model in U. S. DOE's EnergyPlus software tool. Task 7.0 Final Report. Cocoa, FL. Florida Solar Energy Center. FSEC-CR-1965-12.

Raustad, R. (2013). A Variable Refrigerant Flow Heat Pump Computer Model in EnergyPlus. *ASHRAE Transactions*, 119 (Part 1):299-308.

Raustad, R., (2013). Computer Modeling VRF Heat Pumps in Commercial Buildings using EnergyPlus. *ASHRAE Annual Conference*, Denver, Colorado, June 22-27, 2013. DE-13-C071.

Sharma, C. and R. Raustad. 2013. Modeling Variable Refrigerant Flow Heat Pump and Heat Recovery Equipment in EnergyPlus: Task 8.0 – Compare Field Demonstration Building Energy Use to Computer Simulations. Task 8.0 Final Report. Cocoa, FL. Florida Solar Energy Center. FSEC-CR-1966-13.

Sharma, C., R. Raustad, Compare Energy Use in Variable Refrigerant Flow Heat Pumps Field Demonstration and Computer Model. *ASHRAE Annual Conference*, Denver, Colorado, June 22-27, 2013. DE-13-C072.

Torcellini, P., M. Deru, B. Griffith, K. Benne, M. Halverson, D. Winiarski, and D.B. Crawley. 2008. DOE Commercial Building Benchmark Models. National Renewable Energy Laboratory. NREL Report No. CP-550-43291.

US Department of Energy. 2011. Engineering Reference – The Reference to EnergyPlus Calculations, Version 7.0. Washington, DC: U. S. Department of Energy.

US Department of Energy. 2012a. Input Output Reference – The Encyclopedic Reference to EnergyPlus Input and Output, Version 7.2. Washington, DC: U. S. Department of Energy.

U.S. Department of Energy. 2012b. Engineering Reference – The Reference to EnergyPlus Calculations, Version 7.2. Washington, DC: U.S. Department of Energy.

US Department of Energy. 2012c. Auxiliary EnergyPlus Programs – Extra programs for EnergyPlus, Version 7.2. Washington, DC: U. S. Department of Energy.

Zhou, Y.P., J.Y. Wu, R.Z. Wang, and S. Shiochi. 2007. Energy simulation in the variable refrigerant flow air-conditioning system under cooling conditions. *Energy and Buildings* 39: 212–220.

Zhou, Y.P., J.Y. Wu, R.Z. Wang, S. Shiochi, and Y.M. Li. 2008. Simulation and experimental validation of the variable-refrigerant-volume (VRV) air-conditioning system in EnergyPlus. *Energy and Buildings* 40: 1041–1047.

Appendix A: Computer Model Defects Found

Defects, or change requests (CR), found and corrected during **Task 3**:

CR8492 – The VRF heating performance curve boundary temperature selection logic is incorrect. In the VRF flow heat pump model the heating performance curve outdoor temperature type selection in CalcVRF routine checks the boundary temperature against outdoor dry bulb temperature only. While the check for boundary temperature should have been either wet-bulb or dry-bulb depending on user input.

CR8494 – In VRF model Input Power Correction factor that account for defrost effect is calculated but never used. In variable refrigerant flow heat pump model the input power correction factor variable "InputPowerMultiplier" that accounts for defrost effect is calculated In CalcVRFCondenser routine but never used.

CR8497 – When more than 1 VRF condenser is used in a simulation, VRF Terminal Units can be sized based on the first terminal unit that is called from a zone for each unique AirConditioner:VariableRefrigerantFlow object.

CR8500 – VRF Terminal Unit parasitic power is incorrectly reported for both cooling and heating mode report variables (i.e., Zone Terminal Unit Cooling Electric Consumption Rate and Zone Terminal Unit Heating Electric Consumption Rate).

CR8783 – The sum of the VRF terminal unit capacities can be greater than the VRF condenser capacity. Limiting the total VRF system terminal unit capacity (limit of any TU is reported by Variable Refrigerant Flow Heat Pump Maximum Terminal Unit Cooling Capacity) to be less than the VRF condenser capacity may not work correctly when the last terminal unit in the TerminalUnitList is the limiting capacity.

Defects found and corrected during **Task 7**:

CR8909 - AirConditioner:VariableRefrigerantFlow has min/max outdoor limits of operation in both cooling and heating mode. The system does not change mode of operation to meet a heating (cooling) load when the zone loads request cooling (heating) mode and the OA limits of operation for cooling (heating) mode are exceeded.

CR8916 - The ZoneHVAC:VariableRefrigernatFlow terminal unit reports Zone Terminal Unit Latent Cooling Rate in kg/s instead of Watts. This in turn impacts the Zone Terminal Unit Total Cooling Rate report variable.

CR8917 - ZoneHVAC:TerminalUnit:VariableRefrigerantFlow report variables for Zone Terminal Unit Total Cooling/Heating Energy are included on the EnergyTransfer meters when the coils report that information as well. Energy variables for Coil:DX:Heating:VariableRefrigerantFlow are not reported.

CR8936 - Variable Refrigerant Flow Heat Pump Condenser Inlet Temp in Input Output Reference is not the same as the report variable in the rdd file (i.e., the word condenser is missing).

Defects found and corrected during **Task 9**:

CR9011 - The VRF terminal unit defaults to constant fan operating mode when a schedule name is present in the Supply Air Fan Operating Mode Schedule Name input field but the actual schedule is not in the input file.